Università degli Studi di Cagliari

Scuola di Dottorato in Biologia e Biochimica dell'Uomo e dell'Ambiente
Curriculum Biochimica e Biologia Molecolare
Dipartimento di Scienze e Tecnologie Biomediche

Sezione di Chimica Biologica

s.s.d. BIO/10

Supported Metalloporphines As Novel and Bioinspired Ligninolytic Peroxidase–Like Catalysts

PhD Thesis of:

Paolo Zucca

XXIII ciclo

March 10^{th}, 2011

. . . salimmo sù, el primo e io secondo,
tanto ch'i vidi de le cose belle
che porta 'l ciel, per un pertugio tondo.
E quindi uscimmo a riveder le stelle.

This text was formatted by its Author using LaTeX, a free word processing tool, from June 2009 through July 2010.

Cover graphical design and Photography by Arch. Emmanuele Contini ©.

Author's e-mail: pzucca@unica.it
paolo.zucca@gmail.com

Author's address: Sezione Chimica Biologica e Biotecnologie Biochimiche
Dipartimento di Scienze e Tecnologie Biomediche
Università di Cagliari
SP Monserrato–Sestu Km 0.900
09042 Monserrato (CA)
Italy
Tel +39 (0)706754514
Fax +39 (0)706754527

Supervisor: Prof. Enrico Sanjust
Dipartimento di Scienze e Tecnologie Biomediche
Università degli Studi di Cagliari
Italy

Prof. Emil Dumitriu
Facultatea de Inginerie Chimică şi Protecţia Mediului
Universitatea Tehnică "Gheorghe Asachi" din Iaşi
Romania

Reviewers: Prof. Vasile Hulea
Laboratoire de Matériaux Catalytiques et Catalyse
École Nationale Supérieure de Chimie de Montpellier
France

Prof. Francisco Amado
Departamento de Química
Universidade de Aveiro
Portugal

Thesis Committee: Prof. Angelo Cau
Dipartimento di Biologia Animale ed Ecologia
Università degli Studi di Cagliari
Italy

Prof. Adrian Ungureanu
Facultatea de Inginerie Chimică şi Protecţia Mediului
Universitatea Tehnică "Gheorghe Asachi" din Iaşi
Romania

Prof. Nicola Sechi
Dipartimento di Scienze Botaniche
Università degli Studi di Sassari
Italy

List of Original Articles

This thesis is based on the following original publications:

I: Zucca P, Mocci G, Rescigno A, Sanjust E (2007) 5,10,15,20-Tetrakis(4-sulfonato-phenyl)porphine-Mn(III) immobilized on imidazole-activated silica as a novel lignin-peroxidase-like biomimetic catalyst. *Journal of Molecular Catalysis A: Chemical*. 278(1–2): 220–227.

II: Zucca P, Vinci C, Sollai F, Rescigno A, Sanjust E (2008) Degradation of Alizarin Red S under mild experimental conditions by immobilized 5,10,15,20-Tetrakis(4–sulfonato–phenyl)porphine–Mn(III) as a biomimetic peroxidase-like catalyst. *Journal of Molecular Catalysis A: Chemical*. 288(1–2): 97–102.

III: Zucca P, Sollai F, Garau A, Rescigno A, Sanjust E (2009) Fe(III)-5,10,15,20-Tetrakis(pentafluorophenyl)porphine supported on pyridyl-functionalized, crosslinked poly(vinylalcohol) as a biomimetic versatile-peroxidase-like catalyst. *Journal of Molecular Catalysis A: Chemical*. 306(1–2): 89–96.

IV: Zucca P, Sanjust E (2009) Bioinspired routes towards delignification. *La Chimica & L'Industria*. 7: 100–105.

V: Zucca P, Vinci C, Rescigno A, Dumitriu E, Sanjust E (2010) Is the bleaching of phenosafranine by hydrogen peroxide oxidation catalyzed by silica-supported 5,10,15,20–tetrakis–(sulfonatophenyl)porphine–Mn(III) really biomimetic? *Journal of Molecular Catalysis A: Chemical*. 321(1–2): 27–33.

ABBREVIATIONS

ABTS	2,2'–Azino–bis(3–ethylbenzothiazoline–6–sulfonic acid) diammonium salt
APH	2,2'–Azobis(2–methylpropionamidine) dihydrochloride
AP–PVA	3–Aminopropyl–functionalized PVA, crosslinked with glutaraldehyde
APS	Aminopropylsilica
ARS	Alizarin Red S
β–Cl_8–TDCPP	β–octachloro–5,10,15,20–tetrakis(2,6–dichlorophenyl)porphine
AzB	Azure B
DMSO	Dimethyl sulfoxide
FeTFPP	5,10,15,20-Tetrakis(pentafluorophenyl)porphine iron(III) chloride
HRP	Horseradish peroxidase E.C. 1.11.1.7
Im–PVA	Imidazolyl-3-aminopropyl–functionalized PVA, crosslinked with glutaraldehyde
IPS	(3–(1–Imidazolyl)–propylcarbamoyl)–3'–aminopropylsilica
LC	Laccase E.C. 1.10.3.2
LiP	Lignin peroxidase E.C. 1.11.1.14
LP	Generic lignolytic peroxidase
MB	Methylene blue
MG	Methyl Green
MnP	Manganese peroxidase E.C. 1.11.1.13
MnTSPP	5,10,15,20–Tetrakis(4–sulfonato–phenyl)porphine manganese(III) chloride
M–PVA	Mercapto–functionalized PVA, crosslinked with glutaraldehyde
MSG	Mercapto–functionalized silica gel
MO	Methyl Orange
NHS	*N*–hydroxysuccinimide
NHT	*N*–hydroxybenzotriazole

NPH	*N*–hydroxyphthalimide
OH–TEMPO	4–hydroxy-2,2,6,6–tetramethylpiperidine–1–oxyl
PNS	Phenosafranine
PP–PVA	4'–Pyridylmethyl-3-aminopropyl–functionalized PVA, crosslinked with glutaraldehyde
PSG	4–Pyridyl–methylcarbamoyl–3–aminopropylsilica
PVA	Poly(vinylalcohol)
ROS	Reactive oxygen species
SG	Silica gel
TBARS	Thiobarbituric acid reactive substances
VA	Veratryl alcohol (3,4–dimethoxybenzyl alcohol)
TFPP	5,10,15,20–tetrakis(pentafluorophenyl)porphine
TMPP	5,10,15,20-tetrakis–4–(N–pyridiniomethyl)porphine
TPP	5,10,15,20–tetraphenylporphine
TSPP	5,10,15,20–tetrakis(4–sulfonatophenyl)porphine
TDCPP	5,10,15,20–tetrakis(2,6–dichlorophenyl)porphine
VP	Versatile peroxidase E.C. 1.11.1.16
XO	Xylenol Orange

ABSTRACT

Current, classical delignification processes are affected by some economical and environmental drawbacks. These approaches often seem to be inadequate, particularly in the perspective of a sustainable green process. Since immobilized metalloporphines can strictly emulate the active site of ligninolytic peroxidases, their use in delignification processes has been presented and future trends outlined.

In order to achieve a structural emulation, several coordinating groups have been used to coordinatively immobilize metalloporphines. Synthesized adducts have been characterized by UV/vis and IR spectroscopies, and effective coordinative bond between metalloporphine and supports was shown.

The biomimetic catalysts have been also investigated about their peroxidase catalysis and ability to emulate lignolytic peroxidases action and substrate specificity. The adducts showed a remarkable ability to catalyze veratryl alcohol oxidation at the expenses of H_2O_2. Kinetic and operational characterization of the catalysts is also reported. Both lignin peroxidase and manganese peroxidase–like catalysis have been obtained, under very mild experimental conditions, using many lignin model compounds. Redox mediation was possible, allowing also treatment of water–insoluble substrates.

In the perspective of broadening industrial applications of the catalysts, the bleaching of several pollutant and durable textile dyes has been attempted with similar promising results, resulting particularly suitable for industrial scaling–up.

Accordingly, the inexpensiveness of the synthesis and the mild operational conditions allow these adducts to be proposed as feasible catalysts also for industrial large scale processes.

SOMMARIO

La rimozione della lignina dai materiali lignocellulosici costituisce una sfida industriale ancora aperta, poiché gli attuali approcci finora proposti non eccellono per economicità e sostenibilità ambientale del processo. Neppure quello biocatalitico (basato sia sugli enzimi lignolitici, che sui microrganismi loro produttori, i funghi del marciume bianco) ha finora trovato un valido compromesso tra costo ed efficienza del processo.

Le perossidasi ligninolitiche tuttavia costituiscono ottimi modelli per la sintesi di catalizzatori biomimetici in grado di operare una delignificazione più ecocompatibile: in particolare, sono state sviluppate numerose metalloporfine sintetiche che, libere nel mezzo di reazione, hanno mostrato promettenti proprietà catalitiche emulanti le perossidasi lignolitiche. Tuttavia, come tali non presentano alcuna applicabilità su larga scala, per ragioni di ordine economico.

Nel presente lavoro sono stati, dunque, sintetizzati alcuni catalizzatori biomimetici emulanti il sito attivo di questi enzimi, sfruttando supporti organici ed inorganici modificati chimicamente con funzioni in grado di legare tramite legame di coordinazione le metalloporfine sintetiche.

Gli addotti così sintetizzati sono stati dapprima caratterizzati tramite spettroscopia UV/Vis e FT–IR, ed è stato descritto come l'immobilizzazione avvenga effettivamente attraverso un legame di coordinazione, mostrando pertanto un'effettiva emulazione strutturale delle perossidasi lignolitiche.

Successivamente, i catalizzatori sono stati caratterizzati dal punto di vista funzionale, evidenziando proprietà di emulazione sia della lignina perossidasi, che della manganese perossidasi in presenza dell'ossidante più eco–compatibile possibile: il perossido di idrogeno. L'amplissima specificità di substrato, la sintesi poco costosa e le condizioni di reazione estremamente blande (pH neutro,

pressione e temperatura ambiente, ossidante ambientalmente compatibile e totale assenza di solventi organici) rendono questi catalizzatori quantomai adatti allo scaling–up industriale nel trattamento di materiali lignocellulosici in genere. Lo studio di mediatori di ossidoriduzione diffusibili suggerisce anche una loro possibile applicazione con substrati non solubili in acqua, poiché le forme ossidate di questi (ad esempio Mn(III) e $VA^{\bullet+}$) possono efficacemente fungere da tramite tra il catalizzatore eterogeneo e simili substrati.

Le potenzialità applicative degli addotti sono state ulteriormente ampliate attraverso uno screening di decolorazione di coloranti sintetici appartenenti a classi chimiche differenti. Anche in questo caso l'elevata efficienza e le blande condizioni operative risultano essere promettenti in ottica applicativa.

Contents

1 INTRODUCTION **14**
1.1 Lignocelluloses . . . 15
1.2 Cellulose . . . 17
1.3 Hemicelluloses . . . 18
1.4 Lignins . . . 19
1.4.1 Lignin structure . . . 19
1.4.2 Oxidative polymerization of monolignols . . . 22
1.5 Dyes . . . 25
1.6 Classical approaches towards delignification . . . 27
1.6.1 Physical methods . . . 28
1.6.2 Chemical methods . . . 29
1.6.3 Biological methods . . . 34
1.6.4 Enzymatic methods . . . 35
1.6.4.1 Laccase . . . 35
1.6.4.2 Lignolytic peroxidases . . . 36
1.6.5 Drawbacks of biological and enzymatic approaches . . . 41
1.7 Metalloporphines: a "bioinspired" alternative . . . 42
1.7.1 Metalloporphines emulate LPs reactions . . . 44
1.7.2 Immobilization of metalloporphines . . . 45
1.8 Aim of this study . . . 47

2 EXPERIMENTAL **50**
2.1 Materials . . . 50
2.2 Methods . . . 50
2.2.1 APS synthesis . . . 50
2.2.2 IPS synthesis . . . 51
2.2.3 PSG synthesis . . . 51
2.2.4 MSG synthesis . . . 51
2.2.5 AP–PVA synthesis . . . 52
2.2.6 Im–PVA synthesis . . . 52

2.2.7 PP-PVA synthesis . . . 53
2.2.8 M–PVA synthesis . . . 53
2.2.9 Porphination of supports . . . 53
2.2.10 Spettrophotometric analysis . . . 54
2.2.11 Surface area determination . . . 54
2.2.12 Catalytic activity determination . . . 55
2.2.12.1 LP–like assays . . . 55
2.2.12.2 Dye decoloration assays . . . 56
2.2.13 HPLC analysis . . . 57
2.2.14 GC–MS analysis . . . 58
2.2.15 Enzymatic comparison experiments . . . 58

3 RESULTS AND DISCUSSION 60
3.1 IPS/MnTSPP . . . 60
3.1.1 LiP–like activity characterization . . . 65
3.1.2 Reaction mechanism . . . 67
3.1.3 Dyes decoloration . . . 73
3.1.3.1 ARS insights . . . 79
3.1.3.2 PNS insights . . . 84
3.2 PP–PVA/FeTFPP . . . 92
3.2.1 LP–like activity characterization . . . 95
3.2.2 Reaction mechanism . . . 99
3.2.3 Dyes bleaching . . . 104
3.3 M–PVA/FeTFPP . . . 105
3.4 MnTMPP . . . 113

4 CONCLUSIONS 116

References 121

Index 133

1 INTRODUCTION

Not only non-natural chemicals can be regarded as pollutants and environmentally persistent.

Lignocellulosic materials totally derive from natural sources. However, being released in the environment in huge amounts (it has been estimated that every year $\sim$200x10^9 tons of plant biomass are produced [1]), they represent highly durable pollutants whose removal is a serious issue from both a chemical and environmental point of view.

In fact, their cellulosic component can be usually exploited in various ways; so removal should be addressed only towards lignin and hemicelluloses. But the close association in plants of these three constituents makes this goal very complicated.

An efficient method to selectively remove lignocellulosic components could allow complete exploitation of the others. For example, paper [2, 3] and bioethanol [4, 5] can arise from cellulose. Different aromatic compounds can be produced from lignin [6, 7], converting potential wastes in useful sources of chemical featured by high surplus value.

Several methods have been developed to selectively remove lignocellulosic components, including mainly mechanical and oxidative treatments.

Despite of the large efforts of the scientific community, economical feasibility of these processes is however distant. And for instance bioethanol production from lignocellulosic wastes is not yet a large scale process, deserving further enhancements to be economically achievable [4].

Besides treatment of lignocellulosic, such oxidative methods can also find employment in the the removal of many pollutant wastes, like olive mill wastewater [8, 9] and textile dyes [10]. This emphasizes the importance of their development especially with the aim of enhancing their efficiency and inexpensiveness.

1.1 Lignocelluloses

The main part of biomass in nature is composed by wood, grass and most of the plant litter: these materials are collectively called lignocellulose [11] (or better lignocelluloses, due to their high heterogeneity).

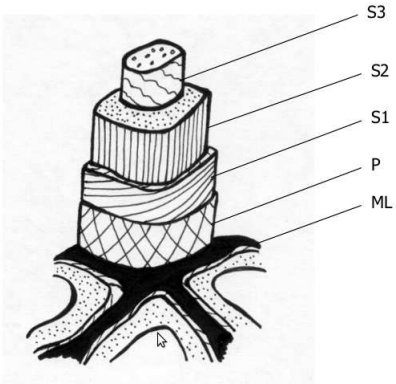

Figure 1: **Structure of a wood cell [12]. S3 secondary wall 3; S2 secondary wall 2; S1 secondary wall 1; P primary wall; ML middle lamella.**

Three major components can be identified in lignocellulosic materials: cellulose, hemicelluloses and lignins. They represents the biggest source of organic matter in earth; Fengel and Wegener [12] estimate the presence of 2.5–4x10^{11} tons of cellulose and 2–3x10^{11} tons of lignins in earth, that correspond about to 40% and 30% of total organic matter carbon.

They are closely associated in plants cell walls, and this makes very difficult

to isolate single components. In Figure 1 a schematic composition of plant cell wall is reported.

In its three major layers (middle lamella, primary and secondary wall) there is not a uniform distribution of cellulose, hemicellulose and lignin, as the former is most present in secondary wall and the latter in predominant in the middle lamella [12, 13].

Also distribution in various plants is very heterogeneous. As reported in Table 1, there are clear differences between different wood plants. Gramineous plants have considerable amounts of hemicelluloses in middle lamella.

Plant Material	**Cellulose (%)**	**Hemicellulose (%)**	**Lignin (%)**
Hardwood stems	40–55	25–40	18–25
Softwood stems	45–50	25–35	25–35
Bark	20–50	10–20	35–50
Wheat	51–54	26–30	16–18
Flax	57	15	2
Hemp	67	16	3.3
Ramie	69	13	0.6
Grass	25–40	35–50	10–30
Nut shells	25–30	25–30	30–40
Leaves	15–20	80–85	0

Table 1: **Lignocellulosic components content in selected plants and agricultural residues [4, 12, 14].**

Usually lignin component slows down plant biomass degradation. In this perspective plant cell wall composition should be carefully taken into account during the devolopment of processes based on the exploitation of plant biomasses.

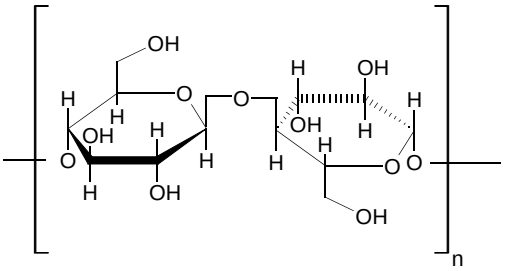

Figure 2: **Cellulose repeating unit.**

1.2 Cellulose

All plant cell walls contain cellulose, that is typically the most valued component of plant biomass.

It is a linear homopolymer consisting of repeating units of β–D–glucopyranose linked together by β–$(1 \rightarrow 4)$−glycosidic bonds as reported in Figure 2. This forces each monomer to be 180° rotated in comparison to the previous and the following residue, explaining the totally different chemical properties of seemingly similar polymers like starch and glycogen.

Because of the high degree of polymerization (up to 15,000) [11], the molecular mass is very high but this does not explain its complete insolubility in water. This feature is due to the crystalline nature of cellulose: 36 monomers are usually associated by hydrogen bonds forming microfibrils which give strength to the wood [11, 12]. Microfibrils can also associate to form ultrastructures like macrofibrilis and fibres.

Crystalline cellulose is much more resistant to degradation than non–crystalline, that is degraded faster. However, microorganisms produce several enzymes able to completely depolymerize cellulose [13]. Endoglucanases and cellobiohydrolases first hydrolyze cellulose to cellobiose (the corresponding disaccharide) and cellodextrins, that are at last hydrolized to glucose by exoglucanases and

β–glucosidases. Glucose can be then introduced in both aerobic and anaerobic metabolisms to be completely oxidized to carbon dioxide or fermentation products.

Many fungi are able to operate this degradation, such as soft and brown rot fungi (*Basidiomycetes*), Ascomycetous and rumen fungi [13]. Moreover, also many bacteria have similar enzymatic equipment.

Besides, also chemical methods (in particular acidic boiling) can efficiently depolymerize this homopolymer, even if a substantial fraction of the obtained glucose is changed into toxic furaldehyde derivatives.

However, as already stressed, usually cellulose represents the most valued component of plant biomass: in this perspective industrial process usually do not require its removal. But they rather consist in cellulose purification from other components. So their aim is usually undamaged cellulose protection during lignins and hemicelluloses depolymerization.

1.3 Hemicelluloses

The term "hemicelluloses" is referred to a heterogeneous class of polysaccharides different from cellulose present in plant cell walls (in particular in secondary wall, but also in the primary one).

They are most often heteropolysaccharides, composed by sugars and acid sugars like uronic acids. They are usually classified on the basis of their principal sugar: so they are divided into glucomannans, galactomannans or arabinoxylans [11, 12, 13].

Monomers are typically linked by β–glycosidic bond, but there can be found different bonds (like β–$(1 \rightarrow 4)$, β–$(1 \rightarrow 3)$, β–$(1 \rightarrow 6)$, but also α–$(1 \rightarrow 2)$ and α–$(1 \rightarrow 6)$ [13]) and frequent branches, leading to gels rather than fibres. Consequently, identification of any ordered structure is usually not possible.

They are usually present in lignocelluloses covalently linked to lignin, enhancing plant tissue strength.

The amorphous nature and the low degree of polymerization (up to 100–200) make hemicelluloses degradation easier than that of cellulose, since milder

acid or basic treatment is able to completely depolymerize and solubilize them. Furthermore, different microbial hydrolases (namely xylanases, xylosidases and mannosidases) are able to completely degrade hemicelluloses [13].

1.4 Lignins

Lignin is a natural polymer present in all vascular plants (and not in *algae*, *bacteria* and *bryophytes* [15]), providing them strength and rigidity. It is particularly present in secondary wall and middle lamella [12]. Total water insolubility of lignin confers impermeability to plants, and this greatly enhances their resistance to biodegradation, chemical, physical, and mechanical attacks [13].

Lignin is an aromatic, cross–linked, three–dimensional and heterogeneous polymer, featured by the peculiar property of not being hydrolyzable, contrary to the other lignocellulose components. This makes lignin the most durable and recalcitrant component of plant biomass (half–life estimated ∼150 years [16]).

Molecular mass is very high (600–1000 KDa), but not uniform between different plants and samples. Lignin is more reduced than polysaccharidic components, with a 50% more carbon content.

1.4.1 Lignin structure

Incredible complexity of lignin structure makes its complete determination a huge effort for scientific community, since it has been only partially understood [15, 17, 18, 19, 20, 21, 22].

The biggest hurdle towards this issue is the great heterogeneity of this polymer, that appears to be significantly different amongst phylogenetically related plants. And the differences are both due to different monomers composition, and to different bonds. This makes more correct the term "lignins", rather than lignin.

Lignin can be described as a high MW polymer composed by three major monomers called phenylpropanoids (or C6C3 compounds, or monolignols, Figure 3): *p*–coumaryl alcohol, coniferyl alcohol, and sinapyl alcohol.

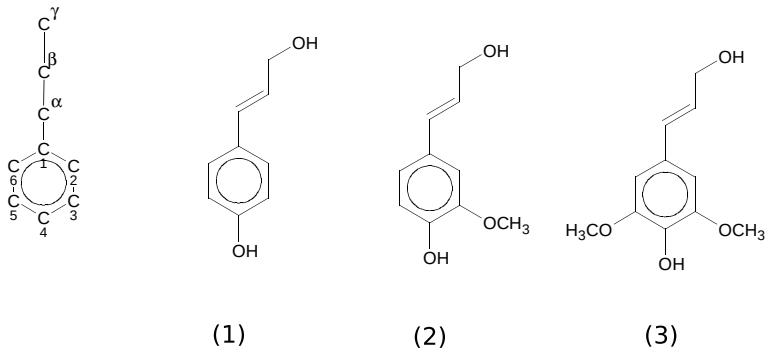

Figure 3: **The three phenylpropanoid monolignols present in lignin structure: *p*–coumaryl alcohol (1), coniferyl alcohol (2) and sinapyl alcohol (3).**

Their definition derives from the presence in their structure of a phenolic ring (variously, methoxy–substituted) and an unsaturated propanoid carbon chain. The γ carbon atom of this chain has primary alcoholic nature.

The monolignols are synthesized by plants starting from aminoacid phenylalanine [20] through the cinnamate pathway [23].

In the first reaction phenylalanine is deaminated by the key enzyme of this metabolic path (Phenylalanine Ammonia Lyase, PAL E.C. 4.3.1.24) to produce cinnamic acid. This is then *para*–hydroxylated, variously methoxylated and lastly reduced in γ position, as summarized in Figure 4.

Plants differ remarkably about relative amounts of this three monomers. Gymnosperm are particularly rich in coniferyl alcohol, as for instance in spruce the ratio between coniferyl, sinapyl and coumaryl alcohols is 94:5:1 [24]. On the contrary in dicotyledons sinapyl alcohol is more frequent (for instance *Eucalyptus globulus* contains about 82–86% syringyl units [25]), and in gramineous and monocotyledons coumaryl alcohol is more widespread.

Besides, the presence of hydroxycinnamate analogs has been described espe-

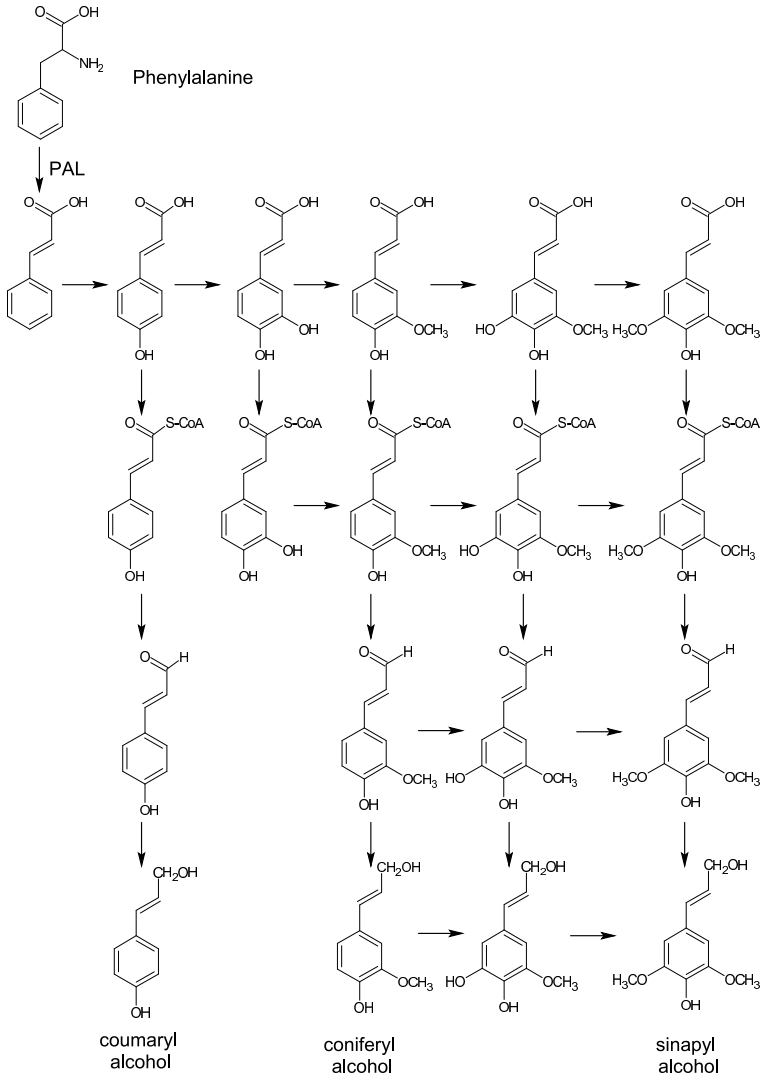

Figure 4: **Cinnamic acid pathway allows plant monolignols biosynthesis starting from phenylalanine.**

cially in grass lignins [26], being particularly involved in covalent bonding with hemicelluloses.

1.4.2 Oxidative polymerization of monolignols

In the presence of hydrogen peroxide and some plant peroxidases [27] (or – it is debatable– by O_2–dependent laccases [28]), monolignols are converted to phenoxy radicals. These are stabilized by electronic delocalization, as unpaired electron is shared among phenolic oxygen, aromatic ring and β carbon.

These radicals then spontaneously undergo addition. Such reaction seems to be quite random, giving the typical three–dimensional and irregular lignin structure, where several type of bonds can be found (Figure 5): β–aryl ether or β–O–4, phenylcoumaran or β–5, resinol or β–β, biphenyl or 5–5,diphenyl ether or 4–O–5, and also α–aryl ether or α–O–4 [13, 21, 25]. Moreover, some other structural motifs have been found such as dibenzodioxocins, arylisochromanes, spirodienones.

None of them is sensible to hydrolysis (unlike polisaccharide components of plant cell wall). This explains the remarkable chemical durability of lignins, that can therefore be considered as recalcitrant pollutants. Especially taking into account the huge amounts of lignin–based wastes produced every year [1].

Lignin biosynthesis is a relatively slow process relying on a continuous monomer supply; monolignol concentrations remain constantly very low so that gradual growth of the three–dimensional lignin structure sharply prevails over monolignol coupling/dimerization [24, 29, 30, 31, 32].

Accordingly, great care should be exerted when inferring structural information from dehydrogenative polymerizates coming from *in vitro* oxidation/dehydrogenation of monolignol mixtures [33], unless the reactant concentrations are kept very low for a long time, and the polymerization process takes place in the presence of lignin, acting as a template [24].

Due to this peculiar polymerization process, it is impossible to outline the precise structure of a lignin molecule. Only pieces of lignin molecules can be hypothesized, as shown in Figure 6.

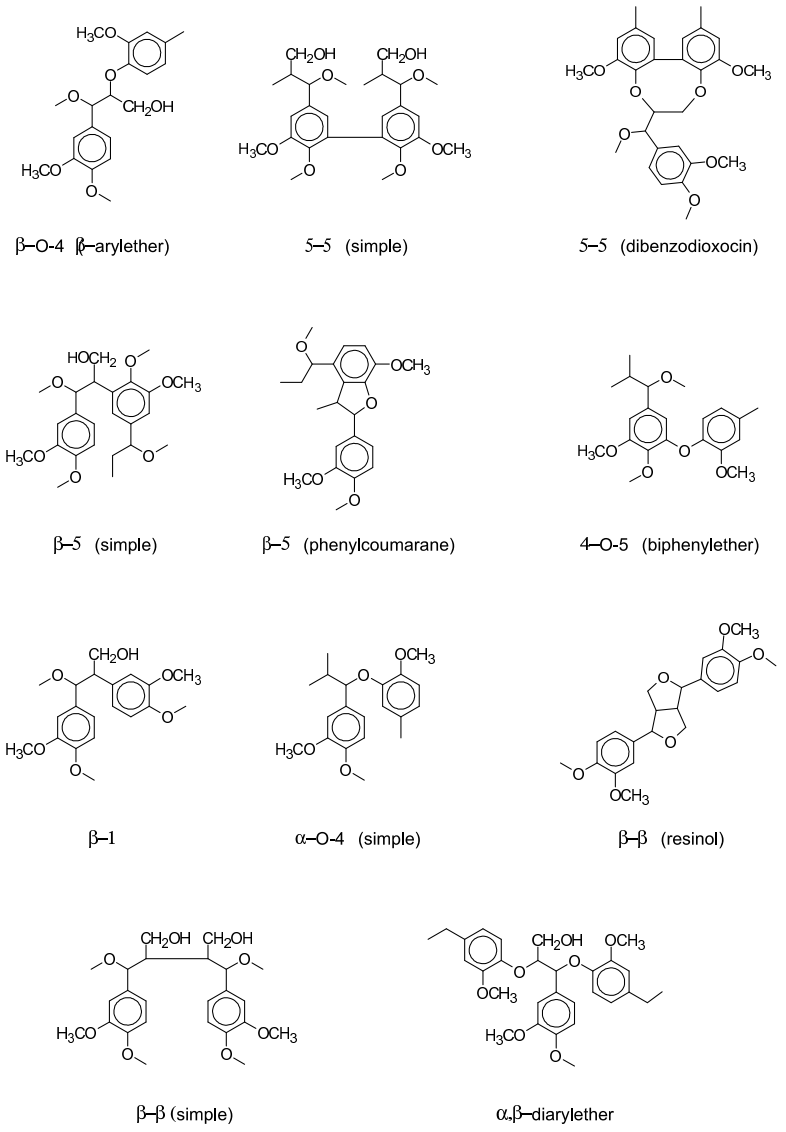

Figure 5: **Most frequent bonds present between monolignols.**

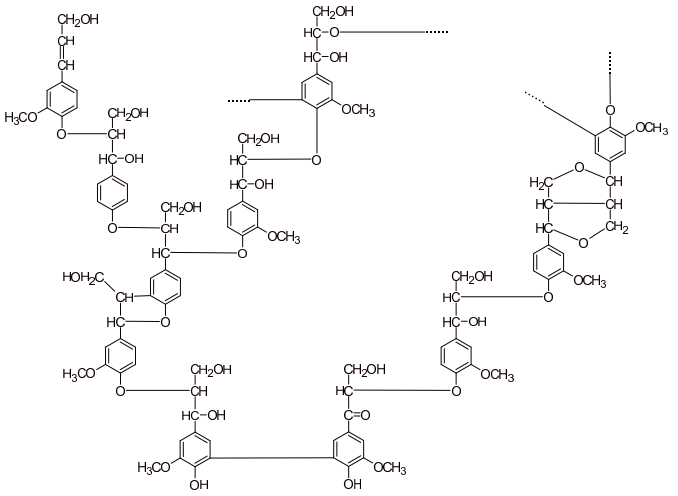

Figure 6: **A simplified scheme of a lignin structure (from spruce) showing some of the chemical bonds commonly found in lignins.**

More recently, an alternative hypothesis on lignin biosynthesis has been developed and corroborated by some experimental findings [22, 34, 35, 36], based on the assumption that monolignol (radical) binding dirigent proteins should direct the biosynthesis, which would therefore be not random, but template–based.

The controversy is quite fascinating [37]; however, the presence of well defined structural domains in lignins such as the hexamers and pentamers of synapyl alcohol found in *Eucalyptus globulus* lignin [38] does not modify the statistical occurrence of the linkages to be (bio)cleaved to accomplish lignin degradation and solubilization. On the other hand, the precise identification of the genes, codifying for dirigent proteins along lignin biosynthesis, could have an outstanding importance in tuning that biosynthesis [39] towards modified, more soluble and/or more degradable lignins.

Besides its inertness, lignin depolymerization and removal from plant bio-

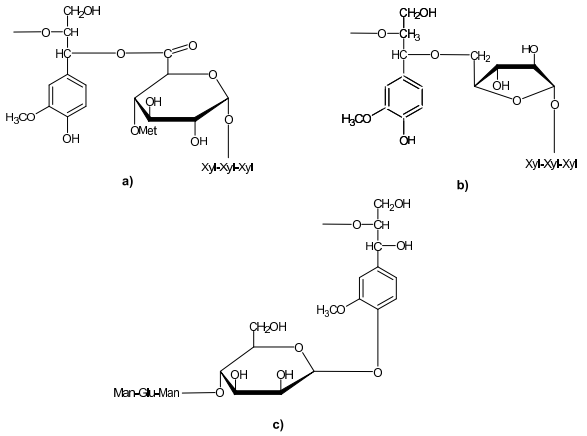

Figure 7: **Most common bonds between lignin and polysaccharides present in the plant cell wall [19].**

masses is made more difficult by non–covalent and covalent bonds present between lignin and polysaccharidic components [19].

Some of these are reported in Figure 7. They are mainly ester and ether bonds. In particular, ester bonds are frequent between hemicelluloses and hydroxycinnamates units [26].

1.5 Dyes

Synthetic dyes are extensively used in many technological fields, such as textile industry, paper production, food technology, hair colorings [40]. Moreover, they have also been employed for monitoring wastewater treatment, and as ground water tracers.

Many chemical classes of synthetic dyes are known and frequently employed on industrial scale. Typical examples are azodyes, anthraquinones, triphenylmethanes, phenothiazine etc (Figure 8). Regardless of their chemical structure, industrial dyes are usually featured by a high resistance to degradation (both

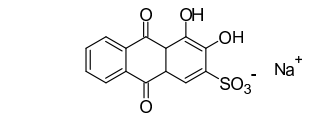

Anthraquinone dye
(Alizarin Red S)

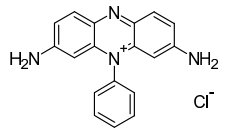

Safranin dye
(Phenosafranine)

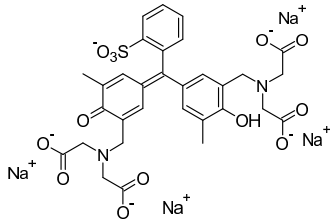

Acid triarylmethane
(Xylenol Orange)

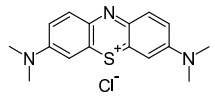

Phenothiazine dye
(Methylene Blue)

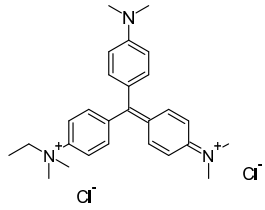

Basic triarylmethane
(Methyl Green)

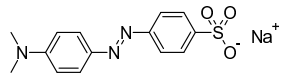

Azo dye
(Methyl Orange)

Figure 8: **Several type of dyes, belonging to different chemical classes, that can be bleached by the same means used for delignification.**

physical and chemical). Accordingly, they represent extremely recalcitrant pollutants.

Lignocellulose and textile dyes share many methods for their oxidative degradation. This usually leads to extend the application of lignin–degrading systems also to their degradation.

This can be usually done for two principal aims. First of all, visible-absorbing dyes can represent easier routine assays for delignifying systems, both chemical and enzymatic, as for instance demonstrated for Azure B and lignin peroxidase [41].

Moreover, industrial dyes represent a serious environmental concern due to their inertness, their high annual production (over 10,000 tons per year [40]) and low yields of textile processes (the percentage of the lost dye in the effluents can reach up to 50% [42]).

The impact of dye wastes can then be easily understood from both aesthetical and economical points of view, as classical approaches towards their removal are usually featured by high costs.

The European community has not been indifferent to such problem, as stated by European directive 2002/61/EC [43]. This directive forbids the use of some products, derivatives of a restricted number of azo dyes. However, these restriction measures are not enough to solve the problems due to the huge amount of dyes discharged in the environment every year.

Besides, their toxicity and carcinogenity have been clearly demonstrated [44, 45, 46, 47]. Accordingly, their removal from wastewater can be a challenging chemical issue. Especially in the perspective of the development of clean and environmentally friendly dyeing processes.

1.6 Classical approaches towards delignification

A wide range of methods have been developed to remove lignin from lignocellulose. They are based on physical treatment, chemical derivatization or oxidation.

Usually, on industrial scale, due to high costs and low yields, combinations

of treatments are employed. Among these, reductive agent like sodium borohydride ($NaBH_4$) are used to reduce the quinones formed during oxidative steps, increasing yield of following treatments [48].

However, especially in pulp and paper production the first step is represented by hemicelluloses removal. For this purpose, enzymatic treatment with xylanases is typically performed, in order to degrade polysaccharides different from cellulose that can affect the following steps [49, 50].

1.6.1 Physical methods

A classical approach in lignocelluloses pretreatment was mechanical comminution [4] through a combination of chipping, grinding and milling. However, by this way the main result is to reduce cellulose crystallinity. The size of the materials is usually 10–30 mm after chipping and 0.2-–2 mm after milling or grinding. But lignin structure is affected very poorly and energy consumption is high.

A significant improvement of mechanical approach is steam explosion [51]. In this method, chipped biomass is treated with high–pressure saturated steam and then the pressure is quickly reduced. This makes the materials undergo an explosive decompression. Steam explosion is typically initiated at a temperature of 160—260℃ (corresponding pressure 0.69—4.83 MPa) for several seconds to a few minutes before the material is exposed to atmospheric pressure.

The process causes hemicellulose degradation and lignin transformation due to high temperature, thus increasing the potential of cellulose hydrolysis. Ninety percent efficiency of enzymatic hydrolysis has been achieved in 24 h for poplar chips pretreated by steam explosion, compared to only 15% hydrolysis of untreated chips [52].

Steam explosion represented an important enhancement of traditional methods, especially in the perspective of the lower energy requirement (comparing to traditional mechanical treatments) and no recycling or environmental costs. Limitations include instead destruction of a portion of the xylan fraction, incomplete disruption of the lignin—carbohydrate matrix, and generation of compounds that may be inhibitory to microorganisms used in the downstream pro-

cesses [53].

Addition of H_2SO_4, or SO_2,, or CO_2, or NH_3 in steam explosion can improve lignin degradation, decrease the production of inhibitory compounds, and lead to more efficient process [54, 55, 56, 57].

In particular Zheng and coworkers showed in 1998 that CO_2 explosion was more cost–effective than ammonia explosion and did not cause the formation of inhibitory compounds that could occur in steam explosion [57].

Unfortunately, all these methods require high temperature and pressure, causing serious economical concerns for both processes and systems.

1.6.2 Chemical methods

Many chemicals can also be used in delignification: in particular, nowadays the chemical lignin removal in the pulp and paper industries is mainly achieved by the Kraft process [58].

The Kraft process is based on a strongly alkaline attack of the woody material, with a caustic liquor, containing concentrate sodium hydroxide and sodium sulfide (the "white liquor") under harsh temperature and pressure conditions [51, 59]. The mechanism of alkaline hydrolysis is believed to be saponification of intermolecular ester bonds crosslinking xylan hemicelluloses and lignin or other hemicellulose. Accordingly, separation of lignin and polysaccharides can occur [4].

The targets of the alkaline attack are also the α–aryl ether and β–aryl ether linkages (mainly α–O–4 and β–O–4), i.e. the linkages joining the C6C3 units together. Cleavage of an α–O–4 linkage is favored when the corresponding phenolic hydroxyl is free; in that case a quinomethide is formed concomitant with the expulsion of the α–OR^- anion as the leaving group. This reaction is responsible for lignin fragmentation but also to a certain extent for the breakage of the main lignin–hemicellulose linkages. In any case, the resulting quinomethide undergoes a nucleophilic attack (usually from hydroxide or water) restoring the aromatic character of the phenylpropanoid unit. When α–hydroxyls are free, the preferred linkage to cleave is the β–O–4, with the intermediate formation of a very reactive α–β–oxirane that quickly undergoes a nucleophilic attack by

water or hydroxide, and an α,β diol is formed.

Hydrosulfide is less basic but more nucleophilic than hydroxide so the presence of sulfide greatly enhances the efficiency of the pulping process; anyway the two anions show similar mechanisms in the attack and breakdown of lignin.

In conclusion, the degraded and solubilized lignin is richer in free phenolic hydroxyls (responsible for its solubility in alkali) and poorer in α–O–4 and β–O–4 linkages; it could be recovered from the spent liquor ("black liquor") by precipitation with acids and is known as Kraft lignin. Conversely, remaining, undissolved lignin in the pulp is poorer in phenolic hydroxyls and should be bleached to obtain white paper.

Caustic treatment of lignocellulosic materials can also cause swelling, and internal surface area is increased. The digestibility of NaOH–treated hardwood increased from 14% to 55% with the decrease of lignin content from 24—55% to 20%. Unfortunately, no effect of dilute NaOH treatment was observed for softwoods with lignin content greater than 26% [60].

Ammonia can substitute NaOH [61]. But described condition are quite extreme: high ammonia concentration (up to 20%) and temperature (170℃) in particular. However, delignification is quite efficient (over 60%).

Conversely, sulfite pulping is based on the nucleophilic properties of hydrogenosulfite ion HSO_3^- which is the prevailing ionic form of sulfite in a wide range of pH, from moderately acidic to about neutral. Hydrogenosulfite is well known as a sulfonating agent for certain organic electrophilic compounds (owing to a relatively high electron density on sulfur atom) and this feature can be well exploited to achieve lignin fragmentation and solubilization. Apart from the so–called labile sulfonate groups (readily hydrolyzable by alkalies) arising from addition reactions to carbonyl groups, the striking feature of the sulfite pulping is the introduction of C–linked sulfonate groups into the lignin backbone.

In particular, both α–O–4 and β–O–4 arylether linkages are broken with release of phenolic hydroxyl groups whereas a sulfonate group $–SO_3^-$ is attached to the α or respectively β carbon atom [62]. Generally speaking, sulfitolysis takes place at acidic pHs on nonphenolic substructures, and at neutral or even

slightly alkaline pHs on the phenolic ones [63]. Moreover, some further sulfonic acid have been characterized in soluble lignosulfonates [64]. The overall result of hydrogenosulfite attack is lignin fragmentation and solubilization of the arising fragments, bearing sulfonate moieties. The obtained lignosulfonates have a number of technical applications [65]. It is worth noting that a minor fraction of (poorly) sulfonated lignin is almost insoluble and remains in the obtained chemical pulp.

Delignification is usually incomplete, and for certain uses the remaining lignin is a problem since it adversely affects the physico–mechanical properties of the paper. Moreover, remaining lignin is brownish and it tends to become more and more colored with time due to oxidation reactions that also give acids off. Such acids, when not neutralized by calcium carbonate added to the paper paste, tend to promote cellulose hydrolysis thus lowering the paper strength.

Therefore, a pulp bleaching step usually follows the delignification, to obtain white pulps and to stop alteration of remaining lignin that cause the problems cited above.

The use of various chlorine–based chemicals (such as ClO_2 and chlorite salts) have been proposed under extreme operational conditions [66, 67]. In this case, the action is due to oxidative attack of chlorine–containing compounds.

Unfortunately their action proceeds with both oxidation and chlorination, and the arising chlorolignins are highly recalcitrant to (bio)degradation and quite toxic. Sodium chlorite and chlorine dioxide, although much more costly than chlorine, act mainly via oxidative reactions. However, a noticeable degree of chlorination is unavoidable.

Also hydrogen peroxide can effectively act as a delignificant agent [68] especially in alkaline environments.

The effectiveness of alkaline delignification or bleaching is due to the formation of important HO_2^- concentrations above pH 11, where this nucleophile can attack electrophilic positions in the oxidizable molecules. Even more important, H_2O_2 becomes unstable within the pH range 10–12, where H_2O_2 and HO_2^- concentrations are comparable. The decomposition reactions are as follows:

$$H_2O_2 + HO_2^- \rightleftharpoons OH\bullet + O_2^-\bullet + H_2O \quad (1)$$

$$OH\bullet + O_2^-\bullet \rightleftharpoons O_2 + OH^- \quad (2)$$

$$2O_2^-\bullet + H_2O \rightleftharpoons^1 O_2 + HO_2^- + OH^- \quad (3)$$

$$^1O_2 + O_2^-\bullet \rightleftharpoons O_2 + O_2^-\bullet \quad (4)$$

The occurrence of reaction 3 explains why at least a fraction of formed molecular oxygen is in its singlet, very reactive state. Undoubtedly, the transient superoxide and hydroxyl radicals arising from reaction 1 play a key role in oxidation reactions by alkaline hydrogen peroxide. According to this hypothesis, the maximum effect of hydrogen peroxide towards lignin reaches its maximum just at pH $\sim$ 11.5 (pK_a for H_2O_2 is 11.6).

Many studies have been performed about alkaline oxidative pulping by H_2O_2, leading to a growing interest not only towards lignin–retaining bleaching but also towards optimization of delignifying/bleaching treatments, alternative to conventional Kraft pulping [69, 70, 71]. In fact, even if hydrogen peroxide is decidedly more expensive than the white liquor of Kraft pulping is, the reaction conditions are much milder, and moreover the effluents could be faced and managed more easily. The reactivity and mechanistic changes observed in the system hydrogen peroxide/lignin in the presence of redox active transition metal ions must be emphasized: in that case, the following reaction take place [72]:

$$Me^{n+} + H_2O_2 \rightleftharpoons Me^{(n+1)+} + OH^- + OH\bullet \quad (5)$$

This is the Fenton reaction, showing hydroxyl generation and scavenging by a metal ion (Fe, Mn, Cu) engaged in a one-electron redox cycle.

In the presence of a phenoxide ion (this discussion is referred to sharply alkaline reaction conditions) further reactions can take place:

$$PhO^- + Me^{(n+1)+} \rightleftharpoons PhO\bullet + Me^{n+} \quad (6)$$

$$PhO^- + OH\bullet \rightleftharpoons PhO\bullet + OH^- \tag{7}$$

$$PhO\bullet + O_2^-\bullet \rightarrow \text{ oxidative degradation} \tag{8}$$

$$PhO^- + {}^1O_2 \rightarrow \text{ oxidative degradation} \tag{9}$$

However, the continuous ferrous salt supply (it does not act as catalyst) and the significant release of ferric ions in the environment restrict practical applications of such reagents.

Lignin oxidation can be also achieved using both molecular oxygen and ozone, that can be combined with various catalysts both chemical (TiO_2, ZnO) and physical (UV radiations) [73, 74, 75, 76, 77].

Ozonolysis has many advantages, since it effectively removes lignin, not producing toxic residues for the downstream processes. Moreover the reactions are carried out at room temperature and pressure [4, 78]. Vidal and coworker for instance showed a decrease for the percentage of lignin from 29% to 8% after ozonolysis pretreatment of poplar sawdust [78].

However, a large amount of ozone is required, making the process expensive. Furthermore ozone is very costly, unstable, toxic and explosive.

Besides these methods, also organic solvents (combined in case with inorganic acid catalysts such as HCl or H_2SO_4) can be used to break the internal lignin and hemicellulose bonds. The organic solvents used in the process include methanol, ethanol, acetone, ethylene glycol, triethylene glycol and tetrahydrofurfuryl alcohol [4].

However, the organic solvent use causes obvious environmental and economical issues, since operational conditions are not always mild. Moreover, solvent removal and recovery from the wastes is strictly necessary.

Furthermore, more recently new catalysts like molybdovanadophosphate polyanions, methyltrioxorhenium derivatives, polyoxometalates, and TAML were proposed, working under quite promising operational conditions [79, 80, 81, 82, 83].

1.6.3 Biological methods

Despite their large industrial applications, physico–chemical approaches towards delignification clearly suffer from economical and operational concerns, since they usually deal with extreme conditions and/or expensive reactants.

Accordingly, in order to achieve a greener alternative, lignin–degrading microorganisms have been deeply studied during the last decades [11, 13]. Particular interest arose around ligninolytic fungi, that due to a specific lignolytic enzymatic pattern are able to live on wood and in some cases to degrade it.

Only two classes of fungi are able to oxidize lignin: brown–rot and white–rot fungi, both belonging to *Basidiomycetes* [13].

Brown–rot fungi, however, degrade mainly cellulose and only marginally lignin. While many white–rot fungi are able to completely oxidize lignin, using it as principal carbon source, and not damaging cellulose. Accordingly, this class is the most promising from an industrial point of view.

Among white–rot fungi, the most investigated species have been *Pleurotus eryngii* and *Phanerochaete chrysosporium*. However, many other *Basidiomycetes* genera belong to this group, like *Trametes*, *Phlebia*, *Ceriporiopsis*, *Dichomitus*, *Ganoderma*, *Stereum* and *Bjerkandera*.

Biological delignification can be achieved using whole cells in bioconversion processes. These processes showed promising milder operational conditions, in comparison to physo–chemical methods. Fungal reactions, in fact, occur at low temperature and pressure, in absence of any organic solvent, and catalysts can be recovered for many reaction cycles in an environmentally sustainable process [84, 85, 86, 87].

1.6.4 Enzymatic methods

Otherwise, ligninolytic enzymes can be purified from producing–fungi and employed in biotransformations processes.

White–rot fungi synthesize two classes of lignin–degrading enzymes: laccases (LC, E.C. 1.10.3.2) and peroxidases (LP).

The former are cuproenzymes known since XIX century, containing in their active site four Cu^{2+}, while the latter are hemoproteins discovered only in 1980s. Lignolytic peroxidases can be further classified into three groups depending on their substrate specificity: lignin peroxidase (LiP, E.C. 1.11.1.14), manganese peroxidase (MnP, E.C. 1.11.1.13), and versatile peroxidase (VP, E.C. 1.11.1.16).

1.6.4.1 Laccase

Laccases (benzenediol:oxygen oxidoreductase, EC 1.10.3.2), belonging to blue multi–copper oxidases, are enzymes able to catalyze the oxidation of various low–molecular weight compounds, including: benzenediols, aminophenols, polyphenols, polyamines, and lignin–related molecules, while concomitantly reducing molecular oxygen to water [88].

Laccases are common enzymes in nature, and they are found widely in plants and fungi as well as in some bacteria and insects. The first laccase was reported in 1883 from *Rhus vernicifera*, the Japanese lacquer tree [89], from which the laccase designation derived. Laccases have subsequently been discovered in numerous other plants.

However, the majority of laccases characterized so far have been derived from fungi, especially from white–rot *Basidiomycetes* that are efficient lignin degraders. Only a few bacterial laccases have been described, like the laccases of the plant root-associated bacterium *Azospirillum lipoferum* [90]. In addition to plants, laccases have been found in some insects, where they have been suggested to be active in cuticle sclerotization [91].

Laccase contains four cupric ions Cu^{2+} with a different complexation by the residues of the active site. These ions are able to accept one electron each during four monoelectron oxidations of substrates. The cuprous ions are then

reoxidized to cupric, releasing the four electrons to molecular oxygen [92, 93, 94], according to global reaction 10.

$$O_2 + 4H^+ + 4e^- \rightarrow 2H_2O \tag{10}$$

Reducing substrates (phenolics or aromatic amines) are oxidized to various radicals, that can evolve in different ways depending on oxygen availability. During delignification for instance non–enzymatic reactions can occur releasing ROS (*Reactive Oxygen Species*, like hydroxyl radical OH•), or further decomposition to quinones is possibile. Then, fungal quinone reductases usually allow to form phenols again [95, 96, 97] in an only apparently futile cycle, that in fact leads to the continous formation of ROS, the real lignin–degrading species.

Many potential applications and production processes of laccases have been suggested [88, 98, 99]. However, this enzyme suffers from a limited substrate spectrum in comparison to lignolytic peroxidases. In particular, as shown in §1.4.1, lignin loses most of its phenolic nature during polymerization: and laccase are not able to oxidize aromatic non–phenolic compounds. Moreover, its oxidation action is limited to quinone step. As shown for model dye alizarin red S [10], this can be a serious concern during wastes detoxification, since only partial oxidation can take place.

Some improvements can be obtained coupling laccase catalysis with redox mediators [88]. In particular, TEMPO and OH–TEMPO are promising compounds towards this issue.

1.6.4.2 Lignolytic peroxidases

The first two lignolytic peroxidases (LP) were discovered in 1980s in a lignolytic *Basidiomycete* (*Phanerochaete chrysosporium*): lignin peroxidase (LiP) and manganese peroxidase (MnP) [100, 101]. More recently, a third LP has been identified: versatile peroxidase (VP) [102]

White–rot fungi synthesize different LPs patterns among various genera. For instance *Phanerochaete crysosporium* only synthetizes LiP and MnP, while *Pleurotus spp.* produce LC and some MnP or VP isozymes only under particular

growth conditions.

All LPs are featured by unusual high redox potential, and significant sequence and structure homology [103].

These enzymes, included in Peroxidase Class II, share general tertiary folding and helical topography with peroxidases in Class I, such as Cytochrome C Peroxidase (CCP, EC 1.11.1.5) [104]. Accordingly, their substrate specificity seems to be modulated by changes near the protein surface, without substantial modification of polypeptide core [105].

LPs are secretory globular proteins (PM $\sim$ 40000 a.m.u.), containing about 340 residues clustered in 11–12 predominantly–α–helices. Two main domains are formed (proximal and distal), delimiting a central cavity harboring the prosthetic group (an iron(III)–coordinating protoporphyrin IX, Figure 9).

Fe^{3+} coordination is completed by proximal His and a water molecule linked by a weak bond. LPs present two Ca^{2+} binding sites and 8 cysteine residues forming 4 disulfide bridges (with exception of MnP having 5 bridges), stabilizing protein structure [103, 106].

VPs, the latter to be identified, have not been structurally characterized. Molecular models are only available [103].

LPs show close similarity also about catalytic cycle, being similar to other peroxidases [107, 108, 109] as reported in Figure 10 and Figure 11.

Hydrogen peroxide is their natural electron acceptor, acting as two–electron oxidizing substrate for LP native form (path **(a)** Figures 10 and 11). In particular, one electron derives from Fe(III), which is oxidized to Fe(IV) forming an oxoferryl specie with oxygen atom deriving from H_2O_2. Second electron is taken from porphyrin delocalized electronic system, forming a cationic π porphyrinic radical. This completely oxidized form of LP is known as Compound I.

This intermediate contains two oxidizing equivalents. Accordingly, particular reducing substrates can release one electron in two consecutive mono–electronic reducing steps, forming firstly Compound II and then native LP (path **(b)** and **(c)** of Figures 10 and 11).

LiP, MnP and VP differ on reducing substrates specificity. For instance

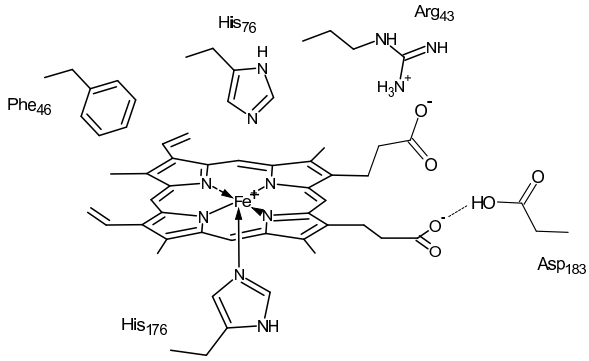

Figure 9: **LiP active site structure shows most important interactions between heme and apoprotein residues, In particular proximal and distal His, and H–bond between heme propionate and Asp_{183} are evidenced [106].**

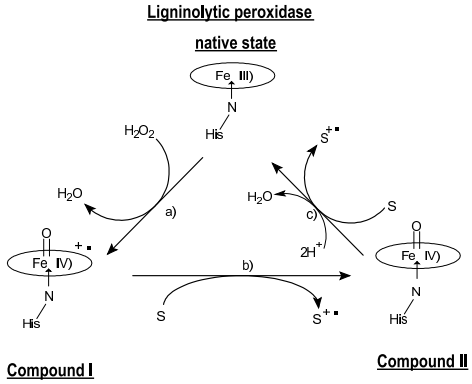

Figure 10: **Lignin peroxidase catalytic cycle is similar to that of other peroxidases.**

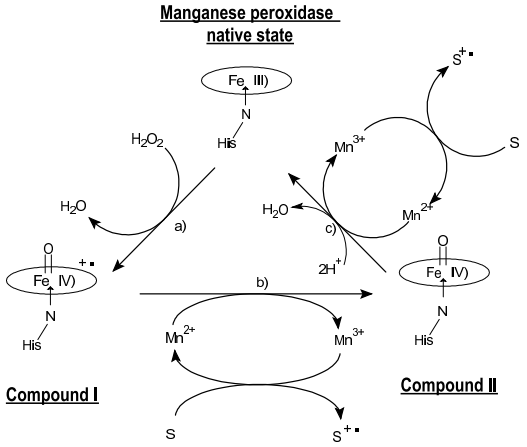

Figure 11: **Manganese peroxidase catalytic cycle differs from LiP's one for reducing substrates specificity.**

LiP is able to oxidize phenolics, but its best substrates are non–phenolic aromatic compounds [93, 103, 109, 110]. These compounds release one electron to Compounds I or II forming phenoxy radical or cationic aromatic radicals, that can evolve variously, leading to lignin oxidative depolymerization through C_α–C_β, C_α–H or C–O bonds breaking. As an alternative, carbonyl groups can be formed entering in cycle similar to LC (already described in §1.6.4.1) with ROS production.

However, lignin is a sterically hindering compound, usually not able to enter into the LiP active site (especially in the early stages of depolymerization). Then, the need of a redox mediator of the reaction is clear.

Several substrates have been proven able to act in this way, such as tryptophan [111], and many methoxy–substituted aromatic compounds [110, 112]. However, one in particular, veratryl alcohol (3,4–dimethoxybenzyl alcohol, VA) has been identified as natural LiP substrate.

Although no LiP crystal structure has been obtained showing VA binding

site, indirect techniques like site–directed mutagenesis suggested at least two binding sites for VA [113].

However, two more schemes of action have been proposed for VA. LiP could be protected from H_2O_2–mediated inactivation by VA. In fact, oxidant excess leads to Compound III formation, since iron has valence III binding O_2^-. Compound III can evolve in catalytically inactive forms. Only VA (and not other aromatic or phenolic compounds) is able to regenerate LiP native (and catalytically active) state [113, 114, 115].

VA has been also suggested to allow catalytic cycle completion [116]. Many substrates can quickly reduce Compound I to Compound II. However limiting stage of the reaction is the second reduction to LiP native state. Only VA has been suggested able to perform this reaction, since in its absence formation of high amounts of Compound II has been observed.

Since no definitive evidence has been showed for real VA role, all three schemes of action have been suggested to coexist [112].

MnP catalytic cycle is definitely less complicated, as only Mn^{2+} ion can act as reducing substrate [109, 117], yielding Mn^{3+}. This acts as redox mediator in Compound I and II reduction. Mn^{3+} is a very unstable chemical species, which is however stabilized in extracellular environment by organic acids (like oxalic [112]) complexation, allowing its diffusion towards real substrates that can release one electron, reducing it to Mn^{2+}.

Such substrates can be phenolics and non–phenolic aromatic compounds, that evolve in a similar way described for LiP. MnP is furthermore able to oxidize, through active specie Mn^{3+}, aromatic amines, carboxylic acids, thiols and unsaturated fatty acids [109], whose arising radicals can degrade lignin.

VP has been the last LP to be identified [102]. Mn–oxidizing peroxidases with Mn–independent activity have been firstly described in *Pleurotus spp.* and *Bjerkandera spp.*. VPs are in fact able to oxidize directly both Mn^{2+} (like MnP), and other aromatic substrates (such as lignin mimicking compounds, like VA). But VPs are also able to oxidize hydroquinones and substituted phenolics (very

weak LiP and MnP substrates).

1.6.5 Drawbacks of biological and enzymatic approaches

In the last decades, LC and LPs have been proposed for many industrial applications related to delignification, pollutants removal from wastewaters, pulp and paper production etc. Both using purified enzymes, and whole white–rot fungi cells [118, 119, 120, 121].

Up to now, however, industrial applications of these enzymes are prevented by some factors: high cost of enzymes and mediators; extreme fragility of LPs; easy enzyme inactivation by excess of H_2O_2; no effective protocols for the heterologous expression of these enzymes.

Redox mediators, in fact, must be almost continuously supplied in reaction media, as they are highly reactive species unavoidably undergoing irreversible degradation.

Moreover, many other proteins seem to be involved in delignification process. It has been demonstrated that *in vivo* lignin oxidation requires the synergistic action of other enzymes such as cellobiose:quinone oxidoreductase, glucose oxidase, aryl alcohol oxidase, glyoxalate oxidase [96, 122] as already described in §1.6.4.2: only in this way ROS are produced (through a quinone redox cycle) and the reaction becomes effective. In this perspective, it is not surprising that purified peroxidases or laccases singly do not delignify intact lignocellulose *in vitro* [123, 124].

The only feasible way could be the use of whole fungal cells in delignification process, which could constantly supply redox mediators and all the other indispensable enzyme activities.

But also this approach suffers by some drawbacks, due to very slow fungal metabolism and large biomass contamination (by the fungal hyphae) of reaction products (and related expensive separation). On the other hand, the mechanical properties of the obtained pulps are sometimes very good (even if an undesired yellowing of the product is often observed).

1.7 Metalloporphines: a "bioinspired" alternative

In order to overcome these drawbacks, new generations of biomimetic catalysts have been developed, with the common aim of emulating LPs activity, under mild and cost–effective operational conditions.

Several biomimetic methods have been proposed involving metalloporphines, molybdovanadophosphate, metallophthalocyanines, polyoxometalates and iron(III) tetraamido macrocycles [79, 80, 81]. Among them, only metalloporphines strictly resemble LPs cofactor (compare Figure 9) and seem to be suitable for real emulation of their active sites.

Metal complexes of porphines and porphyrins (mainly Mn and Fe) have been shown to be able to catalyze many oxidation and oxygenation reactions with several monoxygen donors (iodosylbenzene, NaClO, H_2O_2, peroxyacids etc). These studies have been mainly addressed to the emulation of cytochrome P450 in hydrocarbons oxygenation, but also in oxidation of amines, *N*–demethylation of secondary aromatic amines or oxidative chlorinations [125, 126, 127], while LPs emulation has been quite less investigated [128].

For these purposes, the use of natural metalloporphyrins has been prevented by their insolubility in common solvents and low stability in oxidizing environment: luckily, a broad range of synthetic analogues (mainly unsubstituted in the β positions, therefore being more correctly called metalloporphines) are available since some decades (Figure 12).

The synthesis of the ancestor of this family of molecules was firstly described in 1935, when Rothemund boiled benzaldehyde and pyrrole in refluxing propionic acid to easily afford 5,10,15,20-tetraphenylporphine (TPP). Only more recently catalytic activity of the complexes Fe–TPP and Mn–TPP have been studied, but they were very unstable catalysts being degraded by their own substrates (iodosylbenzene and NaOCl) [125]. However, the way was open and these complexes deserved the label "first generation catalysts".

In a short time, it became clear that increasing electron–withdrawing power of meso–substituents would lead to higher stability and activity of the catalyst. This could be achieved through the presence of halogen atoms as substituents in the meso phenyl groups. Those were the so-called "second generation cat-

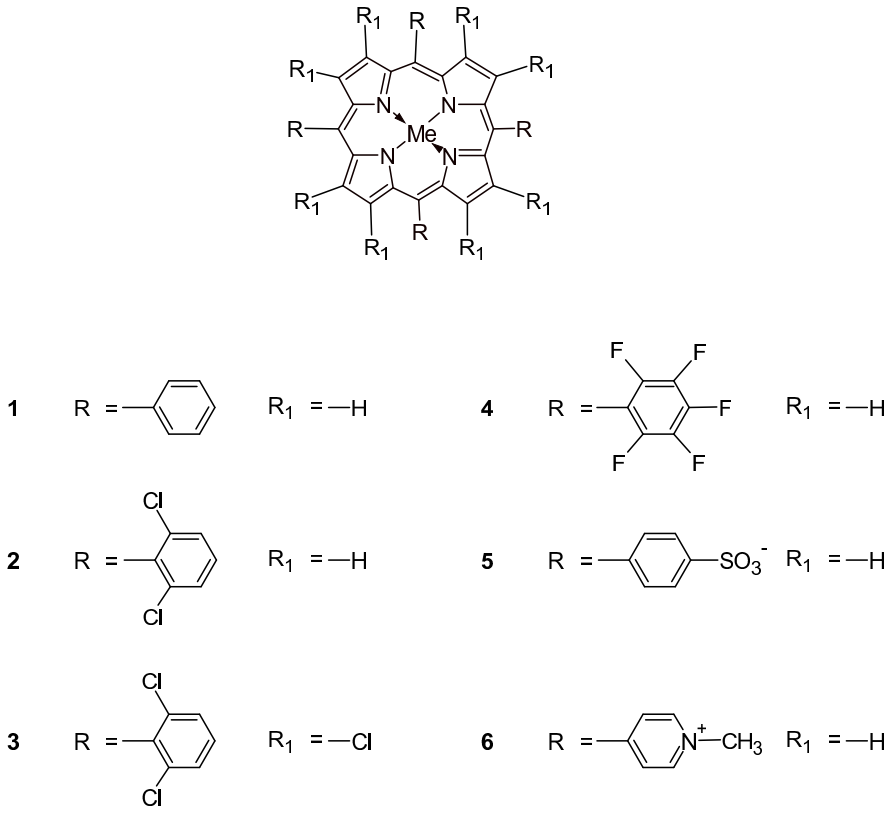

Figure 12: **Chemical structures of the most studied metalloporphines. 1: 5,10,15,20–tetrakisphenylporphine (TPP). 2: 5,10,15,20–tetrakis(2,6–dichlorophenyl)porphine (TDCPP). 3: β–octachloro–5,10,15,20–tetrakis(2,6–dichlorophenyl)porphine (β–Cl_8–TDCPP). 4: 5,10,15,20–tetrakis(pentafluorophenyl)porphine (TFPP). 5: 5,10,15,20–tetrakis(4–sulfonatophenyl)porphine (TSPP). 6: 5,10,15,20-tetrakis(*N*–methyl–4–pyridyl)porphine (TMPP).**

alysts". In particular the insertion of two chlorine atoms in the 2,6 position of phenyls (TDCPP) had positive effects: Fe and Mn–TDCPP were capable of high conversion of the substrates without significant loss of activity, and this led to a dramatic improvement of performances.

Also β–octa–halogenated porphines (like β–Cl_8–TDCPP) were synthesized: however, catalytic studies were quite conflicting and not very promising.

More efficient seemed to be perhalogenated porphines in the phenyl positions: in particular metal complexes of 5,10,15,20-tetrakis(pentafluorophenyl)porphine (TFPP) and their derivatives exhibit excellent catalytic and stability properties [129].

Metal complexes of TFPP are, though, not water–soluble: that could be overcome by sulfonating TFPP β–positions, or by completely changing meso electron–withdrawing pendants. Both use of 4–sulfonatophenyl (TSPP) and N–methyl–4–pyridinio (TMPP) substituents allowed the synthesis of stable, efficient and less expensive catalysts.

Metal complexes of TFPP, TSPP and TMPP could be easily synthesized at laboratory scale, but they are also commercially available and represent a promising base for development of pre–industrial delignification processes.

1.7.1 Metalloporphines emulate LPs reactions

First investigations about biomimetic degradation of lignin and lignin model compounds were performed with natural heme using t–buthylhydroperoxide (tBuOOH) as the oxidant [130]. Catalyst insolubility and instability under oxidizing conditions suggested however employment of next generation porphines.

Fe–β–sulfonated-TDCPP, and both Fe– and Mn–TSPP showed better stability during aqueous oxidation of VA and other lignin model compounds [131, 132], with a product selectivity very similar to LiP.

In those experiments $KHSO_5$, tBuOOH or mCPBA were employed as the oxidants: however, the perfect oxidant from an industrial point of view should be inexpensive, totally miscible with H_2O (no organic solvent should be needed in a "green" process), and its degradation products should not be harmful. From this

perspective, the best "clean" oxidant can only be H_2O_2, as its decomposition produces only O_2 and H_2O.

H_2O_2 has been proposed as oxidant by Artaud and coworkers in 1993 [133]: several Fe metalloporphines (such as TDCPP, TFPP and β–sulfonated–TFPP) were investigated though in a partially organic reaction mixture. Those catalysts led to significant yields with many lignin model compounds.

The oxidation of real lignins has been showed few years later. Kurek and coworkers [134] noticed effective oxidative degradation of spruce lignin in presence of Fe–β–sulfonated–TFPP and H_2O_2. The reaction was managed at very mild temperature (22°C) but in the presence of high concentrations of organic solvent (a mixture 9:1 dioxane:H_2O was used as reaction medium).

Crestini and coworkers in 1999 [135] were able to completely eliminate organic solvent during their screening of some hydrosoluble metalloporphines (the most interesting being Mn–TSPP and Mn–TMPP). Residual kraft lignin was oxidized in presence of H_2O_2 at a slightly higher temperature (50°C) but under very mild pH conditions (pH 6 in citrate buffer).

1.7.2 Immobilization of metalloporphines

Those studies were very promising, but did not allow an immediate application of metalloporphines in delignification processes.

From an economical point of view, catalyst recovery after reaction is essential, in order to completely exploit its activity. Besides, complete toxicological studies of porphines have not yet been completed: so they cannot be released in the environment, but must be (possibly easily) removed from any waste.

Moreover, when metalloporphines work free in solution, they are less stable as side reactions can occur, such as μ–oxo dimers (catalytically inactive) formation or homolytic cleavage of O–O bond to yield Fe(IV)–OH and OH• [136].

In this perspective, immobilization of the catalysts on a solid support should be considered as a mandatory aim.

Many approaches have been developed to immobilize metalloporphines: adsorption, ion–exchange and covalent bond formation in particular. In all cases

catalysts seem to retain much of their activity as LP emulators. Just few studies, however, are reported about LPs–like activity of those immobilized metalloporphines.

Labat and Meunier [131] emulated LiP activity by immobilizing Mn– and Fe–TSPP on ion–exchange resin Amberlite IRA 900: catalyst stability was noticeably enhanced, and repeated use gave excellent results.

More recently Crestini and coworkers [137] used supported Mn–TMPP on a smectite clay to achieve oxidation of lignin and lignin model compounds. Operational conditions were extremely mild and only temperature was quite high (ranging 60–90℃), but no organic solvent was necessary saving dioxane to solubilize reagents. Also in this case porphine stability seemed to be improved: repeated use of the catalyst for the oxidation of model compounds was efficient, leading to quite high conversion rate.

Not even in those cases, however, real LPs emulation was achieved.

In these enzymes, fifth coordination position of heme iron is occupied by imidazole–*N* of proximal histidine (Figure 9): in this perspective closer emulation of their active site requires the presence of an appropriate axial ligand, perhaps imidazole.

Moreover, fundamental effects of axial ligand for porphine catalytic efficiency have been exhaustively demonstrated [125]. Using free bulk ligands, stabilization of high valence metal oxo species has been observed: this can be a problem though, when ligand/porphine interaction is too strong. It can lead to bis–ligated form which can interfere with oxygen donor/metal proper interaction, which is certainly more favored with mono–ligated species. Moreover, if stabilization of high valence metal species is too strong, reduction of oxidized metalloporphine species could be slower. Besides, electron–deficient ligands are also able to increase redox potential of oxidized metalloporphines species, speeding up catalytic cycle completion.

Good ligands have also proven able to affect porphines chemio– and enantioselectivity and to facilitate heterolytic cleavage of O–O bond. This prevents formation of OH•, the main responsible of undesired cellulose damage during

delignification processes.

Several possible ligands have been proposed: pyridine and alkyl substituted derivatives, *N*–amine oxides, and the more bioinspired imidazole.

Among them only the latter allows a real emulation of LPs active site (Figure 9). Moreover, its positive catalytic effects have been clearly demonstrated [138].

However, all those studies have been performed using free ligands.

The need of a good axial ligand for metalloporphine can be, however, combined with that of a suitable immobilization of the catalyst. This can be achieved properly by grafting imidazole (or other coordinating group) residues on solid supports, and immobilizing metalloporphines on these through a coordinative bond.

Such generation of catalysts can be referred as real LPs emulators.

This approach avoids the continuous supply of ligands in a hypothetical multicyclic use of the catalyst: it means an economical saving of the process. Besides, if the support grafting is properly operated, only mono–ligated metalloporphines can be obtained.

Metalloporphine immobilization on an imidazole-grafted support has been already described [139].

In that study 3–imidazolyl–propyl–trimethoxysilane was used to functionalize silica gel surface, on which Fe–TMPP was then supported. The adduct was not characterized about its LP–like activity: however, it showed a poor performance in hydroxylation and epoxidation of hydrocarbons.

This can be partially explained with the very short and hydrophobic spacer between metalloporphine and support. In order to completely emulate enzyme activity, a longer, hydrophilic and flexible spacer should be considered.

1.8 Aim of this study

Emulation of LPs is a challenging task with many promising industrial applications.

This should be based on robust and catalytically efficient metalloporphines

properly immobilized on solid supports providing axial ligands, in order to achieve both structural and functional emulation. This is economically and environmentally crucial as it implies mild operational conditions, strictly resembling natural delignification pathway. In other words, a really green process.

According to these consideration, the first purpose of this study is the development of properly immobilized metalloporphines.

In this perspective, several supports have to be grafted with enough long spacers ending with coordinating chemical groups like the more bioinspired imidazole, but also mercapto (Fe(III)–heme coordinating group in Cytochrome P450 [126]) and pyridine. This is, in fact, a quite more electron–withdrawing group compared to imidazole: this could lead to higher redox potential of coordinated metalloporphine. Some investigations have already been attempted [140], but pyridine seems to be weaker than imidazole as a metalloporphine ligand.

Then, screening of possible metalloporphines/supports combinations is necessary. In order to achieve an economically affordable process, the most common commercially–available metalloporphines are studied: Mn–TSPP, Fe–TFPP and Mn–TMPP.

The catalysts are investigated according to their ability to emulate LPs activity with common lignin–emulating compounds (particularly VA) in the presence of H_2O_2. During this step the main purpose is to obtain extremely mild operational conditions (in terms of pH, temperature, low $[H_2O_2]$, no organic solvents), without any metalloporphine leakage, in order to achieve a real green process. Moreover, catalytic mechanisms are investigated elucidating the similarities between biomimetic and LPs catalysis, and their dependence on coordinating groups.

Moreover, the range of studied substrates is broadened including industrial dyes, since also textile wastewaters represent a serious environmental issue, still needing easy, inexpensive and feasible processes of treatment, as described in §1.5.

In all these contexts, heterogeneous catalysts like immobilized metallopor-

phines should face the necessity of redox mediation, in order to overcome mass transfer issues. Crestini and coworkers [137] already found 1–hydroxybenzotriazole as an efficient mediator in immobilized metalloporphines oxidation of lignin. But, in order to maintain the process as "green" as possible, also redox mediator should be harmless and sustainable: in this perspective, the immediate aim can be not strictly LiP, but rather MnP emulation. As only Mn^{2+} could represent the cleanest redox mediator.

Therefore, redox mediators screening is necessary, with particular attention to MnP emulation.

2 EXPERIMENTAL

2.1 Materials

All the reagents used were of the best grade available, and were used without further purification. In particular, ARS came from Fluka (cat. No. 05600), AzB from Fluka (cat. No. 11660), FeTFPP from Aldrich (cat. No. 252913), glutaraldehyde from Fluka (cat. No. 49629, it was as a 50% aqueous solution, mainly containing oligomers in addition to the monomeric aldehyde), HRP from Sigma–Aldrich (cat. No.P–6782), LiP from Sigma–Aldrich (cat. No. 42603), MB from Fluka (cat. No. 66720), MG from Aldrich (cat. No. 198080), MO from Sigma–Aldrich (cat. No. 234109), MnTMPP from Aldrich (cat. No. 453161), MnTSPP from Sigma–Aldrich (cat. No. 441813), PNS from Fluka (cat. No. 199648), PVA from Aldrich (cat. No. 363138, fully hydrolyzed, Av. MW 30,000–50,000), SG 100 from Fluka (cat. No. 60746), XO from Fluka (cat. No. 9615).

Fungal LC was purified from *Pleurotus sajor–caju* liquid cultures as described elsewhere [141].

2.2 Methods

2.2.1 APS synthesis

Aminopropylsilica (APS) was prepared by reacting 10 mmol of (3–aminopropyl)triethoxysilane in 20 mL of dioxane and 10 g of Silica Gel 100 (SG).

The slurry was kept at 80℃ overnight. The activated silica, was consecutively washed with 0.5 M HCl, with H_2O, with 0.1 M NaOH and again with H_2O. The wet silica was then carefully dried overnight in a vacuum oven at 50℃.

2.2.2 IPS synthesis

Firstly, 3–(1–imidazolyl)propylcarbamoyl–3'–aminopropyl–triethoxysilane was synthesized by reacting 2.6 g (10 mmol) of (3–isocyanatopropyl)triethoxysilane and 1.4 g (11 mmol) of *N*–(3–aminopropyl)imidazole in 20 mL dioxane.

The mixture was allowed to react overnight at 25℃, and to this newly synthesized silane 10 g of SG 100 were added. The slurry was kept at 80℃ overnight. The activated silica, 3–(1–imidazolyl)propylcarbamoyl–3'–aminopropylsilica (IPS), was consecutively washed with 0.5 M HCl, with H_2O, with 0.1 M NaOH and again with H_2O. The wet silica was then carefully dried overnight in a vacuum oven at 50℃.

2.2.3 PSG synthesis

PSG was prepared as described above for IPS §2.2.2, using 4–picolylamine (4–(aminomethyl)pyridine) instead of *N*–(3–aminopropyl)imidazole.

2.2.4 MSG synthesis

Each gram of APS was suspended in 10 mL $NaHCO_3$ 0.1 M containing 0.5 g *N*–acetyl–DL–homocysteine thiolactone. The slurry was then kept for 24 h under gentle stirring at 25℃.

MSG was then consecutively washed with H_2O, KH_2PO_4 0.1 M, H_2O again, sodium dithionite 0.1 M, H_2O again and 2–propanol.

The mercapto–grafted silica was then carefully dried overnight in a vacuum oven at 50℃ and immediately porphinated in order avoid possible oxidation of –SH group.

2.2.5 AP–PVA synthesis

For aminopropyl crosslinked PVA (AP-PVA) synthesis, 500 mL of a 10% *w/v* PVA aqueous solution were treated with 5 mL 4–aminobutyraldehyde diethyl acetal, and pH was adjusted to 2 with 6 M HCl.

Then 10 mL of a 50% *v/v* glutaraldehyde aqueous solution were added under stirring and the pH adjusted to 0 with 6 M HCl. The obtained gel was kept at 90℃ for 1 h into a water bath, and finally overnight at 25℃. The product was broken into coarse lumps with a spatula, soaked with water to remove most HCl, ground for 10' at 16,000 rpm with Ultra Turrax T25 Basic (*IKA Technik*, Milan, Italy), and exhaustively washed with water, 0.1 M NaOH, water again, 2–propanol, and finally carefully dried into a warm oven.

In control experiments, no functionalized crosslinked PVA was obtained omitting 4–aminobutyraldehyde diethyl acetal.

2.2.6 Im–PVA synthesis

Each gram of the AP–PVA powder was suspended in an excess water to form a fluid slurry and treated with 0.1 mL of imidazole–4(5)–carboxaldehyde. The pH was adjusted to 5 with 0.1 M sodium acetate buffer, and reduction of the Schiff base between the aldehyde and amino groups of the support was accomplished by adding 0.5 g sodium cyanoborohydride, under gentle stirring.

After 24 h the support was exhaustively washed with 0.1 M aqueous glycerol, water, 0.1 M NaOH, water again, and 2–propanol. The wet Im–PVA was then carefully dried overnight in a vacuum oven at 50℃. The product was stored in a well–closed bottle at room temperature until use.

To determine the amount of aminopropyl moieties and the extent of their further derivatization with imidazole functions, an already described photometric procedure [142] was used involving the chromogenic reaction with ninhydrin and hydrindantin.

2.2.7 PP-PVA synthesis

PP–PVA was synthesized as described above for Im–PVA (§2.2.6), using 4–pyridinecarboxaldehyde instead of imidazole–4(5)–carboxaldehyde.

2.2.8 M–PVA synthesis

AP–PVA was treated with *N*–acetyl–DL–homocysteine thiolactone, as already described for APS in §2.2.4, leading to thiyl–grafted PVA–based support.

2.2.9 Porphination of supports

Samples of one gram of supports were treated with different amounts of metalloporphines, ranging from 2 to 120 mg (usually 20 mg where not differently specified), solubilized in 10 mL of proper solvent, then the reaction mixtures were kept at 25℃ in the dark (because of metalloporphines photosensitivity) under stirring overnight.

For MnTSPP and FeTMPP solvent, aqueous 50 mM $NaHCO_3$ was chosen, in order to prevent imidazole–*N*, pyridine–*N* and amino–group protonation. During porphination of thiyl–grafted support, water was used. For FeTFPP, dimethylsulfoxide (DMSO) was preferred.

After this, excess of metalloporphine was washed away with aqueous 1 M NaCl and finally with H_2O. For FeTFPP treated support, DSMO and 2–propanol washes were used insted.

Unbound metalloporphines were then quantified through spectrophotometric measurement at specific λ_{max} for each porphine (468 nm for MnTSPP, 460 nm for MnTMPP, and 411 nm for FeTFPP), by using a calibration curve. Thus, the amounts of bound metalloporphine were determined by difference between the two measurements.

The adducts were finally dried at 50℃ in a vacuum oven overnight, and stored in the dark until use.

2.2.10 Spettrophotometric analysis

UV–vis measurements were performed on an UltroSpec 2100 pro spectrophotometer (*Amersham Bioscience*, Uppsala, Sweden). While reflectance spectra were carried out at 25℃ using a Cary 5 UV-Vis-NIR spectrophotometer (*Varian*, Palo Alto, CA, USA).

FT–IR spectra (resolution 4 cm^{-1}) were recorded after the samples were obtained as KBr pellets, with a KBr beam–splitter and KBr windows on a Nicolet 5700 spectrometer (*Thermo Electron Corporation*, Madison, USA) at 25℃.

2.2.11 Surface area determination

Nitrogen physisorption measurements were carried out at –196℃ on an Autosorb-1 volumetric analyzer (*Quantachrome*, Boynton Beach FL, USA) apparatus. The samples (100 mg) were degassed at 70℃ under vacuum for 4 h before of the measurement. The isotherms were used to quantify the textural properties of the samples. The specific surface areas (S_{BET}) of the samples were calculated using the BET method.

The total pore volume V_p was evaluated on the basis of the amount adsorbed at a relative pressure of about 0.98, by converting the amount of nitrogen gas adsorbed at STP to the liquid volume at –196℃ (using the conversion factor $c = 0.001547$). The pore size distributions were obtained from the desorption branch of the isotherm using the corrected form of the Kelvin equation by means of the Barrett–Joyner–Halenda method with a cylindrical pore model. The external surface area (S_{ext}) and the micropore volume ($V_{\mu p}$) were assessed by the *t*–plot method, using the Harkins–Jura equation to estimate the thickness of a monolayer of nitrogen adsorbed at –196℃, $t = [13.99/(0.034\text{-log } p/p^0]^{1/2}$.

2.2.12 Catalytic activity determination

2.2.12.1 LP–like assays

A mixture containing 20 mg of catalyst suspended in 2 mL of 25 mM buffer solution containing 1 mM VA and 8.8 mM hydrogen peroxide, was kept stirring at 25℃ in the dark. Increase in absorbance at 310 nm was measured after 30 min incubation, to detect the formed veratraldehyde (ϵ_{310} = 9,300 M^{-1} cm^{-1} [143]). Both catalysts and substrates amounts have been changed in specified experiments; this was usually done to operate under saturating conditions (according to measured K_M values). For each sample, blank samples without catalyst and substrates were prepared. UV–Vis spectra in the range 230–700 nm were also recorded.

Some McIlvaine buffers at different pH were used: pH 3, pH 4, pH 5, pH 6, pH 7, and pH 8.

To evaluate catalysts multi–cyclic use, assays were repeated several times. Between cycles, catalysts were regenerated through exhaustive washings with H_2O, 2–propanol, and subsequent drying.

Michaelis and Menten kinetic parameters were calculated by using R 2.5.1 software (*R Foundation for Statistical Computing*, Vienna).

Alternatively, the dye Azure B (AzB) was used as the substrate, since it has been suggested as an easy–to–use chromophoric LiP substrate [41]. To a mixture containing 25 mM buffer, 0.88 mM hydrogen peroxide, and 0.01 mM Azure B, in a final volume of 2 mL, 20 mg of catalyst were added. After 30 min of stirring in the dark, decrease in absorbance at 651 nm was detected (ϵ_{651} = 48,800 $M^{-1}cm^{-1}$ [41]).

For certain experiments, the well–known hydroxyl radical scavenger 0.1 M mannitol was also added. In other experiments, 0.1 M 2–deoxyribose was present in the reaction mixtures, that were subsequently analyzed by means of a described method [144] for thiobarbituric acid reactive substances (TBARS) determination.

In order to evaluate hydroxyl radical formation and its effect on catalytic activity, control experiments were performed using, respectively, 100 mM mannitol

and 20 mM APH, at the same conditions as above.

Some other compounds were also tested as substrates: 4–methoxybenzyl alcohol, 4–hydroxy–3–methoxybenzyl alcohol (vanillyl alcohol), 3–hydroxy–4–methoxybenzyl alcohol (isovanillyl alcohol), 3,4,5–trimethoxybenzyl alcohol, 3,4–dimethoxybenzaldehyde (veratraldehyde), 3,4–dimethoxybenzoic acid (veratric acid), 1,2–dimethoxybenzene (veratrole), 1,2,3–trimethoxybenzene, 4–hydroxy–3–methoxycinnamic acid (ferulic acid).

They were always present at the final concentration of 1 mM in the presence of 1,2–dimethoxyethane 10% (to allow their solubilization).

Determination of some non–commercial putative products of VA degradation (4,5–dimethoxy–1,2–benzoquinone, 2–hydroxymethyl–5–methoxy–1,4–benzoquinone, methoxy–1,4–benzoquinone) was performed by separating the individual peaks and comparing retention times and UV/Vis absorption spectra to those of authentic samples synthesized on purpose starting from commmercially available molecules [145, 146, 147].

For MnP–like assay, all the experiments as above were repeated in the presence of 1 mM $MnSO_4$ and 50 mM malonic acid.

2.2.12.2 Dye decoloration assays

During dye decoloration experiments, six dyes belonging to different chemical classes were used (Figure 8 at page 26): alizarin red S (ARS), phenosafranine (PNS), xylenol orange (XO), methylene blue (MB), methyl green (MG), and methyl orange (MO).

Dyes decoloration was quantified at 25℃ by spectrophotometric assay: 20 mg of catalyst were added, in a final volume of 2 mL, to 25 mM buffer, 8.8 mM H_2O_2 and the dye concentration reported in Table 2. Blanks were prepared without hydrogen peroxide and substrates. The mixtures were kept stirring in the dark at 25℃ for 30', and the absorbance decrease at the λ_{max} reported in Table 2 was recorded. When reaction pH was different from 7, before absorbance measurement the pH was corrected to 7 with 0.1 mL of potassium phosphate buffer 1 M (pH 7). UV–Vis spectra in the range 230–700 nm were also recorded.

Dye	**MW** (amu)	λ_{max} (nm)	ϵ ($M^{-1}cm^{-1}$)	**Final concentration used (mM)**
ARS	342.26	520	7,200	0.29
PNS	322.80	525	32,000	0.31
XO	782.56	435	10,500	2.00
MB	319.86	660	79,500	0.15
MG	472.51	632	55,700	1.50
MO	372.34	464	24,800	1.25

Table 2: **Dyes analyzed during this study.**

Some additional experiments were performed in the presence of some well–known redox–mediator: 4–hydroxy-2,2,6,6–tetramethylpiperidine–1–oxyl (OH–TEMPO), *N*–hydroxyphthalimide (NPH), *N*–hydroxysuccinimide (NHS), and *N*–hydroxybenzotriazole (NHT).

When used, they were present in the reaction medium, under the same conditions as above, at the final concentration of 1 mM.

2.2.13 HPLC analysis

Samples for HPLC analysis were centrifuged at 10,000 g for 10', and the resulting supernatants immediately injected.

Identification of the compounds was carried out with a System Gold apparatus (*Beckman*, Cassina de' Pecchi, Italy) equipped with a UV–Vis detector module. The column used for chromatographic separations was an ODS–Hypersil, 250x4 mm i.d., 3.5 mm particle size (*Hewlett–Packard*, Milan, Italy).

Separations of the compounds were achieved at room temperature with 0.085% phosphoric acid in water (solvent A) and 95% acetonitrile in 0.085% phosphoric acid (solvent B) as the mobile phase. Chromatographic conditions: initial 10% B, 10 $\rightarrow$ 90% B in 7 min at 1 mL min^{-1} flow rate.

2.2.14 GC–MS analysis

Analysis of the reaction products was conducted using an HP 5980 gas–chromatograph connected with an HP 5971 A mass spectrometer.

The measurements were carried out by working in electronic impact at 70 eV with a source temperature of 100℃. Gas–chromatographic separation was performed with an HP 5 – MS column (length 30 m, inner diameter 0.25 mm, film thickness 0.25 μm). Analysis conditions: initial temperature 120℃ for 15', then 10℃/minute gradient until 250℃. This temperature was kept for 5'.

2.2.15 Enzymatic comparison experiments

When horseradish peroxidase was used, up to 20 E.U. were present in a final volume of 1 mL of 25 mM buffer (pH 4, 5, 6, or 7) and dyes at the concentration reported in Table 3. H_2O_2 concentration was 8.8 mM.

Dye	**Final concentration used (μM)**
ARS	119
PNS	31
XO	200
MB	15
MG	150
MO	65

Table 3: **Final dyes concentrations used during enzymatic bleaching experiments.**

The same conditions were adopted for the experiments with laccase (23 E.U. added); every experiment was repeated with and without added H_2O_2.

In the case of LiP, 0.2 E.U. were present in the final volume of 1 mL, and

the H_2O_2 concentration was 0.176 mM. For certain experiments, 0.1 mM VA (final concentration) was added to the reaction mixtures.

Moreover, in order to mimick MnP action, other experiments were carried out using Mn(III) as the putative oxidizing agent. To this purpose, 1 mM manganese triacetate was dissolved in 50 mM sodium malonate buffer, pH 6.5 [117], and the final mixture contained this solution along with dyes at the same concentration reported in Table 3.

For PNS also control experiments of uncatalyzed bleaching were performed.

PNS was oxidized by ammonium peroxodisulfate in aqueous HCl, as already described [148]; also additional experiments were carried out with the same oxidant, but with 0.3 mM PNS concentration. In addition, different pH values, i.e. 4 and 7, were tested.

3 RESULTS AND DISCUSSION

3.1 IPS/MnTSPP

The first tested LP–like catalyst was MnTSPP coordinatively immobilized on an imidazole–grafted silica (IPS).

The chosen commercial silica gel is easily available in large amounts at a very low price: this makes it an ideal base for the development of heterogeneous catalysts. The synthesis of the imidazolyl silane (§2.2.2) represents a case of the well–known reaction between alkyl isocyanates and aliphatic primary amines, leading to *N,N'*–disubstituted ureas. The obtained product was subsequently used as a silanizing agent without any need of purification (in order to synthesize IPS), and led to a functionalization degree of 0.29 mmol imidazolyl groups/g silica. In the case of the control experiment with (3–aminopropyl)triethoxysilane, APS was obtained with a functionalization degree of 0.61 mmol amino groups/g silica. This higher yield of functionalization for APS is presumably due to the sharp basic character of aminopropyltriethoxysilane in comparison with the weak basicity of the imidazolyl moiety (silanization reactions usually require a basic catalyst).

With concern to the metalloporphine loading by IPS, a typical hyperbolic saturation curve was obtained (Figure 13), and a proportion of 60 mg metalloporphine per gram of IPS (corresponding to a loading of 40.8 mg per gram IPS) was chosen for further experimental work. With concern to control experiments, SG showed no interaction with MnTSPP, which was completely recovered by simply washing the support with distilled water. This excludes any unspecific

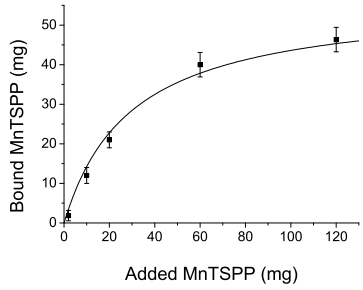

Figure 13: **MnTSPP loading versus MnTSPP concentration. Bound MnTSPP was intended per gram IPS. Added MnTSPP was dissolved in 10 mL aqueous $NaHCO_3$ 50 mM.**

interaction with the metalloporphine. In the case of APS, the metalloporphine was adsorbed at first and it resisted against to the water washings. However, MnTSPP was promptly and almost totally released upon washing with the NaCl solution (contrarily to that was seen with the IPS/MnTSPP adduct).

These results indicate a specific, axial coordinative interaction between the imidazole nitrogen of IPS side chains and the Mn(III) chelated within the porphine macrocycle (Figure 14). This interaction is therefore insensitive to the rise of ionic strength caused by NaCl. Moreover, this specific interaction seems to be rather strong and therefore prevents imidazole protonation (and concomitant MnTSPP release) unless pH drops below 3 (not shown). On the other hand, the interaction between APS side-chains and MnTSPP would be ionic in nature (APS amino groups and MnTSPP sulfonato moieties should be involved), explaining its lability.

Comparison between Figures 9 and 14 reveals the great resemblance between IPS/MnTSPP adduct catalytic site and active site of LPs.

The changes of the support from the commercial SG to IPS and to IPS/MnTSPP adduct could be checked by inspection of the IR spectra (Figure 15): the reaction of 3–(1–imidazolyl)propylcarbamoyl–3'–aminopropyl–triethoxysila-

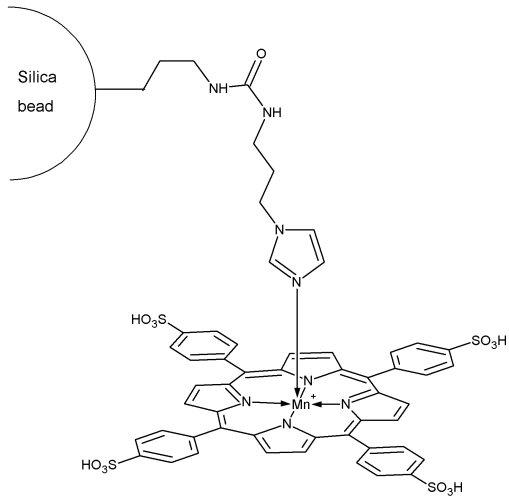

Figure 14: **Schematic representation of the proposed coordinative interaction between IPS and MnTSPP.**

ne with silica led to decrease of -–OH band at 3500 cm^{-1}, and two new bands appeared at 1450–1550 cm^{-1} and 700 cm^{-1}, too. Further differences were also noted after metalloporphine complexation: in particular the band at 1250 cm^{-1}.

Surface area and porosity of IPS was also estimated by liquid–nitrogen physisorption. To have the isotherms, the adsorbed volume is plotted against relative pressure (equilibrium pressure, p/saturation pressure, p^0). The adsorption and desorption isotherms are reported in Figure 16.

Physisorbed molecules are fairly free to move around the surface of the sample. As more gas molecules are introduced into the system, the adsorbate molecules tend to form a thin layer that covers the entire adsorbent surface. Based on the well–known Brunauer, Emmett and Teller (BET) theory, one can estimate the number of molecules required to cover the adsorbent surface with a monolayer of adsorbed molecules (N_m). Multiplying N_m by the crosssectional area of an adsorbate molecule (16.2 $Å^2$ for N_2) yields the sample's surface area (S_{BET}). Furthermonre, computational methods such as the one by Barrett,

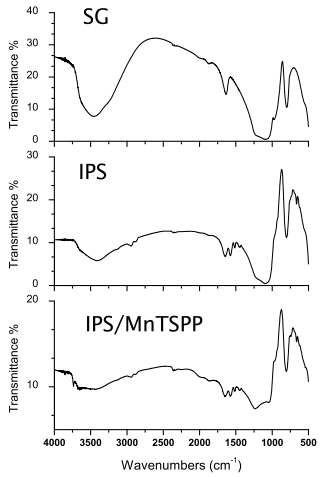

Figure 15: **IR spectra of SG, IPS, IPS/MnTSPP.**

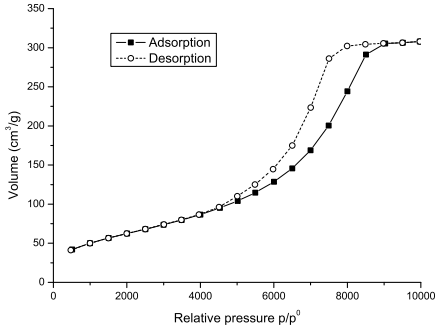

Figure 16: **Adsorption and desorption isotherms generated during physisorption analysis of IPS.**

Joyner and Halenda (BJH) allow the computation of pore sizes from equilibrium gas pressures, from which also total pore volume can be estimated. All these data are summarized in Table 4.

Support	S_{BET} **(m^2g^{-1})**	**Pore Diameter (Å)**	**Pore Volume (cm^3g^{-1})**
SG	335.3	104.1	0.872
IPS	235.1	81.2	0.477

Table 4: **Surface analysis parameters determined on plain SG and functionalized IPS.**

Silanization of IPS led to a slight decrease of all the parameters. In particular surface area of plain SG was 335.3 m^2g^{-1}, while after imidazole–grafting it was 235.1 m^2g^{-1}. However, decrease was quite small, not affecting global porosity properties of the support. Besides, this decrease can be considered as a further evidence of effective functionalization of the support.

Adsorption and desorption mechanisms differ, accordingly adsorption and desorption isotherms do not overlay each other (Figure 16). The resulting hysteresis leads to isotherm shapes that can be mechanistically related to those expected from particular pore–shapes. In particular, in the case of IPS a type IV isotherms with hysteresis type $H2$ (according to IUPAC classification [149]) was found, that is correlated with an ink–bottle–like shape (pores having a narrow neck and wide body). No change on the pore–shape was caused by silanization.

It is worth noting that the amount of bound MnTSPP (about 45 μmol/g under saturating conditions) is by far lower than the imidazolyl moieties (290 μmol/g). This finding could be explained by the above observation on SG structure: the majority of the imidazolyl moieties, although bound at the ends of flexible chains, would be unable (because of sterical hindrance) to properly interact with manganese ions that are firmly complexed within the rigid and

bulky tetraphenylporphine structure.

Whereas SG and APS were almost unable to load MnTSPP, IPS support bound a noticeable amount of metalloporphine, as revealed by the blackish–brown color of the adduct. Accordingly, only this preparation could catalyze the oxidation of veratryl alcohol (VA) at the expenses of hydrogen peroxide at a significant rate. Consequently, further characterization was mainly focused on the IPS/MnTSPP adduct.

3.1.1 LiP–like activity characterization

VA is commonly used as a convenient substrate to assess the LiP activity [41, 150, 151, 152]. In fact, preparation of pure lignin samples is not easy, and the physicochemical properties of the obtained products widely vary depending on both the chosen plant sources and the purification protocols; therefore the results are hardly reproducible. So, various model compounds have been proposed to carry out photometric LiP assays [41], and chosen to avoid interference by other enzymes that often come with LiP, such as peroxidase(s) and laccase. Among these compounds, VA is inexpensive and enough water soluble to obtain aqueous solutions, and thus it is suitable for photometric measurements. In fact, the compound is oxidized by LiP to form the corresponding aldehyde which can be detected by virtue of its adsorption at λ_{max} of 310 nm. VA simply behaves as a nonsubstrate for both peroxidase and laccase, although being oxidized —at the expenses of molecular oxygen and with concomitant H_2O_2 release-– by another fungal enzyme, veratryl alcohol oxidase (VAO, EC 1.1.3.7) [153]. In the present work, VA has been also chosen because its adsorption by the adduct –as well as that one of the corresponding aldehyde– is negligible (not shown). Product formation could be clearly checked by UV spectrophotometry (Figure 17).

Among the wide variety of oxidants proposed for use with metalloporphine catalysts [125, 154, 155, 156], hydrogen peroxide has been chosen in the present study for various reasons: *i*) the substance is easily available in large amounts at a relatively low price, and is suitable for safe transport and stocking; *ii*) it is completely miscible with water thus avoiding the need of using any organic

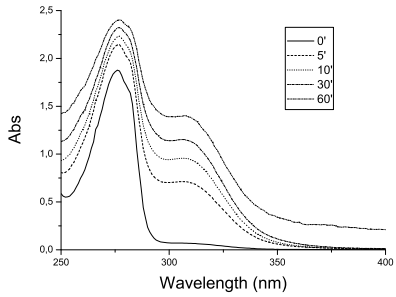

Figure 17: **Spectral changes of VA oxidized by H_2O_2 in the presence of the IPS/MnTSPP adduct.**

solvent; *iii*) the only degradation products are water and molecular oxygen, which are harmless and obviously do not imply any recovery process of the exhausted oxidant. In conclusion H_2O_2 is the oxidant of choice for catalytic oxidative processing of wastewaters, as already stated [157], and was the sole oxidant used throughout this study.

Addition of more hydrogen peroxide when veratraldehyde production ceased, produced no effects on the absorption spectra, thus showing that under the tested conditions no further oxidation of the aldehyde took place, and also suggesting that VA was almost totally consumed. The same inertness of the compound was seen when veratraldehyde was directly subjected to H_2O_2 action in the presence of the catalyst: the former could be regarded as a dead end product of VA oxidation. On the contrary, VA addition to the reaction mixture where the substrate had been apparently exhausted, caused a significant rise of the aldehyde peak, therefore indicating that the aromatic alcohol had been almost entirely consumed whereas an excess of hydrogen peroxide was still present (not shown).

The catalytic activity depended on pH of reaction medium, being the optimum centered at pH 7 (Figure 18).

A Michaelis–Menten–like kinetics was found for both hydrogen peroxide con-

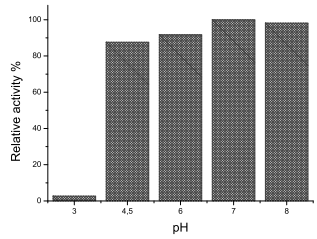

Figure 18: **Catalytic dependence on pH for the IPS/MnTSPP adduct.**

sumption and veratraldehyde formation (Table 5), showing that the catalyst could be saturated by both H_2O_2 and VA.

The catalyst was suitable for repeated use: catalytic activity remained over 90% of the starting one for the first 3 cycles, but it quickly decreased below 20% after 8 cycles. Results are summarized in Table 6. This activity drop is concomitant with a color fading of the adduct, and is perhaps depending on an oxidative degradation of the porphine ring due to a prolonged action of relatively concentrate hydrogen peroxide.

Both kinetic values and multicycle use feasibility are compatible with large scale applications, since catalysts is able to work with a substrate amount in the order of magnitude of millimolar (many enzymes suffer from substrate inhibition and cannot handle such high concentrations). Besides, catalyst recovery seems to be economically profitable.

3.1.2 Reaction mechanism

As it concerns the reaction mechanism, it was observed that the amount of aldehyde production is far to be stoichiometric: after two hours of reaction, the absorption peak at $\lambda = 310$ nm reached a maximum which corresponds to a conversion of about 17%, indicating that the reaction did not proceed further.

This finding was confirmed by GC–MS and HPLC analysis: a conversion of 87.9% was obtained after 24 h, whereas veratraldehyde concentration was

Substrate	Kinetic Parameter	Value
VA	K_M	5.5 ± 0.9 mM
	k_{cat}	18.6 ± 0.9 min^{-1}
	k_{cat}/K_M	3.4 ± 0.7 mM^{-1} min^{-1}
H_2O_2	K_M	10.3 ± 2.1 mM
	k_{cat}	16.5 ± 1.4 min^{-1}
	k_{cat}/K_M	1.6 ± 0.5 mM^{-1} min^{-1}

Table 5: **Kinetic parameters of the IPS/MnTSPP adduct in the presence of the substrates, H_2O_2 and VA. The assay mixture contained, in a final volume of 2 mL, 15 mg of catalyst, 8.8 mM hydrogen peroxide, 1.25 mM VA and 25 mM potassium phosphate buffer pH 7. Absorbance increase at 310 nm was then read after 30' of stirring reaction ($n = 3$).**

only 12.9% of initial VA concentration. HPLC revelead also a small production of veratric acid (about 5%), as stated in Figure 19. No other products were detected by this technique. Therefore, oxidation of VA under the described conditions must go to other products, undetectable by GC–MS and UV–HPLC, but affecting the absorbance at 310 nm, which explains the observed discrepancy of conversion to veratraldehyde between UV, HPLC, and GC–MS data.

A wide range of lignin model compounds was then tested: catalyst showed the ability to oxidize with significant conversion rates both non–phenolic and phenolic substrates (Table 7); with a preference for the latter. Only 1,2,3–trimethoxybenzene was not a substrate of IPS/MnTSPP adduct. Among non–phenolic substrates, the catalyst is able to degrade methoxy–substituted benzyl alcohols: this is a very promising feature since these constituents are common in highly polymerised lignin.

As point of fact, catalysis of IPS/MnTSPP adduct was not affected by the presence of Mn(II) complexes. Accordingly, its activity can be labelled only

Cycle Number	% Catalytic Activity
1	100 ± 1
2	98 ± 2
3	93 ± 3
4	88 ± 2
5	80 ± 4

Table 6: **Catalytic activity of the IPS/MnTSPP adduct upon multicyclic use in the presence of 15 mg of catalyst, 8.8 mM hydrogen peroxide, 1.25 mM VA and 25 mM potassium phosphate buffer pH 7 (final volume 2 mL). After 30' of stirring reaction, absorbance increase at 310 nm was detected. Between cycles, catalyst was regenerated through washings with H_2O and 2–propanol.**

LiP–like, but not MnP or VP–like.

Much work has been spent to the identification of reaction products arising by LiP action on methoxybenzenes and among these on veratryl alcohol [93, 151, 158]. A general agreement nowadays exists on the idea that the first product of LiP–catalyzed oxidation of methoxybenzenes and related compounds, of course including lignin and congeners and derivatives, is an aromatic radical cation, which could evolve in different manners, depending on its chemical nature and on the experimental conditions. In particular, veratraldehyde is the main product in the case of LiP catalysis (Figure 20), where deprotonation and rearrangement of the cation radical lead to veratraldehyde.

A very different pathway could be observed when model metalloporphines have been used [133]. In particular, work with H_2O_2 and electron–deficient Fe(III)–porphines produced high yields of 2–hydroxymethyl–5–methoxy–1,4-benzoquinone (Figure 21), whose formation is not surprising when taking into account that the catalytic center is freely accessible by water molecules. There-

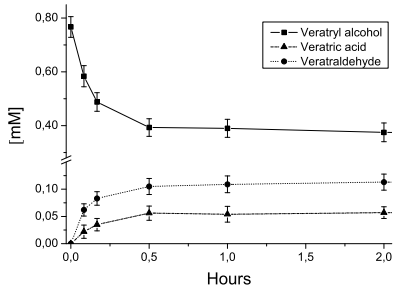

Figure 19: **VA degradation by H_2O_2 in the presence of the IPS/MnTSPP adduct, and concomitant production of veratraldehyde and veratric acid.**

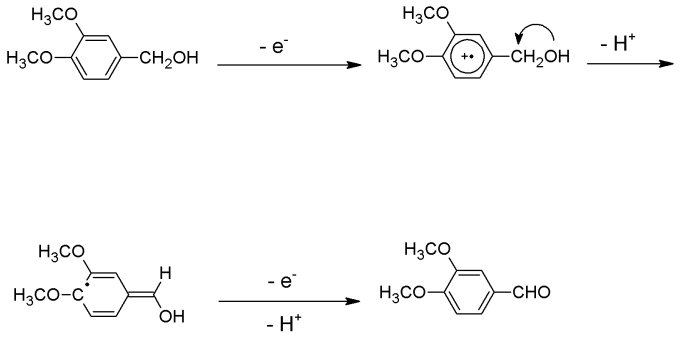

Figure 20: **Putative reaction pathway from VA to veratraldehyde.**

Substrate	Conversion 3 h (%)
Ferulic acid	99 ± 2
Isovanillyl alcohol	98 ± 3
Vanillyl alcohol	98 ± 3
4–Methoxybenzyl alcohol	20 ± 4
Veratryl alcohol	49 ± 5
3,4,5–Trimethoxybenzyl alcohol	28 ± 2
1,2,3–Trimethoxybenzene	0 ± 1
1,2–Dimethoxybenzene	29 ± 3
Veratric acid	9 ± 2

Table 7: **Sustrate specificity of IPS/MnTSPP adduct with various lignin–model compounds. Catalytic activity was detected in the presence of 15 mg of catalyst, 8.8 mM hydrogen peroxide, 1 mM substrate, DME 10%, and 25 mM potassium phosphate buffer pH 7 (final volume 2 mL). Samples were then analyzed through UV–HPLC.**

fore, hydration of the intermediate cation radical prevails over deprotonation. By analogy, this could explain why, also in the case of MnTSPP, only a minor fraction of VA was converted to the corresponding aldehyde even if VA was almost totally consumed. The same quinone unfortunately has not been detected during IPS/MnTSPP adduct catalysis by UV–HPLC analysis. Perhaps, main products could be further oxidized compounds, such as dicarboxylic acids. Or maybe oligomerized or polymerized products arose from VA.

On the contrary, a significant difference was found between the above mentioned Fe(III)–porphines and MnTSPP used here: the former cleave veratraldehyde to muconic dimethylesters [133] while the latter showed no significant action towards the aldehyde.

The different pattern of reaction products between IPS/MnTSPP and LPs

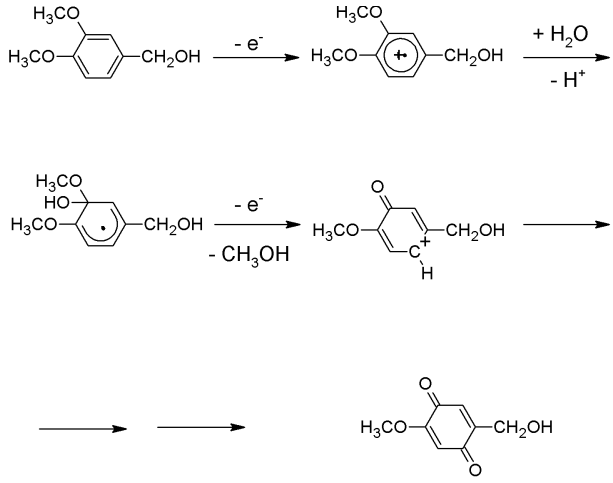

Figure 21: **Putative reaction pathway from VA to 2–hydroxymethyl–5–methoxy–1,4–benzoquinone.**

shows how the structural emulation did not lead to a perfect functional emulation. However, since the IPS/MnTSPP products seem to be more oxidized than the ones deriving from LPs catalysis, these differences could conceivably be welcome from an applicative perspective.

The IPS/MnTSPP adduct appears to be a very promising heterogeneous catalyst, that could be well suitable for the oxidative degradation (by means of hydrogen peroxide) of water soluble lignin derivatives such as those coming from pulp and paper plants. The presented data suggest a deep oxidative action which is a favourable prerequisite for a further mineralization. These findings will conceivably allow to broaden the application fields of the catalyst, such as in the treatment of various industrial substrates and wastewaters.

Time	Remaining Dye %					
(h)	ARS	PNS	XO	MB	MG	MO
0	100	100	100	100	100	100
0.33	80	13	64	23	37	15
0.66	54	9	60	6	22	14
1	38	8	58	4	18	13
3	15	6	43	1	10	11
5	1	6	31	0	6	8

Table 8: **Bleaching of each dye studied by means of IPS/MnTSPP.**

3.1.3 Dyes decoloration

Accordingly, in order to broaden its industrial applications, IPS/MnTSPP adduct has been investigated about its ability to bleaching textile dyes, since they represent high pollutant wastes, released in the environment in significant amounts (§1.5).

In order to completely evaluate IPS/MnTSPP substrate specificity, six dyes belonging to different chemical classes (such as azodyes, anthraquinones, triphenylmethanes, and phenothiazine) have been included in the study (Figure 8 at page 26).

Under the same mild operational conditions described above, the biomimetic catalyst easily degraded all tested dyes, as summarized in Table 8, showing a wide substrate specificity.

In just 1 h about 90% of starting dyes was bleached. Only ARS and XO showed slight slower conversion rates, as 62% and 42% respectively of initial dye were removed during the same time.

However, textile wastewaters are usually composed by a mixture of several dyes. In this perspective, IPS/MnTSPP adduct was also tested about its ability to bleach a mixture of all six dyes. As reported in Figure 22, bleaching was

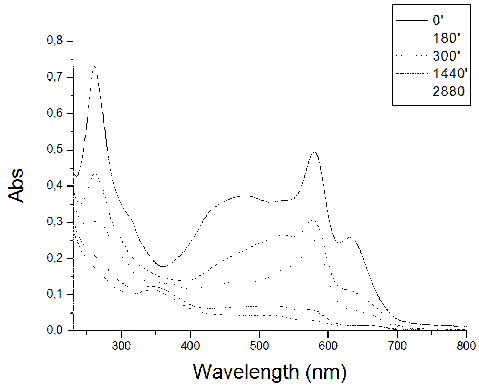

Figure 22: **IPS/MnTSPP adduct in the presence of H_2O_2 is able to effectively bleach a mixture containing high concentrations of the six dyes included in this study.**

effective also in this situation, suggesting the catalyst suitable for real industrial applications.

This statement is further corroborated by the extremely mild operational conditions, at which these results have been obtained: low pressure and temperature (25℃), organic solvents absence, most eco–friendly oxidant (H_2O_2 [157]) at low concentration (8.8 mM).

Also pH was at neutrality: as shown in Table 9, for each dyes pH optimum was determined. In all cases, this value was close to 7, allowing simultaneous degradation of the six dyes to be performed at neutrality.

Bleaching of the six dyes was also kinetically characterized. In all cases, Michealis–Menten kinetics was observed, whose parameter have been reported in Table 10. The inspection of the table revealed that the catalyst showed a K_M for dyes always in the millimolar order of magnitude, not suffering substrate inhibition in this range. This is a crucial feature, since industrial wastes usually contain dyes quite concentrated (the millimolar order of magnitude can be a good approximation). And not all the methods proposed for their bleaching are

Dye	Optimum pH
ARS	7
PNS	8
XO	6
MB	7
MG	7
MO	6

Table 9: **In the presence of H_2O_2, adduct IPS/MnTSPP presents for each dye a pH optimum close to 7.**

able to work under these conditions.

Lignolytic enzymes (studied for comparison) suffered, for instance, from a remarkable substrate inhibition not allowing them to be used at concentrations higher than those reported in Table 3 at page 58. Besides, these enzymes suffer also from H_2O_2 inhibition, leading to use this reagent more diluted than during biomimetic catalysis. Accordingly, under the same operational conditions it is not surprising that enzymatic bleaching efficiency was lower.

The lignolytic enzymes studied were laccase (LC), also in the presence of H_2O_2, horseradish peroxidase (HRP), and lignin peroxidase. Besides, Mn(III) was also used as oxidizing agent, mimicking manganese peroxidase action [117].

Their ability to bleach the dyes, under the studied operational conditions, has been summarized in Table 11.

On the whole, none of the examined enzymes was able to bleach all the studied dyes. In particular, PNS is resistant to LC, HRP, and Mn^{3+}, while only a partial degradation with concomitant irreversible inactivation is observed with LiP (*vide ultra*, §3.1.3.2). On the other hand, IPS/MnTSPP is able to effectively bleach all the studied dyes, as described above and shown in Table 8.

Dye	Reducing substrate			H_2O_2		
	K_M (mM)	k_{cat} (min^{-1})	k_{cat}/K_M ($mM^{-1}min^{-1}$)	K_M (mM)	k_{cat} (min^{-1})	k_{cat}/K_M ($mM^{-1}min^{-1}$)
ARS	2.11 ± 0.74	0.14 ± 0.03	0.066 ± 0.037	3.21 ± 0.12	0.13 ± 0.01	0.040 ± 0.004
PNS	0.32 ± 0.04	2.2 ± 0.1	7.0 ± 1.2	3.0 ± 0.4	1.9 ± 0.1	0.63 ± 0.13
XO	1.33 ± 0.38	98 ± 14	74 ± 31	7.9 ± 1.9	78 ± 8.9	9.9 ± 3.6
MB	0.11 ± 0.02	19.0 ± 1.8	166 ± 52	2.4 ± 0.5	15.2 ± 1.3	6.4 ± 2.1
MG	0.72 ± 0.12	108 ± 9	150 ± 37	0.43 ± 0.08	159 ± 12	369 ± 100
MO	0.63 ± 0.05	67 ± 4	105 ± 16	7.4 ± 1.5	71 ± 8	9.6 ± 3.2

Table 10: **Kinetic parameters measured for the bleaching of each dye by means of IPS/MnTSPP and H_2O_2.**

Dye	LC	LC + H_2O_2	HRP	LiP	Mn^{3+}
ARS	+	++	+/−	+/−	+
PNS	−	−	−	+/−	−
XO	+	+	+	−	+
MB	−	+/−	+/−	+/−	−
MG	+	+	++	+/−	++
MO	+	+/−	+	+/−	+

Table 11: **Enzymatic bleaching of the dyes included in the present study. Experimental conditions are reported in §2.2.15 at page 58.**

All these features allow to consider biomimetic catalysis a more feasible alternative for industrial treatment of textile wastewaters.

According to the hypothesis of a monoelectronic abstraction as the first step of the bleaching process, some redox mediators, capable of cycling between their "resting" states and the oxidized, radical counterparts have been tested for their influence towards the decoloration process (Table 12).

The results, however, were very poor as it was possible only in few cases to double or triplicate catalytic activity. But also in these cases environmental impact of redox mediator should not suggest their routinely employment. In some cases (like for PNS), a noticeable quenching of the catalytic action was observed.

Unluckily, the only environmentally–affordable alternative (Mn^{2+} as redox mediator) was not able to affect IPS/MnTSPP activity (as already stated in §3.1.2).

The catalyst was also investigated for its reuse potential. After bleaching of the dyes, the catalyst was recovered, washed, and reused. Results are reported in Table 13.

Redox	% Remaining Catalytic Activity					
Mediator	ARS	PNS	XO	MB	MG	MO
None	100	100	100	100	100	100
OH–TEMPO	98	45	277	56	336	16
NHT	142	46	162	38	299	121
NHS	141	89	146	90	313	122
NPH	103	32	74	56	340	57

Table 12: **The presence of some redox mediators seems to affect the dyes decoloration rate. Percentage of activity is referred to a control experiment in absence of mediators ($n = 3$).**

Cycle	% Remaining Catalytic Activity					
Number	ARS	PNS	XO	MB	MG	MO
1	100	100	100	100	100	100
2	68	73	100	99	98	44
3	49	70	93	73	97	37
4	33	61	88	49	97	34
5	30	51	47	37	97	28
6	28	49	41	34	96	28
7	28	44	31	34	96	28
8	26	41	30	26	94	27
9	25	39	29	25	94	20
10	25	35	27	24	90	19

Table 13: **Catalytic activity of the IPS/MnTSPP adduct upon multicyclic use during the decoloration of the studied dyes ($n = 3$).**

On the average, a rapid decrease of catalytic activity was observed in the first 2–3 cycles. After that, a stable activity of about 25–30% was still present for at least 8–10 cycles.

This could be explained if one considers that a fraction of some dyes remained tightly adsorbed on to the catalyst even when the supernatant was completely decolorized. This adsorbed dye most probably reduced the catalytic performance through steric hindrance and/or electrostatic repulsion of incoming substrate molecules, explaining the different behavior observed in the case of VA (compare Table 6).

In conclusion, the described catalytic bleaching process is characterized by a high efficiency combined with very mild conditions. Dilute hydrogen peroxide is a relatively safe and inexpensive reagent, and the catalyst could be successfully recycled, rendering on the whole the bleaching process economically feasible.

Furthermore, the comparison with the lignolytic enzymes showed a clearly wider substrate specificity for the biomimetic catalyst, which was also able to remove larger amounts of each dye from the reaction medium. These features definitely broaden its practical applications for textile wastewaters treatment.

3.1.3.1 ARS insights

The bleaching mechanism of some model dyes have been investigated deeply, as in the case of ARS for instance.

As already stressed, in the presence of the heterogeneous IPS/MnTSPP catalyst, hydrogen peroxide became capable of efficiently bleaching ARS under very mild conditions (neutral pH, ambient temperature, low hydrogen peroxide concentration) (Figure 23). As a point of fact, H_2O_2 alone was quite unable to bleach the dye under the same experimental conditions.

The pH dependence of catalytic activity is fully reported in Figure 24. Contrarily to that already seen in the case of the oxidation of VA by H_2O_2 (§3.1.1 and Figure 18), where catalytic activity was almost pH–independent in the range 4.5–8, an optimum at pH 7 was found in ARS decoloration. ARS exists mainly as the monoanion (yellow) below pH 5.5, as the dianion (red) below

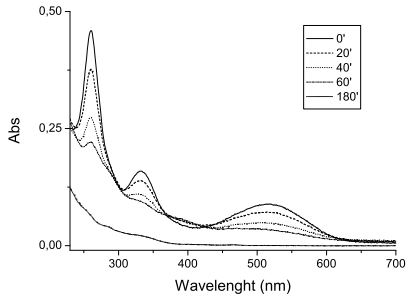

Figure 23: **Spectral changes during oxidative catalytic degradation of ARS by 8.8 mM H_2O_2 in the presence of IPS/MnTSPP catalyst in 25 mM McIlvaine buffer, pH 7.**

pH 11, and is completely deprotonated under sharply alkaline conditions as the trianion (purple) [159]. The pH dependence of the oxidative bleaching strongly suggests that the process takes place on the dianion (Figure 25). Over pH 7, the bleaching efficiency of the H_2O_2/catalyst system slightly decreased, most probably as the catalyst itself became less effective. Therefore pH 7 represents the best compromise between catalyst efficiency and substrate reactivity.

Despite of the widespread occurrence of hydroxyanthraquinones in nature and their use in several application fields, their oxidative degradation has been until now the target of a few studies, so the degradation mechanism(s) is largely unknown. Alizarin (1,2–dihydroxy–9,10–anthraquinone) bleaching by hydrogen peroxide in sharply alkaline environment has been studied in detail [160] and a mechanism involving double bond epoxidations as the key steps has been proposed.

As ARS could well represent a water–soluble, useful model for the oxidative degradation of anthraquinone derivatives, it has been the targed of a number of studies. Electrochemical oxidation of ARS [161, 162] and photoinduced oxidation over titania [163, 164, 165, 166, 167] have been described. All these studies proposed the involvement of reactive oxygen species (namely hydroxyl radicals)

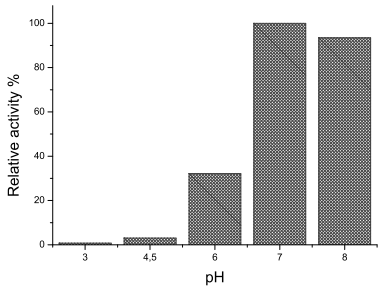

Figure 24: **Dependence on pH of the ARS degradation rate by H_2O_2 and IPS/MnTSPP. Data are obtained in the presence of 10 mg catalyst, 8.8 mM hydrogen peroxide, 290 μM ARS and 25 mM buffer (final volume 2 mL).**

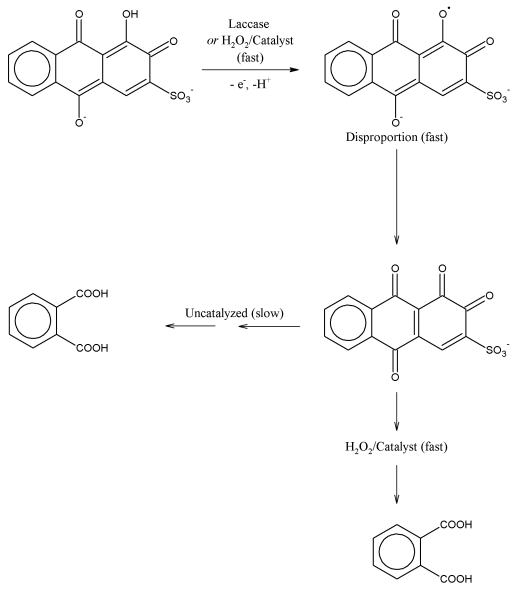

Figure 25: **The proposed route for ARS oxidative degradation.**

attacking the junction between the quinone and the catechol rings of the dye, and leading to a deep oxidative cleavage. The complete mineralization of the isolable intermediate phthalic acid under suitable experimental conditions has also been claimed.

With concern to the biomimetic catalytic system, a mechanism involving hydroxyl radicals must be ruled out. In fact, treatment of ARS with the hydroxyl radical generator APH did not affect the dye under the described conditions. Moreover, addition of the hydroxyl radical scavenger mannitol could not influence ARS bleaching by hydrogen peroxide in the presence of IPS/MnTSPP.

Hydrogen peroxide reacted with IPS/MnTSPP leading to a PorphMn(V)=O intermediate, according to an earlier study [154] and to our finding that syringaldazine and ABTS, classical peroxidase substrates acting as one–electron donors, were rapidly oxidized by H_2O_2 in the presence of MnTSPP/IPS (not shown). Two consecutive monoelectronic reductions of PorphMn(V)=O to the resting state, leading to an ARS semiquinone radical, capable of evolving to the very reactive 1,2,9,10–anthradiquinone–3–sulfonic acid, could well be thus suggested. In other words, a reaction pathway strictly resembling that found with peroxidase or laccase should be considered. However, diquinones arising from hydroxyanthraquinones are (as expected) very prone to nucleophilic attack by water, so their isolation under the described experimental conditions is not possible.

The formation of the same diquinone as above should have taken place also when ARS was treated with fungal laccase (ARS is so weak as a HRP and LiP substrate that the experiments involving these latter enzymes were useless). As laccase cannot catalyze reactions other than the extraction of one electron from phenolics leading to phenoxyl radicals (disproportion to quinones usually follows), the close similarity between the two spectral patterns strongly suggest the proposed formation of the diquinone as a key intermediate in ARS bleaching. However, IPS/MnTSPP in the presence of H_2O_2 was a much more efficient catalyst than laccase, perhaps because the former could act as an oxygen donor and therefore oxidize intermediates (as the above mentioned diquinone) that are simply nonsubstrates for laccase (Figure 25). Accordingly, laccase plus H_2O_2

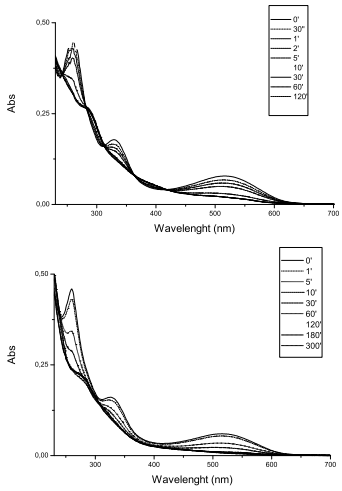

Figure 26: **ARS bleaching by laccase alone (top) and by laccase plus H_2O_2 (bottom). 23 E.U. laccase were present, dissolved in 25 mM McIlavine buffer, pH 6. When present H_2O_2 was 8.8 mM.**

(the chosen concentration of the latter was unable to adversely affect laccase activity) was more efficient than laccase alone was, although not so efficient as seen with our biomimetic catalyst (Figure 26).

However, despite of the speed and efficiency of the bleaching, no complete mineralization was achieved by H_2O_2/MnTSPP/IPS, and HPLC analysis after bleaching completion revealed the presence of phthalic acid as the main product of the process, according to the relative chemical inertness of this compound (Figure 27). This can be, however, considered a substantial progress with respect to the parent anthraquinone dye.

Summing up all the collected data, IPS/MnTSPP do not functionally emulate even in this case any precise enzymic activity, presenting however signifi-

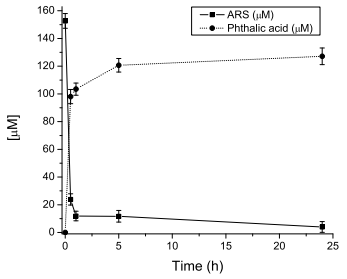

Figure 27: **Phthalic acid formation during ARS bleaching. Data obtained by HPLC analysis of the reaction mixture as described in the text.**

cantly better operational features, especially from an industrial point of view.

3.1.3.2 PNS insights

Another dye, whose bleaching was deeply investigated and compared with other chemical approaches, has been PNS.

As previously described [148], a complex mixture of oligomers and insoluble polymers arose, when 0.2 M PNS was oxidized by 0.5 M potassium peroxodisulfate dissolved in 0.2 M HCl (Figure 28).

However, PNS concentrations as high as 0.2 M are quite unlikely in industrial wastewaters, and, therefore, a far lower concentration was tested in this study. No precipitate was observed when 0.3 mM PNS was oxidized by peroxodisulfate. The dye was gradually bleached under all the tested pH values (Figure 29). This result is not surprising, considering the comparatively low PNS concentration used; the nitrenium dication that formed most probably underwent rapid hydrolysis, leading to a reactive quinone and further decomposing to colorless compounds. The efficacy of peroxodisulfate as an oxidizing agent towards PNS is also dependent on its concentration: below 10 mM, no oxidation was observed.

It is also worth noting that concentrations of residual PNS obtained by

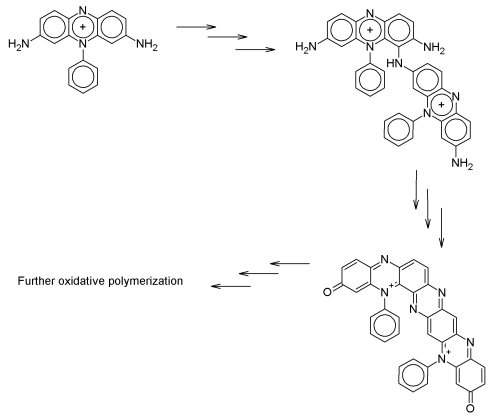

Figure 28: **The oxidative oligomerization of PNS upon treatment with ammonium peroxodisulfate in 0.2 M HCl. The very strong electrophile, a nitrenium dication, arising from peroxodisulfate action, is the key intermediate for PNS dimerization and subsequent oligomerization.**

HPLC analysis were strictly proportional to absorbance decrease at 525 nm, so that decrease was assumed as a measure of PNS degradation.

Under the experimental conditions described here for the biomimetic method (8.8 mM H_2O_2 in the presence of the IPS/MnTSPP catalyst), no oxidative polymerization was evident: on the contrary, a noticeable bleaching of the dye was observed, leading to a clear and almost colorless solution (Figure 30), with 87% of the PNS degraded within 20 min at pH 8. In particular, the observed spectral UV/Vis bleaching pattern noticeably differed from that observed with 0.5 M potassium peroxodisulfate at pH 7: a small absorption peak centered at approximately 295 nm was observed after peroxodisulfate oxidation, whereas a small peak at 340 nm arose upon H_2O_2 treatment in the presence of the biomimetic catalyst. By contrast, no oxidation of PNS was found when 8.8 mM H_2O_2 was used in the absence of the IPS/MnTSPP catalyst.

Moreover, the MnTSPP–derived high–valency specie has been found to be a Mn(V)=O species, and this is presumably further stabilized by a coordinative

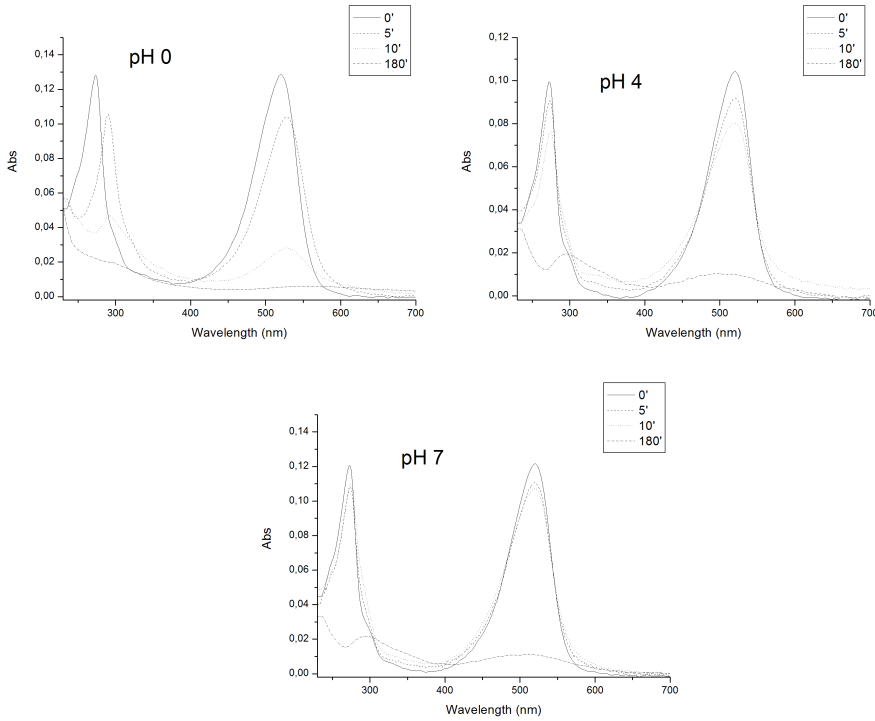

Figure 29: **PNS bleaching in the presence of 0.5 M ammonium peroxodisulfate at different pH values. It was determined that 0.5 M peroxodisulfate was very effective as a bleaching agent for PNS along a wide pH range.**

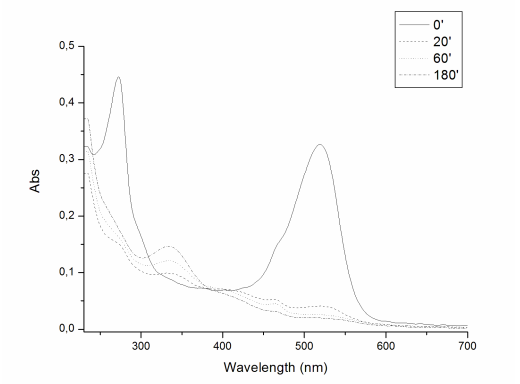

Figure 30: **PNS bleaching in the presence of 8.8 mM H_2O_2 and the IPS/MnTSPP catalyst at pH 8. Nearly complete bleaching of PNS was seen under the described experimental conditions.**

bond with the imidazolyl moiety [168] of the functionalized silica beads. This very reactive "oxomanganyl" intermediate [169], somewhat paralleling "Compound I" in the peroxidase catalytic cycle, could, in principle, evolve further via two different routes: *a*) the addition of one electron (from the oxidizable substrate) leading to a Mn(IV)=O intermediate [170] (and comparable to "Compound II" in the catalytic cycle of peroxidases), or *b*) direct oxygenation of the oxidizable substrate leading to catalyst regeneration. By following this latter path, IPS/MnTSPP could be regarded as a P450 analogue, rather than a peroxidase-like catalyst, with two obvious differences: *i*) the oxygen donor is H_2O_2 instead of the quite inexpensive O_2; *ii*) no costly sacrificial reductant is required to obtain the hypervalent active intermediate.

Obviously, these two routes *a*) and *b*) could potentially co–exist, with the relative importance of each depending on a number of conditions.

An alternative Fenton–like mechanism, involving the direct release of OH• radicals upon the interaction of Mn(III)TSPP with H_2O_2, and the concomitant formation of a Mn(IV) hydroxospecies, has been ruled out by earlier studies

[154]. To corroborate this statement, some additional experiments were performed to gather information for depicting a reasonable reaction mechanism. The addition of the well–known hydroxyl radical scavenger mannitol to the reaction mixture containing the IPS/MnTSPP catalyst had no significant influence on the PNS oxidative bleaching rate; conversely, incubation of PNS with the well–known OH• generator APH resulted in no alteration of the dye. The hydroxyl radical was therefore not involved in PNS bleaching, at least under the experimental conditions adopted here.

In another series of experiments, well–known redox mediators were added to the reaction mixtures (Table 12). Not surprisingly, a noticeable quenching of the catalytic action was observed with all the mediators, which shared the feature of being oxygen-centered radicals, and presumably less reactive than OH•. On the other hand, when another dye (ARS §3.1.3.1) was tested under quite similar conditions, it was bleached more rapidly in the presence of NHS and NHT. The two catalytic routes (*a*) and (*b*) could therefore act at the same time, with a relative contribution depending on the particular substrate to be oxidized. In the case of PNS, its ionization energy of 7.98 eV [148] renders the abstraction of one electron to form the radical dication unlikely (although still possible), and the oxygen–centered radicals produced by the redox mediators used were thus unable to promote this process. Their action rather exhausted the oxidizing power of the oxomanganyl reactive species arising from the reaction of H_2O_2 with the catalyst. This was quite confirmed by the absence of activity on PNS by LC and Mn^{3+} (*vide ultra*).

The direct, comparatively fast oxygenation (as compared to oxidation) of the dye (or/and of any highly reactive intermediate(s)) by the oxomanganyl reactive species could be therefore the main mechanism responsible for the bleaching process. The structure of the colorless species absorbing at 340 nm, which gradually formed as the dye was bleached, is still awaiting chemical characterization.

The bleaching efficiency was dependent on pH (Figure 31), in a different manner from that observed for alizarin red S under the same experimental conditions, therefore suggesting that the actual ionization state of the dyes must play a role at least as important as that of the catalyst itself. PNS exists

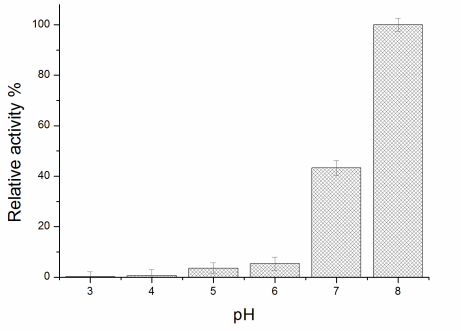

Figure 31: **Bleaching efficiency of PNS by H_2O_2 in the presence of the IPS/MnTSPP catalyst as a function of pH.**

as a monocation within the wide pH range studied here, and therefore, the variation in the catalytic efficiency in this case should be ascribed exclusively to the catalyst.

The chosen pH range was 3–8, taking into account that metalloporphine leaching was observed at pH values below 3 (as a consequence of imidazole protonation), and, on the other hand, slow solubilization of amorphous silica gel above pH 8 is a well-known phenomenon.

As the IPS/MnTSPP adduct is a bio–inspired catalyst resembling hemoenzymes, it seemed reasonable to test and compare the ability of commercial HRP to promote PNS bleaching by H_2O_2. However, no catalytic activity was observed within the tested pH range 3–8, even when a large excess (20 E.U. mL^{-1}) of the enzyme was present, and PNS remained unchanged even after several hours of incubation. This is not surprising, however, considering the comparatively low redox potential of this enzyme.

The same inertness was found when a fungal LC was tested, either alone or in the presence of H_2O_2. This latter was added by following the idea that a putative radical species, arising from the enzymatic action, could be oxidized by hydrogen peroxide, thereby enhancing the action of the enzyme on PNS. In

fact, a synergistic action between LC and H_2O_2 has been described in the case of ARS oxidative bleaching. Such a synergistic action clearly did not take place in the case of PNS, where LC was quite unable to promote the first one–electron abstraction reaction, thus rendering the presence of H_2O_2 useless.

In the case of LiP, dramatically different results were observed. In this case, both H_2O_2 and PNS concentrations were substantially reduced, to prevent inhibition by the substrate (as already described). As expected, the enzyme was inactive at pH 7, but active at pH 4.5, with a maximum activity at pH 3 (Figure 32). The spectral pattern of PNS bleaching versus time was considerably different from that observed with the IPS/MnTSPP catalyst; on the contrary, the spectral pattern was similar to that observed when PNS was treated with potassium peroxodisulfate, therefore suggesting a similar mechanism. This conclusion is in agreement with the well known LiP behavior, as this enzyme is a true peroxidase and cannot act as a mono–oxygenase. At pH 3, LiP action was very fast, but stopped within a few minutes while the PNS degradation reaction was far from completion. This loss of activity was not due to H_2O_2 exhaustion: addition of further hydrogen peroxide to the reaction mixture had no significant effect on the spectrum (not shown). An inspection of the spectral pattern of LiP action reveals that even this enzyme was unable to promote complete PNS degradation, as shown by the formation and persistence of a small absorption peak at about 295 nm, whereas the visible peak centered at 525 nm was replaced by a low peak at 534 nm. This corresponds to a new compound, much more polar than PNS, as chromatographic analysis revealed (not shown). Only 58% PNS was bleached after 10 min, as confirmed by HPLC analysis and the reaction did not proceed further, thus suggesting LiP inactivation by reaction product(s) such as the polar, colored compound absorbing at 534 nm. Therefore one could reasonably conclude that IPS/MnTSPP adduct and LiP differ fundamentally in their action mechanism, and H_2O_2 in the presence of immobilized MnTSPP is not a real functional emulator of LiP/H_2O_2 system.

As the physiological intermediacy of VA in LiP catalysis is well known [171], further experiments were carried out in which this redox mediator was present together with H_2O_2 and LiP. The presence of veratryl alcohol adversely affected

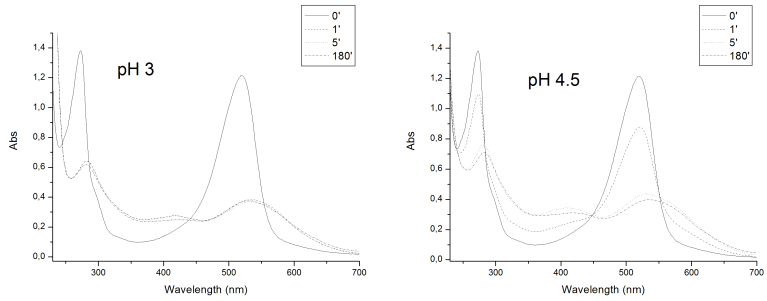

Figure 32: **PNS bleaching in the presence of 0.176 mM H_2O_2 and LiP at pH 3 (left) and pH 4.5 (right). The maximum efficiency of enzymatic bleaching was observed, as expected, at pH 3.**

the bleaching process, which was slow and incomplete, and a new peak, most probably corresponding to veratraldehyde, arose at 310 nm (Figure 33).

Only marginal changes in PNS spectra were observed in the presence of Mn(III)/malonate complex (not shown), therefore suggesting that manganese peroxidase would be substantially inactive towards the dye.

According to these results, PNS (and probably other phenylphenazinium dyes) could be efficiently destroyed in aqueous environments under very mild conditions by oxidation with dilute hydrogen peroxide in the presence of the IPS/MnTSPP catalyst. Two catalytic mechanisms, which probably occur at the same time, were proposed: the one being peroxidase-like, and the other resembling the mono–oxygenase activity of P450.

Biomimetic approach is superior in comparison with alternative treatments involving peroxodisulfate (at oxidant concentrations far higher than stoichiometric ratios) or LiP (incomplete bleaching, poor efficiency due to inactivation by H_2O_2, expensive and rather unstable enzyme). Therefore, the metalloporphine–based system could be developed and scaled up in view of future technological applications also for the removal of PNS and/or chemically related dyes from

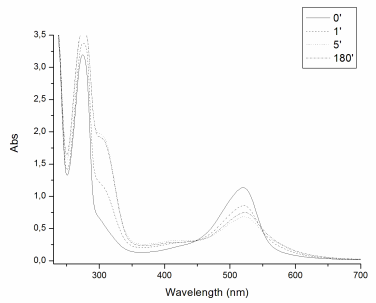

Figure 33: **PNS bleaching in the presence of 0.176 mM H_2O_2 plus 1 mM VA and LiP at pH 3. Veratryl alcohol prevented PNS degradation by LiP, behaving as a competitive substrate rather than a redox mediator.**

industrial wastewaters.

3.2 PP–PVA/FeTFPP

Besides imidazole, also less bioinspired pyridine was tested about its ability to coordinatively immobilize metalloporphines. Pyridine is, in fact, a quite more electron–withdrawing group compared to imidazole: this could lead to higher redox potential of coordinated metalloporphine.

Preliminary studies, however, showed that pyridine ligand leads to higher loading yields with Fe(III)–porphines, while imidazole prefers to bind Mn(III)–porphines.

Accordingly, FeTFPP was immobilized on a pyridine–grafted PVA crosslinked with glutaraldehyde.

PVA is an inexpensive, non–toxic, biodegradable, hydrophilic polymer, suitable for a wide range of modification reactions, including crosslinking, and therefore of potential interest for a number of applications, including enzyme immobilization and topochemical functionalization [172]. In the present study a crosslinked and functionalized structure was obtained by acetalation with glutaraldehyde and 4–aminobutyraldehyde (in the form of the corresponding

diethylacetal) under strong acidic conditions. A transparent, colorless, highly hydrophilic gel was obtained, carrying aminopropyl sidechains, that could in turn be modified by reductive coupling with pyridine–4–carboxaldehyde in the presence of sodium cyanoborohydride.

Yields were satisfactory and the procedure led to a highly functionalized product: 384 μmol aminogroups per gram of AP–PVA (corresponding to 74% of the theoretical value) and 327 μmol pyridyl groups per gram PP-PVA (corresponding to 85% of the theoretical value).

FeTFPP was chosen in the present study as it is well known for its noticeable chemical stability and catalytic efficiency [173]. FeTFPP is insoluble in water and soluble in some organic solvents. Among these, DMSO was chosen because it shows high swelling properties towards PVA, so allowing for metalloporphine entering into the polymer beads. As much as 67 mg FeTFPP per g of PP–PVA (corresponding to 63 μmol metalloporphine) could be loaded at the maximum tested metalloporphine concentration, even if a metalloporphine/PP–PVA ratio of 20 mg/g was chosen (leading to an effective loading of 15 mg FeTFPP per g support, corresponding to 14 μmol of metalloporphine) because it gave the optimum catalytic efficiency in terms of specific activity (data not shown). It should be noted that —although no support saturation was reached even at the highest metalloporphine concentration-– the loading process left a relevant fraction of the pyridyl groups unreacted. This was most probably due to the noticeable sterical hindrance encountered by the planar, bulky, and hydrophobic FeTFPP in diffusing within the macromolecular support network to find the proper alignment between the pyridyl nitrogen atom and the porphine macrocycle.

The FT–IR spectra were not in contradiction with the proposed structures (Figure 34). In particular, some assignments could be reasonably be made: O—H, 3650–3000 cm^{-1} relative to the stretchings of both free and hydrogen–bond–engaged —OH function; 2900 cm^{-1} relative to C–H stretching of C–H bonds, both pertaining to the PVA backbone. The stretching of N–H (from aminopropyl moieties before and after reaction with pyridine carboxaldehyde) could not be seen as it falls into the same region where the O—H stretching

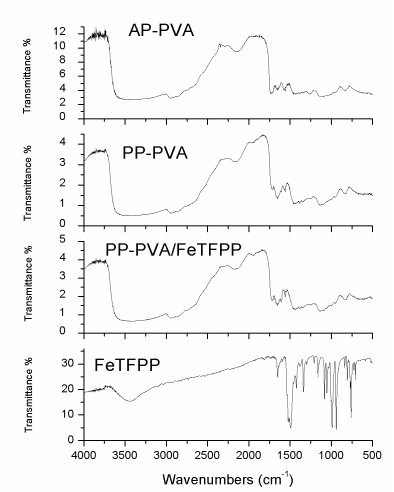

Figure 34: **The FT–IR spectra of AP–PVA; PP–PVA; PP–PVA/FeTFPP; FeTFPP.**

is found. Inclusion of pyridyl moieties led to a new peak around 1950 cm^{-1}, and also the region 1750–1500 cm^{-1} seems clearly modified. Unfortunately, the metalloporphine loading was too low to allow for unambiguous assignments of the complex pattern seen in the fingerprint region of the spectrum of the polymer/metalloporphine adduct.

Despite of the sharp hydrophobic character of the metalloporphine, the dark red PP–PVA/FeTFPP adduct (Figure 35) fully retained the hydrophilic character as well as the swelling properties of the original polymer; therefore the adduct could be tested in aqueous environment to assess its catalytic properties. No metalloporphine loss could be seen in water or by extraction with organic solvents such as acetonitrile, DMSO, 2–propanol, that are good solvents for the free metalloporphine. This is in agreement with a relatively strong coordinative interaction between the iron(III) within FeTFPP and the pyridine nitrogen of the polymer. Accordingly, no metalloporphine was bound by plain crosslinked PVA or by AP–PVA which could no form any coordinative interaction.

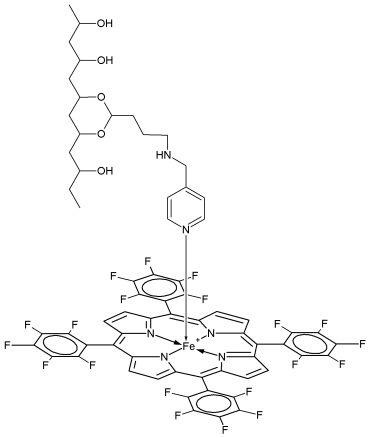

Figure 35: **The chemical structure of the PP-–PVA/FeTFPP adduct.**

Pyridyl instead of the more bioinspired imidazolyl was chosen as a functional substituent on the PVA beads because of its stronger electron–withdrawing effect, which should reasonably increase the oxidizing catalytic efficiency of the bound metalloporphine. Accordingly, a quite similar catalyst but bearing the imidazolyl functionality instead of the pyridyl one was prepared and found to be on the whole less active (not shown) and therefore abandoned.

3.2.1 LP–like activity characterization

VA is one of the known physiological substrates of fungal LiP, its monoelectronic oxidation by the enzyme being also crucial in generate the redox mediator which shuttles between LiP and lignin [174]. VA is the substrate of choice for LiP activity measurements [152], and has been also used to test LiP–like activity of metalloporphines [175]. It behaved as a good substrate for the adduct and was therefore used through the present study for rapid and reliable photometric measurements. Even if veratraldehyde was not the main reaction product, a linear relation was found by means of HPLC analysis between produced veratraldehyde and consumed VA (not shown), so the reliability of the measurements was

assessed.

Alternatively, another photometric assay was based on the quenching of the visible absorption peak (λ_{max} = 651 nm) of the dye Azure B (AzB), which has been recognized as a substrate for LiP whereas it is a nonsubstrate for MnP and resists the oxidizing power of Mn(III) [41], therefore allowing for differentiating between the two catalytic activities.

To assess the ability of the catalyst to oxidize other substrates, either phenolic or non–phenolic, some molecules were chosen among naturally occurring aromatic compounds, more or less (bio)chemically related to lignin. As the oxidation led to product mixtures, quantitative determination of conversion was carried out by HPLC analysis.

The catalytic activity of the adduct was strongly pH–dependent: on a parallel with LiP enzyme, the noticeable activity found at pH 3 quickly dropped as pH increased, and at pH 7 only phenolic substrates were oxidized, whereas the others remained almost unchanged. The conversion yields for both VA and AzB at different pH values are summarized in Figure 36.

A dramatic change in the behavior of the adduct could be seen in the presence of Mn(II): while no significant effect was caused at pH 3, the addition of $MnSO_4$ together with malonic acid (which is capable of stabilizing and solubilizing the true oxidant species, Mn(III) [176]) rendered the catalyst fully active at pH 7, so that the peroxidase–like activity was completely restored also towards non–phenolic substrates. The conversion results obtained at pH 3 and pH 7, both in the presence or in the absence of added Mn^{2+} and malonic acid are summarized in Figure 37.

Some kinetic parameters were calculated under different experimental conditions, and the related results are summarized in Table 14. The catalyst showed a substrate saturation behavior for both hydrogen peroxide and electron donors.

Inspection of the table shows that K_M values fell into the millimolar range, which explains why conversion is only partial for the less reactive substrates; on the other hand, reaction speed could be compatible with potential practical applications.

By this last view, it is worth noting that residual activity after six catalytic

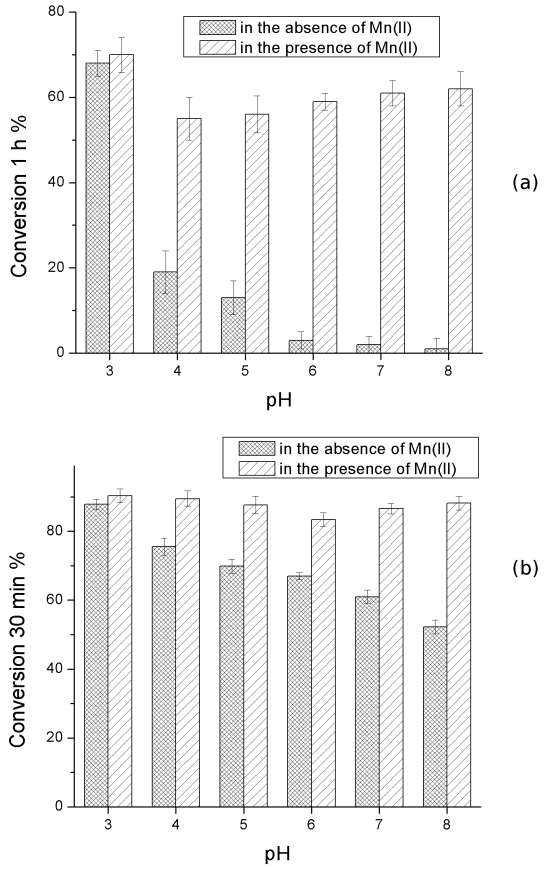

Figure 36: **Conversion yields for (a) VA and (b) azure B in the presence of the PP-–PVA/FeTFPP adduct at various pH values. Effect of pH on VA conversion (a): 100 mg of catalyst, 25 mM of McIlvaine buffer, 4.4 mM hydrogen peroxide and 1 mM VA. Final volume 5 mL. Effect of pH on azure B conversion (b): 100 mg of catalyst, 25 mM McIlvaine buffer, 0.88 mM hydrogen peroxide and 0.01 mM azure B. Final volume 5 mL. When working in the presence of Mn(II), 1 mM $MnSO_4$ and 50 mM malonic acid were added.**

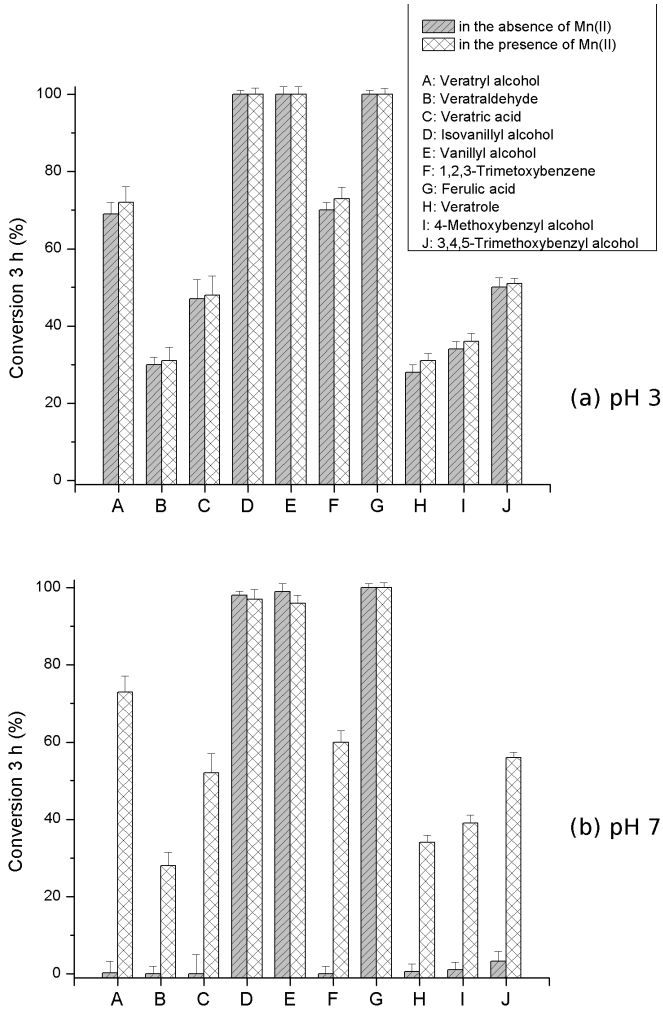

Figure 37: **Conversion yields of various electron donors by the PP–PVA/FeTFPP catalyst at pH 3 (a) and at pH 7 (b), both in the absence and in the presence of Mn^{2+} and malonic acid.**

Reducing Substrate	Substrate Varied	Kinetic Parameter	Value
VA	VA	K_M	1.18 ± 0.45 mM
	VA	k_{cat}	3.1 ± 0.4 min^{-1}
	VA	k_{cat}/K_M	2.6 ± 1.3 mM^{-1} min^{-1}
	H_2O_2	K_M	7.5 ± 1.0 mM
	H_2O_2	k_{cat}	3.2 ± 0.4 min^{-1}
	H_2O_2	k_{cat}/K_M	0.43 ± 0.11 mM^{-1} min^{-1}
AzB	AzB	K_M	0.021 ± 0.005 mM
	AzB	k_{cat}	0.068 ± 0.019 min^{-1}
	AzB	k_{cat}/K_M	3.38 ± 1.3 mM^{-1} min^{-1}
	H_2O_2	K_M	1.83 ± 0.45 mM
	H_2O_2	k_{cat}	0.081 ± 0.007 min^{-1}
	H_2O_2	k_{cat}/K_M	0.044 ± 0.014 mM^{-1} min^{-1}

Table 14: **Some kinetic parameters for the FeTFPP/PP–PVA adduct; *n* = *3*.**

cycles is still >80%, which is a quite encouraging performance (Table 15).

3.2.2 Reaction mechanism

The reaction between redox–active metalloporphines and hydrogen peroxide leading to homolytic cleavage of the O—O bond and OH• generation is well known [140, 177, 178]. Hydroxyl radical rapidly attacks the metalloporphine leading to irreversible catalyst degradation.

Such a situation (which usually prevents practical use of free metalloporphines as catalysts when H_2O_2 is used as the oxidant) dramatically changes

Cycle Number	% Catalytic Activity
1	100 ± 1
2	96 ± 3
3	95 ± 2
4	92 ± 3
5	89 ± 3
6	81 ± 4

Table 15: **Multicyclic activity of FeTFPP/PP–PVA as a LiP emulator in the presence of azure B as the electron donor. For each cycle 20 mg of catalyst were added to a mixture (1 mL final volume) containing 25 mM buffer, 0.88 mM hydrogen peroxide, and 0.01 mM azure B, at pH 3;** n **=** ***3.***

when an axial coordination of the metal ion by imidazole or pyridine takes place: in this case, a high-valent PorphMe=O species arises with a heterolytic cleavage mechanism [179, 180]. This is just the case of the described adduct, where FeTFPP molecules are coordinatively bound to pyridyl moieties on the polymer beads. That no hydroxyl radicals were generated upon H_2O_2 addition was confirmed by the observation that mannitol (a well–known OH• scavenger) was quite unable to affect the catalytic properties of the adduct, and that moreover no TBARS was found at all when 2–deoxyribose was added to the reaction mixtures (not shown).

In point of fact, the catalyst temporarily turned dark brown when treated with H_2O_2, and reverted gradually to red as the hydrogen donor was converted into product(s), when a phenolic substrate was used. This behavior strongly suggests that the catalyst was changed to an analogue of peroxidase Compound I upon addition of hydrogen peroxide. Figure 38 shows the differences that arose in reflectance spectra upon H_2O_2 treatment of the catalyst, and reversion

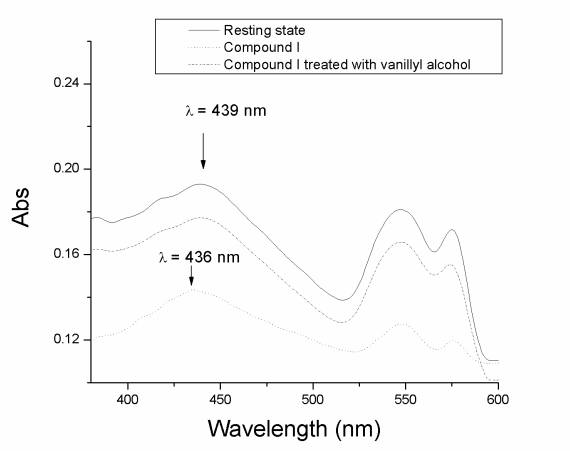

Figure 38: **Reflectance spectra of PP–PVA/FeTFPP upon treatment with H_2O_2 and upon further treatment with vanillyl alcohol (reactions were performed at pH 7).**

of Compound I to the resting state upon treatment with the phenolic substrate, vanillyl alcohol. Figure 39 shows the FT–IR spectrum of Compound I, clearly showing deep differences in comparison with adduct resting state (Figure 34). The hypothesized reaction pathways (including Compund I and II formation) for LiP–like and MnP–like activities are analogous to LiP and MnP reaction scheme (Figures 10 and 11, respectively).

The observation that only a fraction of VA was converted to the corresponding aldehyde prompted further investigation about the other products, arising from VA plus H_2O_2 in the presence of the catalyst. Oxidative degradation of VA (as well as that of other related methoxybenzenes) by LiP and MnP has been the object of a number of deep studies [93, 133, 147, 151, 158], and the conclusion has been reached, that the radical cation which is the first product of peroxidase action, rapidly evolves giving rise to several different products, depending on the experimental conditions tested; at least in the case of LiP and VP the conformation of the enzyme active site should play a role in driving the

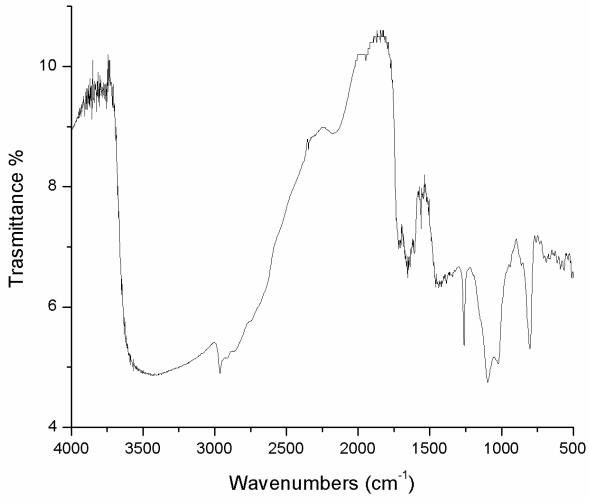

Figure 39: **FT–IR spectrum of Compound I.**

rearrangement of the primary radical cation. In the case of the heterogeneous catalyst described here, no active site comparable to that of true peroxidases is present, one face of the metalloporphine being fully exposed to the aqueous phase surrounding the polymer beads.

Therefore one can reasonably hypothesize that the primary radical cation quickly abandons the catalytic site and diffuses into the aqueous phase, its fate being no longer affected by the catalyst. Despite the sharp structural differences between the true LiP and the catalyst described here, the overall reaction mechanism seemed to parallel that found for LiP and MnP. Under the tested experimental conditions (pH = 3, no Mn^{2+} nor malonic acid added), only a fraction of VA was converted to veratraldehyde (about 9%), and even less to veratric acid (about 3%), as confirmed by HPLC and GC–MS analyses. Among the possible benzoquinone derivatives, already described among the products arising from LiP action on VA [147], only 2–hydroxymethyl–5–methoxy–1,4–benzoquinone was found in noticeable amounts (69%), so it could be well considered as the

main reaction product under the tested experimental conditions.

The compound was found however to be not very stable in aqueous environment (it was not detectable by GC analysis [147]), and this is why it was not used for quantitative determinations instead of veratraldehyde formation or azure B bleaching. The other quinones (if formed) were evidently so unstable under the experimental conditions tested, that most probably quickly underwent oxidative ring fission and/or rearrangement to other products, which escaped the identification by GC–MS. Accordingly, a fraction of VA was converted to a mixture of UV–absorbing, colorless products whose identification was not attempted although the formation of unsaturated lactones arising from VA ring oxidative cleavage could well be suggested [133].

The observed pH dependence of VA oxidation in the presence of the catalyst strongly supports a structural (protonation and/or charge state) change on the metalloporphine side, as VA is an uncharged species and cannot be protonated/deprotonated within the studied pH range.

This behavior strictly parallels that observed for the pH dependence of LiP–catalyzed oxidation of high redox–potential, non–phenolic substrates, and is more probably due to increased redox potentials of Compounds I and II at low pH values (maybe owing to the protonation of the ferryl oxygen) rather than to specific features of the heme pocket [181].

Emulation of MnP is a challenging task when specific catalysis is required, as a Mn^{2+} binding site has been found close to the ferriheme in the enzyme whereas phenolics oxidation is prevented by sterical hindrance and by lack of a long–range electron transfer pathway [103]; PP–PVA/FeTFPP adduct obviously lacks both such binding site and any residue hindering substrate approach to the redox–active centre. Therefore the conclusion could be drawn that its ability to oxidize Mn^{2+} to a (chelated) Mn(III) species must be inherent to FeTFPP axially bound to the pyridyl functionality on to polymer beads. Differently from MnP, Mn^{2+} oxidation took place only around neutrality, where the catalyst was unable to promote VA oxidation. An electrostatic repulsion between Mn^{2+} and positively charged Compounds I and II at low pH values could explain this behavior. This finding, together with the observation that the addition of Mn^{2+}

to the reaction mixtures is of no effect at pH 3 strongly supports the conclusion that the couple Mn(II)/Mn(III) could act under suitable pH conditions as a redox mediator in VA oxidation, but not vice versa.

The study about the PP–PVA/FeTFPP adduct is the first one dealing with the immobilization of the hydrophobic and water–insoluble iron(III)porphine FeTFPP on pyridyl–functionalized, crosslinked PVA polymer beads to obtain a stable, sharply hydrophilic, catalytically active preparation.

The obtained adduct showed interesting catalytic properties in aqueous environment, and in particular behaved as a LiP at acidic pH values, and turned to a MnP–like catalyst around neutrality. These activities render the catalyst potentially interesting for insoluble substrates such as lignin, as the redox couples VA/$VA^{\bullet+}$ and in particular Mn(II)/Mn(III) could easily shuttle between the insoluble catalyst and the insoluble substrate. Therefore this adduct could find future applications in the pulp and paper industry and wherever water–insoluble organic wastes of lignocellulosic nature should be oxidatively degraded.

For what in our knowledge, this is the first report of both LiP–like and MnP–like activity in the same immobilized metalloporphine, strictly resembling in this perspective rather VP catalysis.

3.2.3 Dyes bleaching

Besides AzB, PP–PVA/FeTFPP was also tested about its ability to bleach a complete serie of dyes belonging to different chemical classes (ARS, PNS, XO, MB, MG, and MO). The results are summed up in Figure 40.

PP–PVA/FeTFPP adduct, similarly to IPS/MnTSPP, effectively bleached all dyes. In 1 h the conversion was at least 40%. Conversely, the substrate specificity was completely different. IPS/MnTSPP, in fact, showed in the same time almost complete conversion of basic dyes like PNS and MG (Table 8 at page 73), while the slowest kinetics regarded acid dyes (ARS and XO particularly). In the case of PP–PVA/FeTFPP adduct, acid dyes like MO and XO were bleached almost completely in 1 h, while the other four showed almost similar conversion values (about 40–60%).

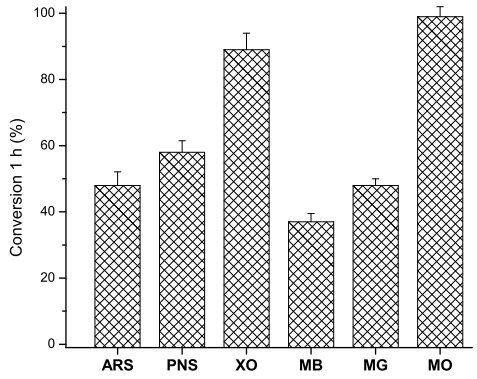

Figure 40: **PP-PVA/FeTFPP adduct effectively bleached several dyes belonging to different chemical classes.**

However, the wide substrate specificity and the conversion rates can be regarded in all cases as satisfactory, and promising in the perspective of the treatment of real textile wastewaters.

3.3 M–PVA/FeTFPP

Cytochrome P450 is a large superfamily of hemoproteins, catalyzing monooxygenase reactions [182], since O_2 is the oxidizing agent and NADPH the reducing agent.

In this enzyme, a mercapto group of a cysteine is present in the active site as proximal ligand of heme.

Since the ability of metalloporphines to emulate P450 catalysis during monooxygenase reactions has been deeply studied [126], some mercapto–grafted supports have been synthesized (both SG and PVA–based) and their ability to immobilize commercial metalloporphines has been investigated, as reported on Table 16.

Metalloporphine	% Relative Activity	
	MSG	M–PVA
MnTSPP	n.a.	25
FeTFPP	28	100
MnTMPP	32	38

Table 16: **Relative activity of some mercapto–grafted supports during immobilization of metalloporphines ($n = 3$). In the case of MSG/MnTSPP, no stable bounding between metalloporphine and support was experienced.**

The inspection of the table shows that the best combination was M–PVA/FeTFPP, while both silica–based and MnTMPP–containing catalysts gave poor results. Accordingly, the study was mainly focused on the former adduct.

M–PVA was able to bind 8.81 mg FeTFPP per g of support (when 20 mg of metalloporphine was added), showing a saturating behavior similar to that described for IPS/MnTSPP and PP-PVA/FeTFPP. This FeTFPP concentration was chosen since it allowed the highest specific catalytic activity (data not shown).

As a point of fact, M–PVA/FeTFPP was not able in the presence of O_2 and NADPH to act as a monooxygenase with various possible oxygen–acceptors. The situation, however, drastically changed when H_2O_2 was present in the reaction mixture: under these conditions, M–PVA/FeTFPP became able to act as a peroxidase–like catalyst, both in VA and ARS oxidations. In the case of VA, a pattern of oxidation similar to that obtained with IPS/MnTSPP (Figure 17 at page 66) was observed, as a rising peak at 310 nm was present likely due to veratraldehyde production. This hypothesis was corroborated by UV–HPLC data, showing in 3 h a 22% yield in aldehyde, while no veratric acid was formed. Unfortunately, VA conversion was very poor as in 3 h only 18% of starting substrate was oxidized. Small amounts of 2–hydroxymethyl–5–methoxy–1,4–benzoquinone were also detected (less than 5%), suggesting a quite different

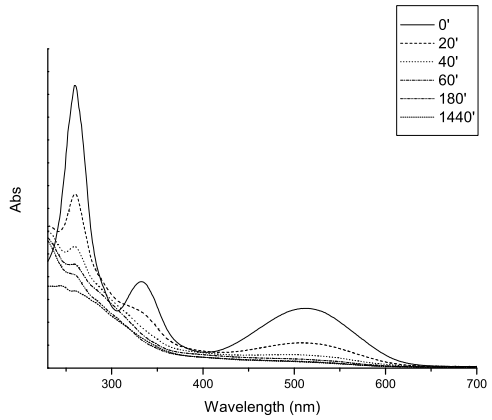

Figure 41: **Spectral changes during oxidative catalytic degradation of ARS by 8.8 mM H_2O_2 in the presence of M–PVA/FeTFPP catalyst in 25 mM McIlvaine buffer, pH 3.**

catalytic route if compared with PP–PVA/FeTFPP.

In the case of ARS, instead, better performances were observed, conversion being over 80% in 1 h (Figure 41).

This behavior can be explained as VA can be only oxidized through mono–electronic oxidations. While ARS (or better ARS partial oxidation–deriving species) can be also substrate for monooxygenase reactions (§3.1.3.1).

During this study, the possibility for metalloporphines to act both as mono–electronic oxidant and as oxygen donor, has already been stressed. This results suggest that mercapto–coordinating group is able to make the latter route more likely, according with attempted structural emulation. In fact, enzymes like LiP, MnP, and VP present imidazole as proximal coordinating group. These enzymes are only able to perform mono–electronic oxidations In good agreement, imidazolyl–supported metalloporphines (such as IPS/MnTSPP) are able of almost complete conversion of substrates like VA. Mercapto coordinating group,

instead, changed their activity towards oxygen—donor ability, as in cytochrome P450.

The M–PVA/FeTFPP catalysis with both VA and ARS has been investigated on a broad pH range, also in presence of Mn(II) to emulate MnP–like action. The results are reported in Figure 42.

VA oxidation showed a maximum at pH 3, but Mn(II) presence was able to dramatically increase this activity, with maximum at pH 4 and 6. However, the values are quite similar in the whole pH range tested, in a similar manner as shown when the same metalloporphine was pyridyl–immobilized (Figure 36).

On the other hand, a quite different pattern was observed for ARS bleaching. In this case, Mn(II) clearly affected catalytic activity, that was lower and stable through pH range test. In its absence, ARS bleaching was faster, presenting an optimum at pH 3.

Catalyst was also kinetically characterized, showing a typical Michaelis–Menten saturation for both VA and ARS (Table 17).

A comparison with similar data for IPS/MnTSPP and PP-PVA/FeTFPP, clearly confirms lower M–PVA/FeTFPP specificity for VA, and also k_{cat} was lower. While, performances with ARS were comparable to analogous data for IPS/MnTSPP.

The poor LiP–like performances of M–PVA/FeTFPP were confirmed during oxidation screening of various lignin–model compounds (Figure 43).

Conversion was only partial also with phenolic substrates, since 87% of ferulic acid, and only 30% and 46% respectively of isovanillyl and vanillyl alcohol were removed in 1 h, while both IPS/MnTSPP and PP-PVA/FeTFPP were able of almost complete conversions.

Veratric acid, 1,2,3–trimethoxybenzene, and 3,4,5–trimethoxybenzyl alcohol were not M–PVA/FeTFPP substrates at all. In all other cases, 1 h conversion was comprised between 10 and 20%. This is a very low value, especially if compared with IPS/MnTSPP and PP–PVA/FeTFPP results (Table 7 and Figure 37, respectively).

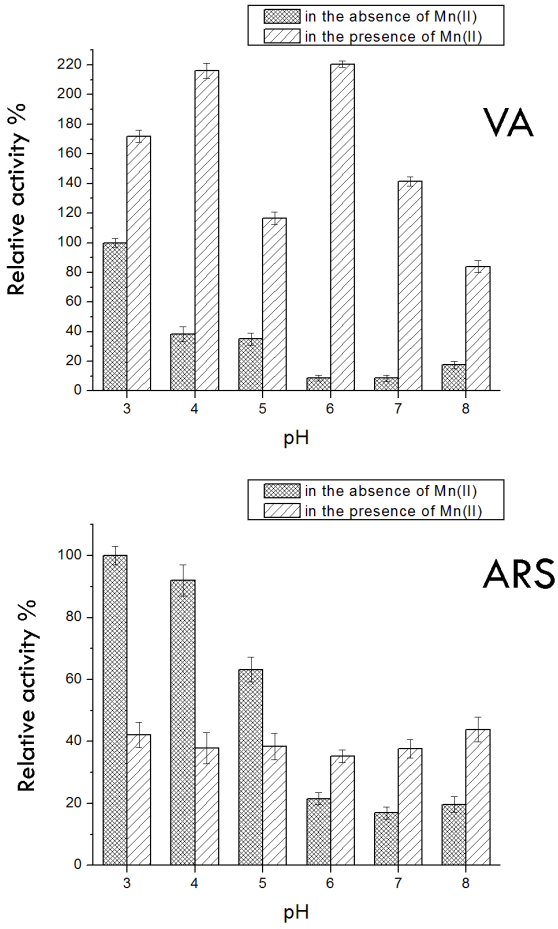

Figure 42: **Relative activity for VA and ARS in the presence of the M–PVA/FeTFPP adduct at various pH values. When working in the presence of Mn(II), 1 mM $MnSO_4$ and 50 mM malonic acid were added.**

Reducing Substrate	**Substrate Varied**	**Kinetic Parameter**	**Value**
VA	VA	K_M	7.6 ± 2.5 mM
	VA	k_{cat}	0.47 ± 0.04 min^{-1}
	VA	k_{cat}/K_M	0.06 ± 0.02 mM^{-1} min^{-1}
	H_2O_2	K_M	1.5 ± 0.2 mM
	H_2O_2	k_{cat}	0.41 ± 0.06 min^{-1}
	H_2O_2	k_{cat}/K_M	0.28 ± 0.07 mM^{-1} min^{-1}
ARS	ARS	K_M	1.12 ± 0.02 mM
	ARS	k_{cat}	2.0 ± 0.2 min^{-1}
	ARS	k_{cat}/K_M	1.8 ± 0.5 mM^{-1} min^{-1}
	H_2O_2	K_M	2.3 ± 0.3 mM
	H_2O_2	k_{cat}	1.46 ± 0.05 min^{-1}
	H_2O_2	k_{cat}/K_M	0.65 ± 0.09 mM^{-1} min^{-1}

Table 17: **Some kinetic parameters for the M–PVA/FeTFPP adduct; *n* = *3*.**

Besides Mn(II), also other redox mediators were tested with similar results (Table 18).

While ARS bleaching was not greatly affected by their presence, VA oxidation was triplicated for instance in the presence of OH–TEMPO.

According to all these data reported, M–PVA/FeTFPP was not a good LiP emulator. This finding was corroborated also by multicycle analysis. During VA oxidation, only 7% of activity was still present at the second cycle. Afterwards, catalytic activity was completely lost.

More promising results were, instead, obtained for ARS (Table 19).

Inspection of table suggests quite a similar behavior if compared with IPS/Mn-

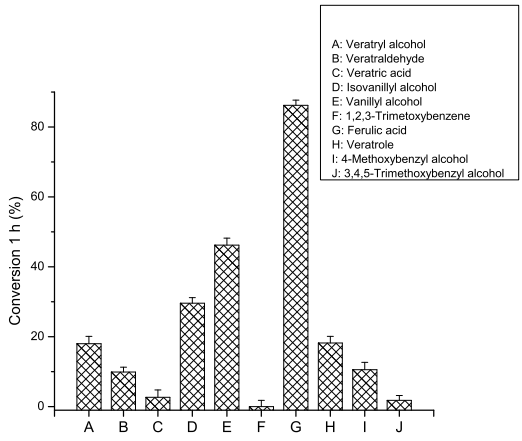

Figure 43: **Sustrate specificity of M–PVA/FeTFPP adduct with various lignin–model compounds. Catalytic activity was detected in the presence of 10 mg of catalyst, 8.8 mM hydrogen peroxide, 1 mM substrate, DME 10%, 1 mM $MnSO_4$ and 50 mM malonic acid, and 25 mM buffer pH 4 (final volume 2 mL). Samples were then analyzed through UV–HPLC.**

Redox	% Remaining Activity	
Mediator	VA	ARS
None	100	100
OH–TEMPO	314	68
NHT	20	110
NHS	259	106
NPH	104	116

Table 18: **The presence of some redox mediators seems to affect the oxidation rate of VA and ARS. Percentage of activity is referred to a control experiment in absence of mediators ($n = 3$).**

TSPP bleaching.

The ability of M–PVA/FeTFPP to bleach a complete serie of dyes belonging to different chemical classes (ARS, PNS, XO, MB, MG, and MO) was also tested. The results are summarized in Figure 44.

The acid dyes MO and ARS were almost completely degraded in 1 h, whereas PNS, MG, and MB conversuib rate were about 50% in the same time. Only XO were decolorated with a slower kinetics (only 20% conversion).

However, in all cases the adduct was catalytically active, confirming the wide substrate specificity of immobilized metalloporphine.

The comparison of these results with the analogous ones for IPS/MnTSPP and PP–PVA/FeTFPP (Table 8 and Figure 40 respectively) clearly shows how, in the worst circumstance, the combination of these three catalysts could conceivably allow a complete decoloration of any textile waste.

In conclusion, the use of the mercapto group to immobilize metalloporphines gave quite poor results, not comparable to what observed in the cases of imidazole and pyridine. Particularly, in the perspective of industrial applications.

Cycle Number	% Catalytic Activity
1	100 ± 1
2	85 ± 4
3	67 ± 5
4	55 ± 3
5	38 ± 2
6	28 ± 4
7	16 ± 2
8	12 ± 2
9	11 ± 1
10	11 ± 2

Table 19: **Multicyclic activity of M–PVA/FeTFPP in the presence of ARS as the electron donor. For each cycle 10 mg of catalyst were added to a mixture (1 mL final volume) containing 25 mM buffer, 8.8 mM hydrogen peroxide, and 2.36 mM ARS, at pH 3;** $n = 3$.

However, the collected data suggest mercapto function to change FeTFPP route of catalysis, since oxygen—donor behavior became more likely than mono–electronic oxidative one.

3.4 MnTMPP

During this study a hydrosoluble acid metalloporphine and a hydrophobic one were studied. In order to complete the chemical spectrum of analyzed metalloporphines, a basic hydrosoluble metalloporphine was included: MnTMPP. This can be regarded as an ideal catalyst for industrial processes, since it is a very stable and catalytically active metalloporphine commercially available at a reasonable price.

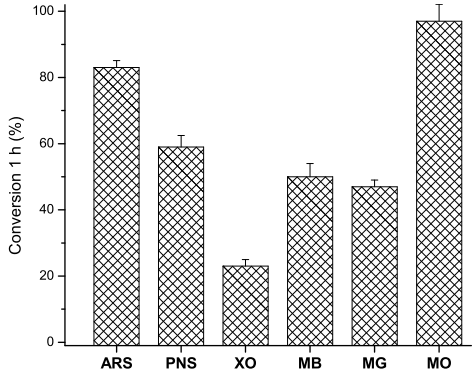

Figure 44: **M–PVA/FeTFPP adduct effectively bleached several dyes belonging to different chemical classes.**

Accordingly, this metalloporphine was immobilized on the already synthesized supports, imidazolyl and pyridyl–grafted, both SG and PVA–based. Some control experiments with plain SG and PVA were also performed. The results are summarized in Table 20.

The sharp basicity of MnTMPP (four quaternary ammonium cations per molecule) strongly affected its immobilization on supports that were grafted with basic functions. Consequently, no effective immobilization was possible neither on pyridine and imidazole–grafted supports.

The highest metalloporphine loading was obtained with plain SG, probably due to its acid properties and cation exchange ability. Quite surprisingly, also plain crosslinked PVA was able to load a small (but comparable to grafted supports) amounts of MnTMPP.

Besides, all the tiny amounts of immobilized MnTMPP presented negligible catalytic activity.

Accordingly, no real LP emulation was obtained with MnTMPP. The collected data suggested ion exchange as the most feasible way for its immobiliza-

Support	**MnTMPP bound (mg/g support)**
SG	4.1 ± 0.8
IPS	n.d.
PSG	n.d.
PVA	2.9 ± 0.3
Im–PVA	3.6 ± 0.2
PP-PVA	2.8 ± 0.4

Table 20: **MnTMPP was not effectively immobilized neither with pyridine, or imidazole–grafted supports; $n = 3$, n.d.: not detectable.**

tion (for instance using a more acid support than plain SG). However, such case falls beyond the scope of this work since no LP emulation could be obtained.

In this perspective, MnTMPP use was then abandoned.

4 CONCLUSIONS

Oxidative approaches towards removal of lignocellulosic and related materials are not currently featured by enough efficiency and inexpensiveness. Accordingly, in order to decrease environmental impact and economical costs of industrial processes, new methods need to be proposed.

In this perspective, during this study several catalysts have been developed, using properly immobilized commercial metalloporphines mimicking lignolytic peroxidase catalysis.

Emulation of these enzymes was achieved by grafting on inexpensive supports (such as SG and PVA) coordinating groups like imidazole and pyridine, resembling heme coordination in active site of peroxidases. In particular acid hydrosoluble MnTSPP was best immobilized on imidazole–grafted support, while hydrophobic FeTFPP gave optimum results when coordinated by pyridyl functions, leading to real LP structural emulation.

The catalysts were then catalytically characterized about LiP, and MnP–like activity, in order to elucidate if structural emulation was also able to lead to functional emulation.

IPS/MnTSPP showed very promising LiP–like catalytic abilities in VA and other lignin–model compounds oxidation, while no action upon Mn(II) was observed. However, it appears suitable for applications in many industrial fields, since a deep oxidative action was shown. Furthermore, the mild operational conditions used (low temperature, neutral pH, low pressure, "clean" oxidant,

absence of any organic solvents) strongly suggest future industrial applications in treatment of lignocellulosic materials.

IPS/MnTSPP was also investigated about the bleaching of several textile dyes, belonging to different chemical classes. The catalyst was able to degrade all dyes, showing a wide substrate specificity. Even in this case, catalysis was featured by a high efficiency combined with very mild conditions, quite promising for real textile wastewaters treatment. Biomimetic bleaching was also compared with enzymatic catalysis, the former being more effective especially in the perspective of industrial applications.

PP–PVA/FeTFPP adduct showed, on the contrary, both a LiP and MnP–like activity, closer resembling VP emulation. This is the first report of such catalytic activity for an immobilized metalloporphine. The oxidative action was also in this case deep, effective, and featured by extremely mild operational conditions.

Its ability to use both VA/$VA^{\bullet+}$ and Mn(II)/Mn(III) redox couples allows PP–PVA/FeTFPP to found application in industrial treatment of many water–insoluble wastes, since both Mn(III) and $VA^{\bullet+}$ can easily shuttle between the insoluble catalyst and the insoluble substrate.

Some molecular details of the catalysis were also obtained, identifying similarities and differences between biomimetic and enzymatic catalysis. In particular, the ability of immobilized metalloporphines to act as oxygen–donor was showed, explaining deeper oxidative action. This can be a crucial feature in order to make feasible industrial applications of these catalysts.

Also cytochrome P450 structural emulation was attempted, but catalytic features of the adducts were quite poor.

Basic metalloporphine MnTMPP was also tested, but no effective immobilization resembling LPs was achieved.

On the whole, these data outline new perspectives for oxidative removal of lignocellulosic and related materials, both water–soluble and water–insoluble. The described catalysts represent effective and economical feasible alternative

towards this issue, since they are particularly suitable for large scale scaling–up.

In particular, the extremely mild operational conditions can dramatically change the approach during pulp and paper bleaching, and oxidation of industrial wastewaters.

Accordingly, the next step will be the treatment of real industrial substrates (such as lignocellulosic, textile, and olive mill wastewaters), in the perspective of developing scaled–up industrial processes.

However, the number of tested supports and metalloporphines can also be broadened, in order to optimize operational conditions and catalytic efficiency. In this context, the effect of redox mediators would be also taken in extreme care, as it can allow to treat also water–insoluble substrates.

Acknowledgment

This work has been possible due to my supervisor Prof. Enrico Sanjust, Dr. Antonio Rescigno and Dr. Francesca Sollai from the laboratory of Biological Chemistry section of Cagliari University.

Some grants funded my experiments: in particular, funding came from Italian Ministry of University and Research (FIRB Project RBAU01CJP9), and Regione Autonoma Sardegna (PO Sardegna FSE 2007–2013, LR 7/2007 "Promozione della ricerca scientifica e dell'innovazione tecnologica in Sardegna", project CRP1_27).

I would like to thank Prof. Emil Dumitriu for his kind assistance, and all the Catalysis Laboratory of Technical University "Gheorghe Asachi" (in particular Brindusa and Alex) that helped me during my research period in Iasi.

This work would not be the same without some GC–MS and FT–IR analysis: for these, I would thank Prof. Roberto Monaci and Dr. Alessandra Garau.

The contribute of the reviewers (Prof. Francisco Amado and Prof. Vasile Hulea) has also been crucial, their criticism and suggestions substantially improving my work.

Il dottorato è un percorso molto più lungo dei tre anni di cui sarebbe composto. Non foss'altro perché sono tre, ma mi hanno fatto invecchiare per cento, e soprattutto poiché giunge al culmine di un intero cammino di studio e di ricerca che ha radici lontane, e che comunque non avrei potuto intraprendere da solo. Non è semplice pertanto menzionare tutte le persone che in questi anni mi hanno aiutato, incoraggiato ed in qualche maniera sostenuto.

A cominciare dalla mia famiglia, che ha permesso che io mi potessi dedicare a questo lavoro. Non sono stati anni facili, ma spero che loro siano i primi a

comprendere l'importanza ed il valore di questo traguardo, e pertanto il valore e l'importanza che ha avuto per me il loro sostegno.

Non vorrei tralasciare tutte le persone che sono passate in laboratorio in questi anni, che in maniera più o meno diretta hanno contribuito ben più forse di quanto loro stessi immaginano (un lavoro di così tanti anni non è fatto solo di esperimenti): Lau, Carletta, Simo, Cla. Sono i primi che mi vengono in mente, ma non certo i soli. Vorrei ringraziare i miei amici (soprattutto per essermi rimasti tali nonostante le numerose batoste che gli ho rifilato a fantacalcio in questi anni, e che hanno permesso al mio morale di mantenersi sempre e comunque alto, volendo escludere la spiacevole parentesi di questi ultimi mesi), ed in particolare Emmanuele, che col suo lavoro professionale (e gratuito) ha notevolmente abbellito la tesi.

References

[1] Lin Y and Tanaka S. Ethanol fermentation from biomass resources: current state and prospects. *Applied Microbiology and Biotechnology*, (69):627–642, 2006.

[2] Akhtar M, Attridge MC, Myers GC, Kirk TK, and Blanchette RA. Biochemical pulping of lobolly pine with different strains of the white-rot fungus *Ceriporiopsis subvermispora*. *TAPPI Journal*, (75):105–109, 1992.

[3] European Commission. Reference document on best available techniques in the pulp and paper industry. 2001.

[4] Sun Y and Cheng J. Hydrolysis of lignocellulosic materials for ethanol production: a review. *Bioresource Technology*, (83):1–11, 2002.

[5] Inderwildi O and King D. Quo vadis biofuels? *Energy Environmental Science*, (2):343–346, 2009.

[6] Biørsvik HM and Minisci F. Fine chemicals from lignosulfonates. 1. Synthesis of vanillin by oxidation of lignosulfonates. *Organic Process Research & Development*, (3):330–340, 1999.

[7] Biørsvik HM and Minisci F. Fine chemicals from lignosulfonates. 2. Synthesis of veratric acid from acetovanillon. *Organic Process Research & Development*, (3):341–346, 1999.

[8] Hamdi M. Future prospects and constraints of olive oil mill wastewater use and treatment: a review. *Bioprocess Engineering*, (8):208–214, 1993.

[9] Ayed L, Assas N, Sayadi S, and Hamdi M. Involvement of lignin peroxidase in the decolourization of black olive mill wastewaters by *Geotrichum candidum*. *Letters in Applied Microbiology*, (40):7–11, 2005.

[10] Zucca P, Vinci C, Sollai F, Rescigno A, and Sanjust E. Degradation of Alizarin Red S under mild experimental conditions by immobilized 5,10,15,20-tetrakis(4-sulfonatophenyl)porphine–Mn(III) as a biomimetic peroxidase-like catalyst. *Journal of Molecular Catalysis A: Chemical*, (288):97–102, 2008.

[11] Kuhad RC, Singh A, and Eriksson K-EL. *Microorganisms and enzymes involved in the degradation of plant fiber cell walls*. In: Eriksson K–EL (ed.) *Advances in Biochemical Engineering Biotechnology*. Springer–Verlag, Berlin, 1997.

[12] Fengel D and Wegener G. *Wood – Chemistry, Ultrastructure, Reactions*. Walter de Gruyter, Berlin, 1989.

[13] Eriksson K-EL, Blanchette RA, and Ander P. *Microbial and enzymatic degradation of wood components*. Springer–Verlag, Berlin, 1990.

[14] McDougall GJ, Morrison IM, Stewart D, Weyers JDB, and Hillman JR. Plant fibres: Botany, chemistry and processing for industrial use. *Journal of the Science of Food and Agriculture*, (62):1–20, 1993.

[15] Higuchi T. Lignin biochemistry: biosynthesis and biodegradation. *Wood Science and Technology*, (24):23–63, 1990.

[16] Dittmar T and Lara RJ. Molecular evidence for lignin degradation in sulfate-reducing mangrove sediments (Amazonia, Brazil). *Geochimica et Cosmochimica Acta*, (65):1417–1428, 2001.

[17] Billa E, Koukios EG, and Monties B. Investigation of lignins structure in cereal crops by chemicaldegradation methods. *Polymer Degradation and Stability*, (59):71–75, 1998.

[18] Nada AA, El-Sarkhawy M, and Kamel SM. Infra-red spectroscopic study of lignins. *Polymer Degradation and Stability*, (60):247–251, 1998.

[19] Kögel-Knaber I. The macromolecular organic composition of plant and microbial residues as inputs to soil organic matter. *Soil Biology & Biochemistry*, (34):139–162, 2002.

[20] Goujon T, Sibout R, Aymerick E, MacKay J, and Jouanin L. Genes involved in the biosynthesis of lignin precursors in *Arabidopsis thaliana*. *Plant Physiology & Biochemistry.*, (41):677–687, 2003.

[21] Boerjan W, Ralph J, and Baucher M. Lignin biosynthesis. *Annual Review of Plant Biology*, (54):519–546, 2003.

[22] Davin LB and Lewis NG. Lignin primary structures and dirigent sites. *Current Opinion in Biotechnology*, (16):407–415, 2005.

[23] Umezawa T. The cinnamate/monolignol pathway. *Phytochemistry Reviews*, (9):1–17, 2010.

[24] Adler T. Lignin chemistry – past, present and future. *Wood Science and Technology*, (11):69–218, 1977.

[25] Evtuguin DV, Neto CP, Silva AMS, Domingues PM, Amado FML, Robert D, and Faix O. Comprehensive Study on the Chemical Structure of Dioxane Lignin from Plantation *Eucalyptus globulus* Wood. *Journal of Agricultural and Food Chemistry*, (4):4252–4261, 2001.

[26] Ralph J. Hydroxycinnamates in lignification. *Phytochemistry Reviews*, (9):65–83, 2010.

[27] Elfstrand M, Sitbon F, Lapierre C, Bottin A, and von Arnold S. Altered lignin structure and resistance to pathogens in spi 2-expressing tobacco plants. *Planta*, (214):708–716, 2002.

[28] Ranocha P, Chabannes M, Chamayou S, Danoun S, Jauneau A, Boudet AM, and Goffner D. Laccase down–regulation causes alterations in phenolic metabolism and cell wall structure in poplar. *Plant Physiology*, (129):145–155, 2002.

[29] Terashima N, Atalla RH, Ralph SA, Landucci LL, Lapierre C, and Monties B. New preparations of lignin polymer models under conditions that approximate cell well lignification. I: Synthesis of novel lignin polymer models and their structural characterization by 13C NMR. *Holzforschung*, (49):521–527, 1995.

[30] Guan SY, Mlynar J, and Sarkanen S. Dehydrogenative polymerization of coniferyl alcohol on macromolecular lignin templates. *Phytochemistry*, (45):911–918, 1997.

[31] Syrjanen K and Brunow G. Regioselectivity in lignin biosynthesis. The influence of dimerization and cross-coupling. *Journal of the Chemical Society, Perkin Transaction 1*, (2):183–187, 2000.

[32] Grabber JH. How do lignin composition, structure, and cross-linking affect degradability? A review of cell wall model studies. *Crop Science*, (45):820–831, 2005.

[33] Matsuita Y, Sekiguchi T, Ichino R, and Fukushima K. Electropolymerization of coniferyl alcohol. *Journal of Wood Science*, (55):344–349, 2009.

[34] Burlat V, Kwon M, Davin LB, and Lewis NG. Dirigent proteins and dirigent sites in lignifying tissues. *Phytochemistry*, (57):883–897, 2001.

[35] Lourith N, Katayama T, and Toshisada S. Stereochemistry and biosynthesis of 8-O-4' neolignans in Eucommia ulmoides: diastereoselective formation of guaiacylglycerol-8-O-4'-(sinapyl alcohol) ether. *Journal of Wood Science*, (51):370–378, 2005.

[36] Chen YR and Sarkanen S. Macromolecular replication during lignin biosynthesis. *Phytochemistry*, (71):453–462, 2010.

[37] Hatfield R and Vermerris W. Lignin formation in plants. The dilemma of linkage specificity. *Plant Physiology*, (126):1351–1357, 2001.

[38] Evtuguin DV and Amado FML. Application of electrospray ionization mass spectrometry to the elucidation of the primary structure of lignin. *Macromolecular Bioscience*, (3):339–343, 2003.

[39] Vanholme R, Morreel K, Ralph J, and Boerjan W. Lignin engineering. *Current Opinion in Plant Biology*, (11):278–285, 2008.

[40] Forgacs E, Cserháti T, and Oros G. Removal of synthetic dyes from wastewaters: a review. *Environmental International*, (30):953–971, 2004.

[41] Archibald FS. A new assay for lignin type peroxidase employing the dye Azure B. *Applied & Enviromental Microbiology*, (58):3110–3116, 1992.

[42] Pierce J. Colour in textile effluents - the origins of the problem. *Journal of the Society of Dyers and Colourists*, (110):131–134, 1994.

[43] European Commission. European directive relating to restrictions on the marketing and use of certain dangerous substances and preparation (azocolourants). 2002/61.

[44] Platzek T, Lang C, Grohmann G, Gi US, and Baltes W. Formation of a carcinogenic aromatic amine from an azo dye by human skin bacteria in vitro. *Human & Experimental Toxicology*, (18):552–559, 1999.

[45] Walthall WK and Stark JD. The acute and chronic toxicity of two xanthene dyes, fluorescein sodium salt and phloxine B, to Daphnia pulex. *Environmental Pollution*, (104):207–215, 1999.

[46] Guarantini CCI and Zanoni MVB. Textile dyes. *Quimica Nova*, (23):71–78, 2000.

[47] Tsuda S, Murakami M, Kano K, Taniguchi K, and Sasaki YF. DNA damage induced by red food dyes orally administered to pregnant and male mice. *Toxicological Sciences*, (61):92–99, 2001.

[48] Roncero MB, JF Colom, and Vidal T. Application of post–treatments to the ozone bleaching kinetics of an XO–kraft pulp. *Journal of Wood Chemistry and Technology*, (20):147–167, 2002.

[49] Pham PL, Alric Y, and Delmas M. Incorporation of xylanase in total chlorine flee bleach sequences using ozone and hydrogen peroxide. *Appita J*, (48):213–217, 1995.

[50] Roncero MB, Torres AL, JF Colom, and Vidal T. Effects of xylanase treatment on fibre morphology in totally chlorine free bleaching (CFC) of Eucaliptus pulp. *Process Biochemistry*, (36):45–50, 2000.

[51] McMillan JD. *Pretreatment of lignocellulosic biomass.* In: Himmel ME, Baker JO and Overend RP (eds.)*, Enzymatic Conversion of Biomass for Fuels Production*. American Chemical Society, Washington DC, 1994.

[52] Grous WR and Saddler JN. Effect of steam explosion pretreatment on pore size and enzymatic hydrolysis of poplar. *Enzyme and Microbial Technology*, (8):274–280, 1986.

[53] Mackie KL, Brownell HH, West KL, and Saddler JK. Effect of sulphur dioxide and sulphuric acid on steam explosion of aspenwood. *Journal of Wood Chemistry and Technology*, (5):405–425, 1985.

[54] Morjanoff PF and Gray PP. Optimization of steam explosion as method for increasing susceptibility of sugarcane bagasse to enzymatic saccharification. *Biotechnology and Bioengineering*, (29):733–741, 1987.

[55] Mes-Hartree M, Dale BE, and Craig WK. Comparison of steam and ammonia pretreatment for enzymatic hydrolysis of cellulose. *Applied Microbiology and Biotechnology*, (29):462–468, 1988.

[56] Vlasenko EY, Ding H, Labavitch JM, and Shoemaker SP. Enzymatic hydrolysis of pretreated rice straw. *Bioresource Technology*, (59):109–119, 1997.

[57] Zheng YZ, Eddy C, Deanda K, Finkelstein M, and Picataggio S. Pretreatment for cellulose hydrolysis by carbon dioxide explosion. *Biotechnology Progress*, (14):890–896, 1998.

[58] Chakar FS and Ragauskas AJ. Review of current and future softwood kraft lignin process chemistry. *Industrial Crops and Products*, (20):131–141, 2004.

[59] Pinto PC, Evtuguin DV, Neto CP, Silvestre AJD, and Amado FML. Behavior of *Eucalyptus globulus* lignin during kraft pulping. II. Analysis by NMR, ESI/MS, and GPC. *Journal of Wood Chemistry and Technology*, (22):109–125, 2002.

[60] Millet Ma, Baker AJ, and Scatter LD. Physical and chemical pretreatment for enhancing cellulose saccharification. *Biotechnology & Bioengineering Symposium*, (6):125–153, 1976.

[61] Iyer PV, Wu ZW, Kim SB, and Lee YY. Ammonia recycled percolation process for pretreatment of herbaceous biomass. *Applied Biochemistry and Biotechnology*, (57/58):121–132, 1996.

[62] Marques AP, Evtuguin DV, Magina S, Amado FML, and Prates A. Structure of Lignosulphonates from Acidic Magnesium–Based Sulphite Pulping of *Eucalyptus globulus*. *Journal of Wood Chemistry and Technology*, (29):337–357, 2009.

[63] Gellersted G and Gierer J. The reactions of lignin during neutral sulphite pulping. Part III. The mechanism of formation of styrene-b-sulphonic acid structures. *Acta Chemica Scandinavica*, (24):1645–1654, 1970.

[64] Gellersted G and Gierer J. The Reactions of Lignin during Neutral Sulfite Pulping. Part VIII. Sulfonic Acids Isolated after Treatment of Spruce Wood Meal with Neutral Sulfite. *Acta Chemica Scandinavica*, (31B):729–730, 1977.

[65] Lebo SE, Gargulak JD, and McNally TJ. Lignin. *Kirk–Othmer Encyclopedia of Chemical Technology*, pages 1–32, 2001.

[66] Lopez F, Ariza J, Eugenio ME, Díaz J, Pérez I, and Jiménez L. Pulping and bleaching of pulp from olive tree residues. *Process Biochemistry*, (37):1–7, 2001.

[67] Lehtimaa T, Tarvo V, Kuitunen S, Jaaskelainen AS, and Vuorinen T. The Effect of Process Variables in Chlorine Dioxide Prebleaching of Birch Kraft Pulp. Part 1. Inorganic Chlorine Compounds, Kappa Number, Lignin, and Hexenuronic Acid Content . *Journal of Wood Chemistry and Technology*, (30):1–18, 2010.

[68] Jiménez L, Navarro E, Ferrer JL, Lopéz F, and Ariza J. Biobleaching of cellulose pulp from wheat straw with enzymes and hydrogen peroxide. *Process Biochemistry*, (35):149–157, 1999.

[69] Lopez F, Diaz MJ, Eugenio ME, Ariza J, Rodriguez A, and Jiménez L. Optimization of hydrogen peroxide in totally chlorine free bleaching of cellulose pulp from olive tree residues. *Bioresource Technology*, (87):255–261, 2003.

[70] Gellersted G and Petterson I. Chemical aspects of hydrogen peroxide bleaching. Part II The bleaching of Kraft pulps. *Journal of Wood Chemistry and Technology*, (2):231–250, 1982.

[71] Yamashita Y, Shono M, Sasaki C, and Nakamura Y. Alkaline peroxide pretreatment for efficient enzymatic saccharification of bamboo. *Carbohydrate Polymers*, (79):914–920, 2010.

[72] Bentivenga G, Bonini C, D'Auria M, and De Bona A. Degradation of steam exploded lignin from beech by using Fenton's reagent. *Biomass and Bioenergy*, (24):233–238, 2003.

[73] Mansilla HD, Yeber MC, Freer J, Rodríguez J, and Baeza J. Homogeneous and heterogeneous advanced oxidation of a bleaching effluent from the pulp and paper industry. *Water Science and Technology*, (36):273–278, 1997.

[74] Tanaka K, Calanag RC, and Hisanaga T. Photocatalyzed degradation of lignin on TiO_2. *Journal of Molecular Catalysis*, (138):287–294, 1999.

[75] Roncero MB, Torres AL, JF Colom, and Vidal T. TFC bleaching of wheat straw pulp using ozone and xylanase. Part A: paper quality assessment. *Bioresource Technology*, (87):305–314, 2003.

[76] Machado AE, de Mirand JA, Freitas RF, Duarte ET, Ferreira LF, Albuquerque YD, Ruggiero R, Sattler C, and de Oliveira L. Destruction of the organic matter present in the effluent from a cellulose and paper industry using photocatalysis. *Journal of Photochemistry and Photobiology*, (155):231–241, 2003.

[77] Hostachy JC, Lenon G, Pisicchio JL, Coste C, and Legay C. Reduction of pulp and paper mill pollution by ozone treatment. *Water Science and Technology*, (35):261–268, 1997.

[78] Vidal PF and Molinier J. Ozonolysis of lignin – improvement of in vitro digestibility of poplar sawdust. *Biomass*, (16):1–17, 1988.

[79] Evtuguin DV, Daniel AID, Silvestre AJD, Amado FML, and Neto CP. Lignin aerobic oxidation promoted by molybdovanadophosphate polyanion $[PMo_7V_5O_{40}]^{8-}$. Study on the oxidative cleavage of β–O–4 aryl ether structures using model compounds. *Journal of Molecular Catalysis A: Chemical*, (154):217–224, 2000.

[80] Collins TJ. TAML Oxidant Activators: A New Approach to the Activation of Hydrogen Peroxide for Environmentally Significant Problems. *Accounts of Chemical Research*, (35):782–790, 2002.

[81] Weinstock IA, Atalla RH, Reiner RS, Moen MA, Hammel KE, Houtman CJ, Hill CL, and Harrup MK. A new environmentally benign technology for transforming wood pulp into paper. engineering polyoxometalates as catalysts for multiple processes. *Journal of Molecular Catalysis A: Chemical*, (116):59–84, 1997.

[82] Crestini C, Caponi MC, Argyropoulos DS, and Saladino R. Immobilized methyltrioxo rhenium (MTO)/H_2O_2 systems for the oxidation of lignin and lignin model compounds. *Bioorganic and Medicinal Chemistry*, (14):5292–5302, 2006.

[83] Saladino R, Ginnasi MC, Collalto D, Bernini R, and Crestini C. An Efficient and Selective Epoxidation of Olefins with Novel Methyltrioxorhenium/(Fluorous Ponytailed) 2,2–Bipyridine Catalysts. *Advanced Synthesis & Catalysis*, (352):1284–1290, 2010.

[84] Breen A and Singleton FL. Fungi in lignocellulose breakdown and biopulping. *Current Opinion in Biotechnology*, (10):252–258, 1999.

[85] Martínez AT, Camarero S, Gutiérrez A, Bocchini P, and Galletti GC. Studies on wheat lignin degradation by *Pleurotus* species using analytical pyrolysis. *Journal of Analytical and Applied Pyrolysis*, (58–59):401–411, 2001.

[86] Shi J, Chinn MS, and Sharma-Shivappa RR. Microbial pretreatment of cotton stalks by solid state cultivation of *Phanerochaete chrysosporium*. *Bioresource Technology*, (99):6556–6564, 2008.

[87] Yu H, Guo G, Zhang X, Yan K, and Xu C. The effect of biological pretreatment with the selective white–rot fungus *Echinodontium taxodii* on enzymatic hydrolysis of softwoods and hardwoods. *Bioresource Technology*, (100):5170–5175, 2009.

[88] Witayakran S and Ragauskas AJ. Synthetic applications of laccase in green chemistry. *Advanced Synthesis & Catalysis*, (351):1187–1209, 2009.

[89] Reinhammar B. *Laccase.* In: Lontie R (ed.) *Copper proteins and copper enzymes*, pages 1–35. CRC Press, Boca Raton, 1984.

[90] Givaudan A, Effose A, Faure D, Potier P, Bouillant ML, and Bally R. Polyphenol oxidase in *Azospirillum lipoferum* isolated from rice rhizosphere: evidence for laccase activity in non–motile strains of *Azospirillum lipoferum*. *FEMS Microbiology Letters*, (108):205–210, 1993.

[91] Dittmer NT, Suderman RJ, Jiang H, Zhu YC, Gorman MJ, Kramer KJ, and Kanost MR. Characterization of cDNAs encoding putative laccase–like multicopper oxidases and developmental expression in the tobacco hornworm, *Manduca sexta*, and the malaria mosquito, *Anopheles gambiae*. *Insect Biochemistry and Molecular Biology*, (34):29–41, 2004.

[92] Xu F. Oxydation of phenols, anilines and benzenethiols by fungal laccases: correlation beetween activity and redox potentials as well as halide inhibition. *Biochemistry*, (35):7608–7614, 1996.

[93] Kersten PJ, Kalyanaraman B, Hammel KE, Reihammar B, and Kirk TK. Comparision of lignin peroxidase, horseradish peroxidase and laccase in the oxidation of methoxybenzenes. *Biochemical Journal*, (268):475–480, 1990.

[94] Youn HD, Hah YC, and Kang SO. Role of laccase in lignin degradation by white-rot fungi. *FEBS Microbiology Letters*, (132):183–188, 1995.

[95] Guillén F, Muñoz C, Gómez-Toribio V, Martínez AT, and Martínez MJ. Oxygen activation during oxidation of methoxyhydroquinones by laccase from *Pleurotus eryngii*. *Applied & Environmental Microbiology*, (66):170–175, 2000.

[96] Guillén F, Gómez-Toribio V, Martínez MJ, and Martínez AT. Production of hydroxyl radical by the sinergistic action of fungal laccase and aryl alcohol oxidases. *Archives of Biochemistry & Biophysics*, (383):142–147, 2000.

[97] Guillén F, Martínez MJ, Muñoz C, and Martínez AT. Quinone redox cycling in the lignolitic fungus *Pleurotus eryngii* leading to extracellular production of superoxide anion radical. *Archives of Biochemistry & Biophysics*, (339):196–199, 1997.

[98] Galhaup C, Wagner H, Hinterstoisser B, and Haltrich D. Increased production of laccase by wood–degraing basidiomycete *Trametes pubescens*. *Enzyme and Microbial Technology*, (30):529–536, 2002.

[99] Xavier AMRB, Tavares APM, Ferreira R, and Amado F. *Trametes versicolor* growth and laccase induction with by–products of pulp and paper industry. *Electronic Journal of Biotechnology*, (10):444–445, 2007.

[100] Tien M and Kirk TK. Lignin degrading enzyme from the hymenomycete *Phanerochaete crysosporium* Burds. *Science*, (221):661–663, 1983.

[101] Kuwahara M, Glenn JK, Morgan MA, and Gold MH. Separation and characterization of two extracellular H_2O_2–dependent oxydases from ligninolitic cultures of *Phanerochaete crysosporium*. *FEBS Letters*, (169):247–250, 1984.

[102] Camarero S, Sarkar S, Ruiz–Dueñas F, Martínez MJ, and Martínez AT. Description of a versatile peroxidase involved in the natural degradation of lignin that has both manganese peroxidase and lignin peroxidase substrate interaction sites. *Journal of Biological Chemistry*, (274):10324–10330, 1999.

[103] Martinez AT. Molecular biology and structure–function of lignin–degrading heme peroxidases. *Enzyme and Microbial Technology*, (30):425–444, 2002.

[104] Welinder KG. Superfamily of plant, fungal and bacterial peroxidases. *Current Opinion in Structural Biology*, (2):388–393, 1992.

[105] Poulos TL, Patterson WR, and Sundaramoorthy M. The crystal structure of ascorbate and manganese peroxidases: the role of non-haem metal in the catalytic mechanism. *Biochemical Society Transactions*, (23):228–232, 1995.

[106] Edwards SL, Raag R, Wariishi H, Gold MH, and Poulos TL. Crystal structure of lignin peroxidase. *Proceedings of the National Academy of Science USA*, (90):750–754, 1993.

[107] Schoemaker HE and Piontek K. On interaction of lignin peroxidase with lignin. *Pure & Applied Chemistry*, (68):2089–2096, 1996.

[108] Baciocchi E, Fabbri C, and Lanzalunga O. Lignin peroxidase–catalyzed oxidation of non–phenolic trimeric lignin model compounds: fragmentation reactions in the intermediate radical cations. *Journal of Organic Chemistry*, (68):9061–9069, 2003.

[109] Hofrichter M. Review: lignin conversion by manganese peroxidase (MnP). *Enzyme and Microbial Technology*, (30):454–466, 2002.

[110] Tien M and Ma D. Oxidation of 4–methoxymandelic acid by lignin peroxidase. Mediation by veratryl alcohol. *Journal of Biological Chemistry*, (272):8912–8917, 1997.

[111] Collins PJ, Fiel JA, Teunissen P, and Dobson ADW. Stabilization of lignin peroxidases in white rot fungi by tryptophan. *Applied & Environmental Microbiology*, (63):2543–2548, 1997.

[112] Zapanta LS and Tien M. The roles of veratryl alcohol and oxalate in fungal lignin degradation. *Journal of Biotechnology*, (53):93–102, 1997.

[113] Johjima T, Wariishi H, and Tanaka H. Veratryl alcohol binding sites of lignin peroxidase from *Phanerochaete crysosporium*. *Journal of Molecular Catalysis B: Enzymatic*, (17):49–57, 2002.

[114] Cai D and Tien M. Kinetic studies on the formation and decomposition of compounds II and III. *The Journal of Biological Chemistry*, (267):11149–11155, 1992.

[115] Barr DP and Aust SD. Conversion of lignin peroxidase compound III to active enzyme by cation radicals. *Archives of Biochemistry and Biophysics*, (312):511–515, 1994.

[116] Koduri RS and Tien M. Kinetic analysis of lignin peroxidase: explanation for the mediation phenomenon by veratryl alcohol. *Biochemistry*, (33):4225–4230, 1994.

[117] Wariishi H, Valli K, and Gold MH. Manganese(II) oxidation by manganese peroxidase from the basidiomycete *Phanerochaete crysosporium*. *Journal of Biological Chemistry*, (267):23688–23695, 1992.

[118] Mester T and Field JA. Optimization of manganese peroxidase production by the white rot fungus *Byerkandera sp.* strain BOS55. *FEMS Microbiology Letters*, (155):161–168, 1997.

[119] Sigoillot JC, Petit-Conil M, Herpoël I, Joseleau JP, Ruel K, Kurek B, de Choudens C, and Asther M. Energy saving with fungal enzymatic treatment of industrial poplar alkaline peroxide pulps. *Enzyme and Microbial Technology*, (29):160–165, 2001.

[120] Herpoël I, Asther M, and Sigoillot JC. Design and scale up of a process for manganese peroxidase production using the hypersecretory strain *Phanerochaete crysosporium* I–1512. *Biotechnology and Bioengineering*, (65):468–473, 1999.

[121] Nüske J, Scheibner K, Dornberger U, Ullrich R, and Hofrichter M. Large scale production of manganese–peroxidase using agaric white–rot fungi. *Enzyme and Microbial Technology*, (30):556–561, 2002.

[122] Leonowicz A, Matuszewska A, Luterek J, Ziegenhagen D, Wojtas-Wasilewska ;, Cho NS, Hofrichter M, and Rogalski J. Biodegradation of lignin by white rot fungi. *Fungal Genetics and Biology*, (27):175–185, 1999.

[123] Galliano H, Gas G, Seris JL, and Boudet AM. Lignin degradation by *Rigidoporus lignosus* involves synergistic action of two oxidizing enzymes: Mn peroxidase and laccase. *Enzyme and Microbial Technology*, (13):478–482, 1991.

[124] Hammel KE and Cullen D. Role of fungal peroxidases in biological ligninolysis. *Current Opinion in Plant Biology*, (11):349–355, 2008.

[125] Rocha Gonsalves AMA and Pereira MM. State of art in the development of biomimetic oxidation catalysts. *Journal of Molecular Catalysis*, (113):209–221, 1996.

[126] Mansuy D. A brief history of the contribution of metalloporphyrin models to cytochrome P450 chemistry and oxidation catalysis. *Comptes Rendus Chimie*, (10):392–413, 2007.

[127] Zhou W, Hu B, and Liu Z. Metallo–deuteroporphyrin complexes derived from heme: A homogeneous catalyst for cyclohexane oxidation. *Applied Catalysis A: General*, (358):136–140, 2009.

[128] Crestini C, Pastorini A, and Tagliatesta P. Metalloporphyrins immobilized on motmorillonite as biomimetic catalysts in the oxidation of lignin model compounds. *Journal of Molecular Catalysis*, (208):195–202, 2004.

[129] Baciocchi E, Gerini MF, and Lapi A. Synthesis of sulfoxides by hydrogen peroxide induced oxidation of sulfides catalyzed by iron tetrakis(pentafluorophenyl)porphyrin: scope and chemoselectivity. *Journal of Organic Chemistry*, (69):3586–3589, 2004.

[130] Paszczynski A, Crawford RL, and Blanchette RA. Delignification of wood chips and pulps by using natural and synthetic porphyrins: Models of fungal decay. *Applied and Environmental Microbiology*, (54):62–68, 1988.

[131] Labat G and Meunier B. Factors controlling the reactivity of a ligninase model based on the association of potassium monopersulfate to manganese and iron porphyrin complexes. *Journal of Organic Chemistry*, (54):5008–5011, 1989.

[132] Cui F, Wijesekera T, Dolphin D, Farrell R, and Skerer P. Biomimetic degradation of lignin. *Journal of Biotechnology*, (30):15–26, 1993.

[133] Artaud I, Ben-Aziza K, and Mansuy D. Iron porphyrin-catalyzed oxidation of 1,2–dimethoxyarenes: a discussion of the different reactions involved and the competition between the formation of methoxyquinones or muconic dimethyl esters. *Journal of Organic Chemistry*, (58):3373–3380, 1993.

[134] Kurek B, Artaud I, Pollet B, Lapierre C, and Monties B. Oxidative Degradation of *in Situ* and Isolated Spruce Lignins by Water–Soluble Hydrogen Peroxide Resistant Pentafluorophenylporphyrin. *Journal of Agricultural and Food Chemistry*, (44):1953–1959, 1996.

[135] Crestini C, Saladino R, Tagliatesta P, and Boschi T. Biomimetic degradation of lignin and lignin model compounds by synthetic anionic and cationic water soluble manganese and iron porphyrins. *Bioorganic & Medicinal Chemistry*, (7):1897–1905, 1997.

[136] Meunier B. *General Overview on Oxidations Catalyzed by Metalloporphyrins* In: Montanari F and Casella L (eds.)*, Metalloporphyrins catalyzed oxidations* . Kluwer Academics Publishers, Dordrecth, 1994.

[137] Crestini C, Pastorini A, and Tagliatesta P. The immobilized porphyrin-mediator system Mn(TMePyP)/clay/HBT (clay–PMS): A lignin peroxidase biomimetic catalyst in the oxidation of lignin and lignin model compounds. *European Journal of Inorganic Chemistry*, (22):4477–4483, 2004.

[138] Moghadam M, Tangestaninejad S, Habibi MH, and Mirkhani V. A convenient preparation of polymer–supported manganese porphyrin and its use as hydrocarbon monooxygenation catalyst. *Journal of Molecular Catalysis A: Chemical*, (217):9–12, 2004.

[139] Iamamoto Y, Idemori YM, and Nakagaki S. Cationic ironporphyrins as catalyst in comparative oxidation of hydrocarbons: homogeneous and supported on inorganic matrices systems. *Journal of Molecular Catalysis A: Chemical*, (99):187–193, 1995.

[140] Meunier B. *Biomimetic oxidations catalyzed by transition metal complexes*, chapter 4. Imperial College Press, London UK, 2000.

[141] Rescigno A, Zucca P, Flurkey A, Inlow J, and Flurke WH. Identification and discrimination between some contaminant enzyme activities in commercial preparations of mushroom tyrosinase. *Enzyme and Microbial Technology*, (41):620–627, 2007.

[142] Amat di San Filippo P, Fadda MB, Rescigno A, Rinaldi A, and Sanjust E. A new synthetic polymer as a support for enzyme immobilization. *European Polymer Journal*, (26):545–547, 1990.

[143] Sarkanen S, Razal RA, Piccariello T, Yamamoto E, and Lewis NG. Lignin peroxidase: toward a clarification of its role in vivo. *The Journal of Biological Chemistry*, (266):3636–3643, 1991.

[144] Halliwell B, Gutteridge JMC, and Aruoma OI. The deoxyribose method: A simple "test–tube" assay for determination of rate constants for reactions of hydroxyl radicals. *Analytical Biochemistry*, (165):215–219, 1987.

[145] Wanzlick HW and Jahnke U. Synthesen mit naszierenden Chinonen, IV. Basenkatalysierte Alkoholaddition an in situ erzeugte o–Chinone. *Chemische Berichte*, (101):3744–3752, 1968.

[146] Witty TR and Remers WA. Synthesis and antitumor and antibacterial activity of benzoquinones related to the mitomycins. *Journal of Medicinal Chemistry*, (16):1280–1284, 1973.

[147] Haemmerli SD, Schoemaker HE, Schmidt HWH, and Leisola MSA. Oxidation of veratryl alcohol by the lignin peroxidase of *Phanerochaete chrysosporium* Involvement of activated oxygen. *FEBS Letters*, (220):149–154, 1987.

[148] Ciric-Marjanovic G, Blinova NV, Trchova M, and Stejskal J. Chemical Oxidative Polymerization of Safranines. *Journal of Physical Chemistry B*, (111):2188–2199, 2007.

[149] International Union of Pure and Applied Chemistry. Reporting physisorption data for Gas/Solid systems with special reference to the determination of surface area and porosity. *Pure and Applied Chemistry*, (57):603–619, 1985.

[150] Gold MH, Kuwahara M, Chiu AA, and Glenn JK. Purification and characterization of an extracellular H_2O_2–requiring diarylpropane oxygenase from the white rot basidiomycete, *Phanerochaete chrysosporium*. *Archives of Biochemistry and Biophysics*, (234):353–362, 1984.

[151] Kersten PJ, Tien M, Kalyanaraman B, and Kirk TK. The ligninase of *Phanerochaete chrysosporium* generates cation radicals from methoxybenzenes. *Journal of Biological Chemistry*, (260):2609–2612, 1985.

[152] Sarkanen S, Razal RA, Piccariello T, Yamamoto E, and Lewis NG. Lignin peroxidase: Toward a clarification of its role in vivo. *Journal of Biological Chemistry*, (266):3636–3643, 1991.

[153] Ferreira P, Medina M, Guillén, Martínez MJ, Van Berkel WJH, and Martínez AT. Spectral and catalytic properties of aryl–alcohol oxidase, a fungal flavoenzyme acting on polyunsaturated alcohols. *Biochemical Journal*, (389):731–738, 2005.

[154] Powell MF, Pai EF, and Bruice TC. Study of (tetraphenylporphinato)manganese(III)–catalyzed epoxidation and demethylation using *p*–cyano–N,N–dimethylaniline N-oxide as oxygen donor in a homogeneous system. Kinetics, radiochemical ligation studies, and reaction mechanism for a model of cytochrome P–450. *Journal of the American Chemical Society*, (106):3277–3285, 1984.

[155] Meunier B, Guilmet E, De Carvalho ME, and Poilblanc R. Sodium hypochlorite: A convenient oxygen source for olefin epoxidation catalyzed by (porphyrinato)manganese complexes. *Journal of the American Chemical Society*, (106), 1984.

[156] Mohajer D and Solati Z. Rapid and highly selective epoxidation of alkenes by tetrabutylammonium monopersulfate in the presence of manganese meso–tetrakis(pentafluorophenyl)porphyrin and tetrabutylammonium salts or imidazole co–catalysts. *Tetrahedron Letters*, 2006.

[157] Noyori R. Pursuing practical elegance in chemical synthesis. *Chemical Communications*, pages 1807–1811, 2005.

[158] Koduri RS, Whitwam RE, Barr D, Aust SD, and Tien M. Oxidation of 1,2,4,5–tetramethoxybenzene by lignin peroxidase of *Phanerochaete chrysosporium*. *Archives of Biochemistry and Biophysics*, (326):261–265, 1996.

[159] Ghasemi J, Lotfi S, Safaeian M, Niazi A, MM Ardakani, and Noroozi M. Spectrophotometric determination of acidity constants of alizarine red S in mixed aqueous–organic solvents. *Journal of Chemical and Engineering Data*, (51):1530–1535, 2006.

[160] Thompson KM, Griffith WP, and Spiro M. Mechanism of bleaching by peroxides. Part 2. - Kinetics of bleaching of alizarin and crocetin by hydrogen peroxide at high pH. *Journal of the Chemical Society, Faraday Transactions*, (8):4035–4043, 1993.

[161] Faouzi AM, Nasr B, and Abdellatif G. Electrochemical degradation of anthraquinone dye Alizarin Red S by anodic oxidation on boron–doped diamond. *Dyes and Pigments*, (73):86–89, 2007.

[162] Gao J, Yu J, Lu Q, He X, Yang W, Li Y, Pu L, and Yang Z. Decoloration of alizarin red S in aqueous solution by glow discharge electrolysis. *Dyes and Pigments*, (76):47–52, 2008.

[163] Liu G, Li X, Zhao J, Horikoshi S, and Hidaka H. Photooxidation mechanism of dye alizarin red in TiO_2 dispersions under visible illumination: An experimental and theoretical examination. *Journal of Molecular Catalysis A: Chemical*, (153):221–229, 2000.

[164] Lachheb H, Puzenat E, Houas A, Ksibi M, Elaloui E, Guillard C, and Herrmann JM. Photocatalytic degradation of various types of dyes (Alizarin S, Crocein Orange G, Methyl Red, Congo Red, Methylene Blue) in water by UV–irradiated titania. *Applied Catalysis B: Environmental*, (39):75–90, 2002.

[165] Chen C, Li X, Ma W, Zhao J, Hidaka H, and Serpone N. Effect of transition metal ions on the TiO_2–assisted photodegradation of dyes under visible irradiation: A probe for the interfacial electron transfer process and reaction mechanism. *Journal of Physical Chemistry B*, (106):318–324, 2002.

[166] Sivalingam G, Nagaveni K, Hegde MS, and Madras G. Photocatalytic degradation of various dyes by combustion synthesized nano anatase TiO_2. *Applied Catalysis B: Environmental*, (45):23–38, 2003.

[167] Yang Y, Qiu Z, Li X, Zhao D, Xie Z, and Kuang T Bai X. Amorphous formation ability and compression strength of CuNiAlNb alloys. *Special Casting and Nonferrous Alloys*, (25):203–204, 2005.

[168] Ingol KU and MacFaul PA. *Distinguishing biomimetic oxidations from oxidations mediated by freely diffusing radical*. In: Meunier B (ed.)*Biomimetic oxidations catalyzed by transition metal complexes*, pages 45–89. Imperial College Press, London UK, 1998.

[169] Groves JT, Lee J, and Marla J. Detection and characterization of an oxomanganese(V) porphyrin complex by rapid-mixing stopped–flow spectrophotometry. *Journal of the American Chemical Society*, (119):6269–6279, 1997.

[170] Groves JT and Stern MK. Synthesis, characterization, and reactivity of oxomanganese(IV) porphyrin complexes. *Journal of the American Chemical Society*, (110):8628–8638, 1988.

[171] Goodwin DC and Aust SD. Evidence for veratryl alcohol as a redox mediator in lignin peroxidase-catalyzed oxidation. *Biochemistry*, (34):5060–5065, 1995.

[172] Finch CA. *Polyvinyl Alcohol – Developments*. Wiley, Chichester, 1992.

[173] Traylor TG, Hill KW, Fann WP, Tsuchiya S, and Dunlap BE. Aliphatic hydroxylation catalyzed by iron(III) porphyrins. *Journal of the American Chemical Society*, (114):1308–1312, 1992.

[174] Tinoco R, Verdin J, and Vazquez-Duhalt R. Role of oxidizing mediators and tryptophan 172 in the decoloration of industrial dyes by the versatile peroxidase from *Bjerkandera adusta*. *Journal of Molecular Catalysis B: Enzymatic*, (46):1–7, 2007.

[175] Cui F and Dolphin D. Iron porphyrin catalyzed oxidation of lignin model compounds: the oxidation of veratryl alcohol and veratryl acetate. *Canadian Journal of Chemistry*, (70):2314–2318, 1992.

[176] Boe JF, Goulas P, and Seris JL. Effect of Organic Acids on Reactions Catalyzed by Manganese Peroxidase from *Phanerochaete chrysosporium*. *Biocatalysis and Biotransformation*, (7):297–308, 1993.

[177] Meunier B. Metalloporphyrins as versatile catalysts for oxidation reactions and oxidative DNA cleavage. *Chemical Reviews*, (92):1411–1456, 1992.

[178] Mansuy D, Battioni P, and Renaud JP. In the presence of imidazole, iron– and manganese–porphyrins catalyse the epoxidation of alkenes by alkyl hydroperoxides. *Journal of the Chemical Society, Chemical Communications*, (19):1255–1257, 1984.

[179] Harris DL. High-valent intermediates of heme proteins and model compounds. *Current Opinion in Chemical Biology*, (5):724–735, 2001.

[180] Traylor TG, Tsuchiya S, Byun YS, and Kim C. High–yield epoxidations with hydrogen peroxide and *tert*–butyl hydroperoxide catalyzed by iron(III) porphyrins: Heterolytic cleavage of hydroperoxides. *Journal of the American Chemical Society*, (115):2775–2781, 1993.

[181] Poulos TL, Edwards SL, Wariishi H, and Gold MH. Crystallographic refinement of lignin peroxidase at 2Å. *Journal of Biological Chemistry*, (268):4429–4440, 1993.

[182] Sigel A, Sigel H, and Sigel RKO. *The Ubiquitous Roles of Cytochrome 450 Proteins. In:* Metal Ions in Life Sciences. Wiley, Chichester, 2007.

Index

A
Alkaline hydrolysis 29
Amberlite 46
Ammonia 29, 30
Anthraquinone 25, 73
AP–PVA 52
ARS 50, **79**, 104, 107, 109, 112
Aryl alcohol oxidase 41
Azodye 25, 73
Azospirillum 35
Azure B 27, 50, 55, 97, 104

B
Basidiomycetes 18, 34, 35
Bioethanol 14
Bjerkandera 34, 40
Black liquor 30
Brown–rot fungi 18, 34
t–Butylhydroperoxide 44

C
Cellobiose 17
Cellobiose:quinone oxidoreductase ... 41
Cellodextrins 17
Cellulose 14, 15, **17**, 28, 34
Ceriporiopsis 34
Chlorine dioxide 31
Chlorolignins 31
Cinnamate pathway 20
β–Cl_8–TDCPP 43
CO_2 explosion 29
Compound I 37, 87, 100–102
Compound II 37, 87, 103
Compound III 40
Coniferyl alcohol 19
p–Coumaryl alcohol 19
Cytochrome C Peroxidase 37
Cytochrome P450 .. 42, 48, 87, 105, 117

D
Delignification 27, 29, 41
Dichomitus 34
Dimethylsulfoxide 93
Dioxane 45
Dirigent proteins 24
Distal His 37
Dyes 15, **25**, 48, 73, 104, 112

E
Endoglucanase 17
Eucalyptus 20, 24
Exoglucanase 17

F
Fenton reaction 32
FeTFPP 53, 92, 101, 105
FeTMPP 53
FT–IR 54, 61, 94

G
Galattomannan 18
Ganoderma 34
GC–MS 58, 67
Glucomannan 18
Glucose 17
Glucose oxidase 41
β–Glucosidase 18
Glutaraldehyde 50, 92
Glycosidic bond 17, 18
Glyoxalate oxidase 41

H
Heme 37, 48

Hemicelluloses 14, 15, **18**, 29
Histidine 46
HPLC 57, 67, 90, 96
HRP 50, 58, 75, 82, 89
Hydrogen peroxide 22, 31, 37, 40–42, 45, 48, 55, 65, 74, 90, 101
Hydrogen sulfide 30
Hydroxy–TEMPO 36, 57
Hydroxybenzotriazole 49, 57, 78, 88, 106, 112
Hydroxycinnamates 20, 25
Hydroxyl radical 32, 36, 45, 80, 99
Hydroxyphthalimide 57, 78, 112
Hydroxysuccinimide 57, 78, 88, 112

I
Im–PVA 52
Imidazole 46, 48, 92
Immobilization 45
Iodosylbenzene 42
IPS 51, 61

K
Kraft 29, 30, 32

L
Laccase 35, **35**, 39, 58, 75, 82, 89
Lignin . 14, 15, 18, **19**, 29, 34, 36, 45, 49
  biosynthesis 22
  structure 19, 24
Lignin peroxidase 27, 35, **36**, 49, 50, 58, 75, 82, 90, 104, 107
Lignocelluloses 15
Lignolytic peroxidase 35, **36**, 42, 47

M
M–PVA 53, 105
Manganese peroxidase ... 35, **36**, 40, 49, 59, 75, 103, 108
MB 50, 104, 112
Mercapto group 48, 107
Metalloporphines **42**, 48
Methyltrioxorhenium 34
MG 50, 104, 112
Middle lamella 16
MnTMPP 113
MnTSPP 53, 64
MO 50, 104, 112
Molybdovanadophosphate 34
Monolignols 19, 22
MSG 51, 105

N
Ninhydrin 52

O
Olive Mill Wastewater 15
Ozonolysis 33

P
Paper 14, 28, 41
Peroxodisulfate 59, 85
Phanerochaete 34, 36
Phenothiazine 25, 73
Phenylalanine 20
Phenylalanine Ammonia Lyase 20
Phenylpropanoids 19
Phlebia 34
Plant cell wall 15, 18
Pleurotus 34, 36, 40, 50
PNS 50, **84**, 104, 112
Polyoxometalates 34
Porphination 53
PP–PVA 53, 95
Primary wall 16
Protoporphyrin IX 37
Proximal His 37
PSG 51

Pulp 28
PVA 50, 114
Pyridine 48, 92

R
Redox mediator 36, 39, 49, 77, 112
Reflectance spectroscopy 54, 101
ROS 36, 39, 41
Rothemund synthesis 42

S
Secondary wall 16, 19
Silica gel 47, 50, 114
Sinapyl alcohol 19
Sodium chlorite 31
Sodium hypochlorite 42
Steam explosion 28
Stereum 34
Sulfite 29, 30
Superoxide 32

T
TAML 34
TDCPP 43
TEMPO 36
TFPP 43, 48, 50
Titanium dioxide 33
TMPP 43, 46, 50
TPP 43
Trametes 34
Triphenylmethane 25, 73
Tryptophan 39
TSPP 43, 48, 50

V
Vanillyl alcohol 101
Veratraldehyde 55, 106
Veratryl alcohol .. 39, 48, 55, 59, 65, 97, 107, 109
Versatile peroxidase 35, **36**, 40, 104

W
White liquor 29, 32
White–rot fungi 34–36, 41
Wood 34

X
XO 50, 104, 112
Xylan 18, 29
Xylanase 28